DEVELOPMENT OF A PROTEIN MICROARRAY FOR ANALYSIS OF HUMORAL IMMUNE RESPONSES TO FLAVIVIRUS INFECTION AND VACCINATION

by

Christine L. Pugh

B.A. (Hood College) 2007

THESIS

Submitted in partial satisfaction of the requirements

for the degree of

MASTER OF SCIENCE

in

BIOMEDICAL SCIENCE

in the

GRADUATE SCHOOL

of

HOOD COLLEGE

April 13, 2018

Accepted:

_____	_____
Craig S. Laufer, Ph.D. Committee Member	Ann L. Boyd, Ph.D. Director, Biomedical Science Program
_____	
Stefan Fernandez, Ph.D. Committee Member	
_____	_____
Robert G. Ulrich, Ph.D. Thesis Adviser	April M. Boulton, Ph.D. Dean of the Graduate School

STATEMENT OF USE AND COPYRIGHT WAIVER

I do authorize Hood College to lend this thesis, or reproductions of it, in total or in part, at the request of other institutions or individuals for the purpose of scholarly research.

DEDICATION

With love and gratitude beyond words, I dedicate this thesis to my amazing husband and best friend, Andy, and my three beautiful daughters, Ella, Liliana, and Olivia. They are my whole world.

ACKNOWLEDGEMENTS

First, I would like to thank my advisor, Dr. Robert Ulrich for his invaluable guidance and unwavering support and encouragement throughout the years. Dr. Ulrich is a wealth of knowledge and an incredible person that I am fortunate to know and have as a mentor. His wisdom, patience, work ethic, and dedication are truly an inspiration. I am beyond thankful for every opportunity he has given to me. Moreover, I am beyond grateful for Dr. Ulrich's faith in my abilities, and me especially during times that I could not find it myself.

I would also like to thank my thesis committee members, Dr. Stefan Fernandez and Dr. Craig Laufer, for patiently serving on my committee. It was a long road, thank you for not giving up on me! Thank you both for your guidance and for encouragement throughout my Master's project and beyond.

I am very fortunate to be part of such a supportive lab group at USAMRIID and I would like to thank all of them for their encouragement, guidance, and help over the years. Dr. Jessica Smith, Beverly Dyas, Dr. Kamal Saikh, Dr. M. M. Shahabuddin Alam, Dr. Mohan Natesan, Dr. Bryan Zhao, Dr. Moo-Jin Suh, Dr. Anna Mielech, and Dr. Stig Jensen-thank you. A special thank you goes to Cyra Ranjii for all of her technical assistance on many of the laboratory tasks involved in this project. I would particularly like to thank Sarah Keasey, who I am very fortunate to have as a coworker, but even more fortunate and blessed to have as a best friend. Sarah is a one in a million kind of person and there are absolutely no words that would ever be enough to explain my sincere gratitude and appreciation for her and the friendship that we share. Sarah's super hero strength and abilities as a wife, mother, and scientist are truly an inspiration. Her patience, encouragement, understanding, and wisdom have guided me through many deadlines and difficult projects; while her sense of humor, supply of coffee and chocolate treats, and mere presence have made those stressful times that much easier.

Lastly, my deepest appreciation and heartfelt love go to my family. I could not have done this without them and their support. Andy is THE most amazing husband and father to our three beautiful girls. I could never thank him enough for all that he is and has done for me. He has been my rock and my biggest supporter through all of this. There is no one else I rather go through life's ups and downs with. Andy and my girls, Ella, Lily, and Olivia, are my biggest blessings in life and mean everything to me. They were my reason for smiling during stressful days and they were my true source of inspiration, strength, motivation, and perseverance. Also, my wonderful parents thank you for your unending love and support that goes far beyond this project. I would not be the person that I am today without you. To my extended family and friends, your love and support near and far is beyond appreciated and never goes unnoticed. Thank you all from the bottom of my heart for your unconditional love, understanding, support, and encouragement. I am beyond blessed to have such amazing people in my life.

This research was supported in part by an appointment to the Postgraduate Research Participation Program administered by Oak Ridge Institute for Science and Education through an interagency agreement with the U.S. Department of Energy.

Opinions, interpretations, conclusions, and recommendations are those of the authors and are not necessarily endorsed by any branch of the U.S. government.

TABLE OF CONTENTS

ABSTRACT

Dengue virus (DENV), yellow fever virus (YFV), West Nile virus (WNV), and Zika virus (ZIKV) are the leading causes of mosquito-borne human flavivirus infections in the Americas. Serological assays for diagnosis and surveillance are generally directed towards one specific virus and disregard the potential for antibody cross reactivity between nearest neighbors. Here, a comprehensive assay was developed that included whole virus preparations and recombinant antigens from 15 human pathogenic flaviviruses. Using the printed microarrays, serological immune responses to ZIKV, WNV, DENV, and YFV infections of humans and nonhuman primates (NHPs) were examined in order to examine specificity and cross reactivity of antibody responses among the viral antigens. Sera were further employed from yellow fever vaccine studies to demonstrate the utility of using multiple viral antigens for obtaining a detailed analysis of antibody responses to vaccination. Results from the microarray assays indicated that antibody recognition of isolated flaviviral antigens can be used to resolve complex infection histories, as well as provide a detailed understanding of immune responses to YFV vaccination in areas of flavivirus endemicity.

LIST OF TABLES

LIST OF FIGURES

LIST OF ABBREVIATIONS

aa	amino acid
ADCC	antibody-dependent cell-mediated cytotoxicity
ADE	Antibody dependent enhancement
AFR	African
ANOVA	analysis of variance
AS	Asian
ATCC	American Type Culture Collection
AUC	area under the curve
BEI Resources	Biodefense and emerging infections
BioLINCC	Biologic Specimen and Data Repository Information Coordinating Center
BSA	bovine serum albumin
C	capsid
CDC	Center for Disease Control
cDNA	complementary DNA
CMV	cytomegalovirus
CoV	coefficient of variance
CV	column volume
D	domain
DENV	dengue virus
DENV1-4	dengue virus serotypes 1-4
DMEM	Dulbecco's Modification of Eagle's Medium
DoD	Department of Defense
DPI	days post infection
DTT	dithiothreitol
E	envelope
E.coli	*Escherichia coli*
EDTA	ethylenediamine tetraacetic acid
ELISA	enzyme-linked immunosorbent assay
F.tularensis	*Francisella tularensis*
FBS	Fetal bovine serum
FDA	Food and Drug Administration
FN	false negative
FP	false positive
FPR	false positive rate
gB	glycoprotein B
HA	Influenza hemagglutinin
HepC	Hepatitis C virus
His	Histidine

HisMBP	His-maltose-binding protein
HIT	hemagglutination inhibition assay
HSD	honest significance difference
ID	identification
IFA	indirect fluorescence assay
IgA	immunoglobulin A
IgG	immunoglobulin G
IgM	immunoglobulin M
IMAC	immobilized metal affinity chromatography
IPTG	isopropyl β-D-1-thiogalactopyranoside
IRB	institutional review board
JEV	Japanese encephalitis virus
K	Kernal function
KLH	keyhole limpet hemocyanin
M	membrane
mAb	monoclonal antibody
MAC	IgM antibody capture
MFI	mean fluorescence intensity
MOI	multiplicity of infection
mRNA	messenger RNA
MSA	multiple sequence alignment
MVEV	Murray valley encephalitis virus
Nab	neutralizing antibody
NAMRU-6	Naval Medical Research Unit No. 6
NHLBI	National Heart, Lung, and Blood Institute
NHP	non-human primates
NIAID	National Institute of Allergy and Infectious Disease
NIH	National Institute of Health
NS	non-structural
ns	non-significant
N-term	amino (NH_2)-terminus
N.V.	non-vaccinated
ORF	open reading frame
pAb	polyclonal antibody
PAGE	polyacrylamide gel electrophoresis
PAHO	Pan American Health Organization
PCA	principal component analysis
PCR	polymerase chain reaction
PFU	plaque forming units
pM	precursor membrane

PT	patient
POWV	Powassan virus
PRNT	plaque reduction neutralization test
PV	post-vaccination
RB	relative binding
RBF	radial basis function
ROC	receiver-operator characteristics
ROCV	Rocio virus
RT-PCR	real-time polymerase chain reaction
SDS	sodium dodecyl sulfate
SEM	standard error of the mean
SLEV	St. Louis encephalitis virus
SVM	support vector machine
TBEV	tick-borne encephalitis virus
TBEV-E	tick-borne encephalitis virus, eastern strain
TBEV-EUR	tick-borne encephalitis virus, European strain
TLAV	tetravalent live, attenuated virus
TN	true negative
TP	true positive
TPIV	tetravalent purified inactivated virus
TPR	true positive rate
U.S.	United States
Vacc.	vaccinated
VACV	vaccinia virus
WHO	World Health Organization
WNPRC	Wisconsin National Primate Research Center
WNV	West Nile virus
Y.Pestis	*Yersinia Pestis*
YFV	yellow fever virus
ZIKV	Zika virus
ZIKV-CAfrR	Zika virus, Central African Republic strain
ZIKV-Sen	Zika virus, Senegal strain

INTRODUCTION

Flaviviridae background

The *Flaviviridae* family includes over 100 enveloped, single-stranded RNA viruses that are agents of animal and human diseases (Lindenbach 2007; Simmonds *et al.* 2017; Stapleton *et al.* 2011). The four *Flaviviridae* genera of flavivirus, hepacivirus, pestivirus, and pegivirus share similar virion morphology, genomic organization, and replication mechanisms. Viruses within *Flaviviridae* are small (~9.5-13kb) positive-strand RNA viruses that enter host cells by receptor-mediated endocytosis (Pierson and Kielian 2013; Simmonds et al. 2017; Smit et al. 2011). Acidification of endosomes induces viral membrane fusion and un-coating of the immature virion, which leads to the release of RNA into the cytoplasm (Pierson and Kielian 2013; Smit *et al.* 2011), which serves as both viral mRNA and a template for genomic replication. The viral RNA is translated into a single polyprotein that is further processed by internal and host proteases into approximately ten structural or non-structural proteins (Heinz and Stiasny 2012; Hollidge *et al.* 2010; Lindenbach 2007). The assembled immature virion buds from the endoplasmic reticulum into the Golgi for further processing. The surface proteins (envelope (E) and precursor membrane protein (pM)) on the immature virion undergo significant conformational change that allows furin-mediated cleavage of the precursor peptide from the virus-associated transmembrane M before exocytosis of the mature infectious virus (Heinz and Mandl 1993; Smit et al. 2011; Stadler et al. 1997).

Despite the similarities, each *Flaviviridae* genus is characterized by distinct biological properties and disease presentations. Flaviviruses are typically transmitted to humans and animals by infected mosquitoes or tick vectors. While most human infections

are mild and self-limiting, flaviviral diseases such as dengue and West Nile can progress to hemorrhagic fever and encephalitis, respectively (Halstead *et al.* 1976; Kliks *et al.* 1988). Hepatitis C virus (HepC), the only human hepacivirus within the genus, is transmitted to humans through infected blood. There are six HepC genotypes that are distributed throughout the world. Hepatitis C infections cause approximately 400,000 deaths each year due to liver related disease ([WHO] World Health Organization 2017a). Pegivirus, formally referred to as GB virus type C, is most similar to HepC. However, disease pathogenesis caused by pegivirus infections in humans remains unresolved, partly due to its high prevalence in individuals co-infected with HepC or human immunodeficiency virus (Berg *et al.* 2015; Gutierrez *et al.* 1997; Mohr and Stapleton 2009). Pestiviruses, such as bovine viral diarrhea virus cause a significant number of deaths and economic loss in the livestock industry, but are not commonly associated with disease in humans (Leyssen *et al.* 2000). Overall, *Flaviviridae* viruses are considered a major global health and economic burden, though differences in epidemiology and pathogenesis exist between each genus.

Flavivirus background information

Approximately half of the 75 known flaviviruses are human pathogens (Solomon and Mallewa 2001). Human flavivirus infections are typically seasonal and occur through the blood-meal bite of an infected mosquito or tick. The infected saliva of the arthropod is transferred into the host's bloodstream, which then goes through a series of steps leading to viremia (Hollidge *et al.* 2010; Schmaljohn and McClain 1996). However, infections can also be transmitted without a vector, such as: through infected blood or organ transplant donations, transmitted from mother to child, through contact with infected animal tissue or

fluids, via sexual transmission, or laboratory acquired infections (Foy *et al.* 2011; Sampathkumar 2003). There are no specific anti-flaviviral drugs, and licensed vaccines for humans exist for only a few flaviviruses, for example YFV, Japanese encephalitis virus (JEV), and tick-borne encephalitis virus (TBEV) (Heinz and Stiasny 2012). Recently a live, attenuated dengue virus (DENV) vaccine was licensed in a number of countries where the disease is endemic. However, the chimeric DENV vaccine has only demonstrated modest efficacy and it is likely to be many years before it is fully implemented in all dengue-endemic areas ([WHO] World Health Organization 2017b; Capeding et al. 2014). In regards to human disease impact, the major pathogenic flaviviruses are DENV, YFV, JEV, TBEV, WNV, as well as the rather newly emergent and rapidly spreading ZIKV. Several other flaviviruses, such as St. Louis encephalitis virus (SLEV), Murray valley encephalitis virus (MVEV), Rocio virus (ROCV), and Powassan virus (POWV), have the ability to cause severe and fatal disease in humans, but outbreaks are currently sporadic and the number of reported annual cases is relatively small (Cleton *et al.* 2012; Heinz and Stiasny 2012).

The 11kb flavivirus genome is translated into a single polyprotein that is cleaved into three structural proteins (capsid (C), envelope (E), and precursor membrane/membrane (pM/M)) and seven non-structural proteins (NS1, NS2A, NS2B, NS3, NS4A, NS4B, and NS5) (Heinz and Stiasny 2012; Hollidge *et al.* 2010; Lindenbach 2007) (Figure 1). The structural proteins are incorporated into the virus particle and have primary roles in virus assembly, mediating cell attachment, and fusion with the host membrane (Lindenbach and Rice 2003; Lindenbach 2007). The non-structural proteins are mainly involved in processing of the polyprotein, RNA replication, and evasion of the host immune response

(Avirutnan *et al.* 2010; Avirutnan *et al.* 2007; Chuang *et al.* 2013; Lindenbach 2007; Patkar and Kuhn 2008; Perera and Kuhn 2008). The E, pM/ M, and NS1 proteins are thought to be the primary targets of humoral immune responses in infected individuals, although antibody responses to NS3 and NS5 proteins has also been detected in humans (Churdboonchart et al. 1991; Cleton et al. 2012; Duangchinda et al. 2010; Fernandez et al. 2011; Wahala and Silva 2011). Further, T-cell (CD4+/CD8+) immune responses have been demonstrated to all flavivirus proteins, but may preferentially target NS proteins (NS3, NS5, and NS4B) (Rivino and Lim 2017) .

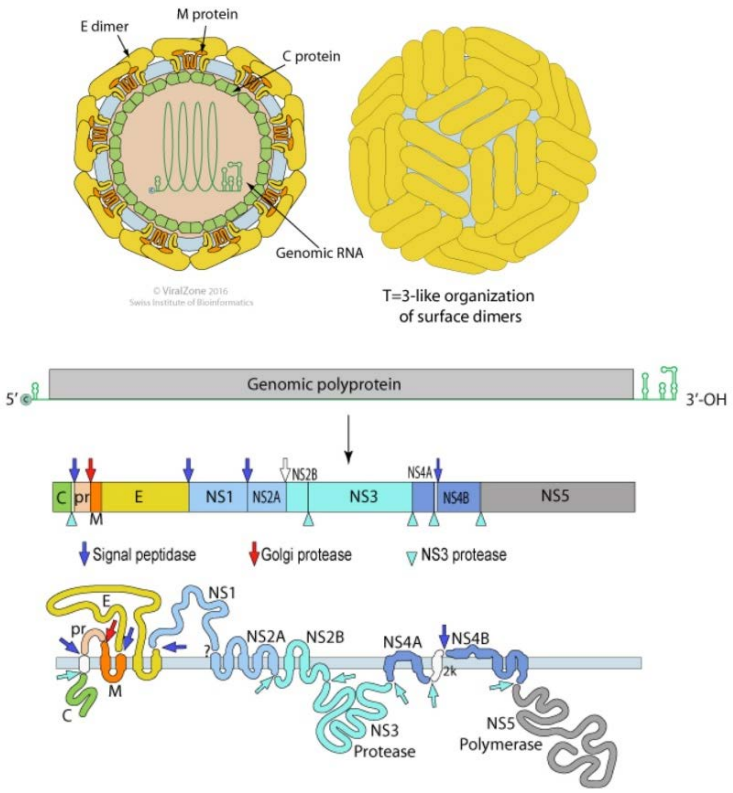

Figure 1. Schematic model of flavivirus virion and proteome. Mature flavivirus particles are composed of a tightly packed surface of 90 E homodimers that are organized in rafts of three parallel dimers. The virions contain two membrane proteins (M and E), while the capsid (C) surrounds the viral positive strand RNA. The virion RNA is infectious and serves as both the genome and the viral mRNA. A single polyprotein is translated and processed by host and viral proteases into three structural proteins (capsid (C), membrane (M), and envelope (E)) and seven non-structural proteins (NS1, NSS2A, NS2B, NS3, NS4A, NS4B, NS5). Picture obtained from ViralZone (www.viralzone.expasy.org), copyright of Swiss Institute of Bioinformatics ([SIB] Swiss Institute of Bioinformatics: ExPasy 2016).

Genomic sequences are useful for categorizing the various flaviviruses. Nucleotide sequence comparisons based on the polymerase (NS5) separate three major phylogenetic clades: mosquito-borne flaviviruses, tick-borne flaviviruses, and a group of flaviviruses with no known vectors (Cook *et al.* 2012; Kuno *et al.* 1998). Another distant group consists of flaviviruses that infect insect, but not mammalian cells (Blitvich and Firth 2015). However, insect-specific flaviviruses should not be overlooked as studies have

demonstrated that mosquitoes co-infected with insect-specific flaviviruses and human pathogenic flaviviruses have the ability to suppress or enhance viral replication (Blitvich and Firth 2015; Goenaga *et al.* 2015). Additional flavivirus associations can be made based on antigenic relatedness, vector of disease, symptoms of their causative disease, and the primary amplifying host (Gaunt *et al.* 2001; Troupin *et al.* 2017). The first subdivision includes JEV, WNV, SLEV, MVEV, and ROCV that are primarily carried by *Culex* species mosquitoes, with avian species serving as natural amplifying hosts. Infections with this group of viruses typically cause mild human disease, but are distinct from other flaviviruses in that severe forms of the disease lead to neurological symptoms of meningitis and encephalitis (de Barros *et al.* 2011; Schmaljohn and McClain 1996; Schweitzer *et al.* 2009). A second subdivision is comprised of viruses transmitted by *Aede*s mosquitoes, with primates as the primary amplifying host (Schmaljohn and McClain 1996). Severe infections with *Aedes*-borne flaviviruses manifest more as a multisystem or systemic disease that can include rash, hemorrhagic fever, arthralgia, and liver damage (Schmaljohn and McClain 1996). From this second group, there are three viruses that have a major global impact on human health: DENV serotypes 1-4, YFV, and ZIKV. However, it should be noted that current human ZIKV infections have not led to hemorrhagic fever, but instead have been linked to congenital microcephaly via *in utero* infections and Guillain-Barré syndrome in adults (Song *et al.* 2017). A third subdivision includes tick-borne flaviviruses that primarily cause neurological disease symptoms, with a small subset that can cause hemorrhagic fever (Yoshii *et al.* 2014). Tick-borne flaviviruses further divide into two distinct groups with either seabirds or rodents as the primary reservoir, with the possibility of a third evolutionarily distinct group containing Kadam virus (Grard *et al.* 2007). Seabird

tick-borne flaviviruses infect only seabirds, whereas mammalian tick-borne flaviviruses, which include Far Eastern, European, and Siberian strains of tick-borne encephalitis virus (TBEV), are a significant cause of human disease (Mansfield et al. 2009). Despite the availability of a licensed vaccine, TBEV subtypes account for more than 10,000 human infections annually in Europe and parts of Asia (Dobler 2010). Powassan virus (POWV) is the only tick-borne flavivirus that is reported in the United States (U.S.), and although the number of human infections has remained low, the number of reported known neuroinvasive cases has increased in recent years ([CDC] Centers for Disease Control and Prevention 2016; Ebel 2010). Overall, viruses within the mosquito and tick-borne flavivirus groups represent a significant threat to the public health by causing diseases that lead to a range in severity of symptoms from general malaise to death (Meltzer 2012). Further, flaviviruses are globally distributed, with many species co-circulating (Figure 2), thus confounding efforts to detect and diagnose current and past infections.

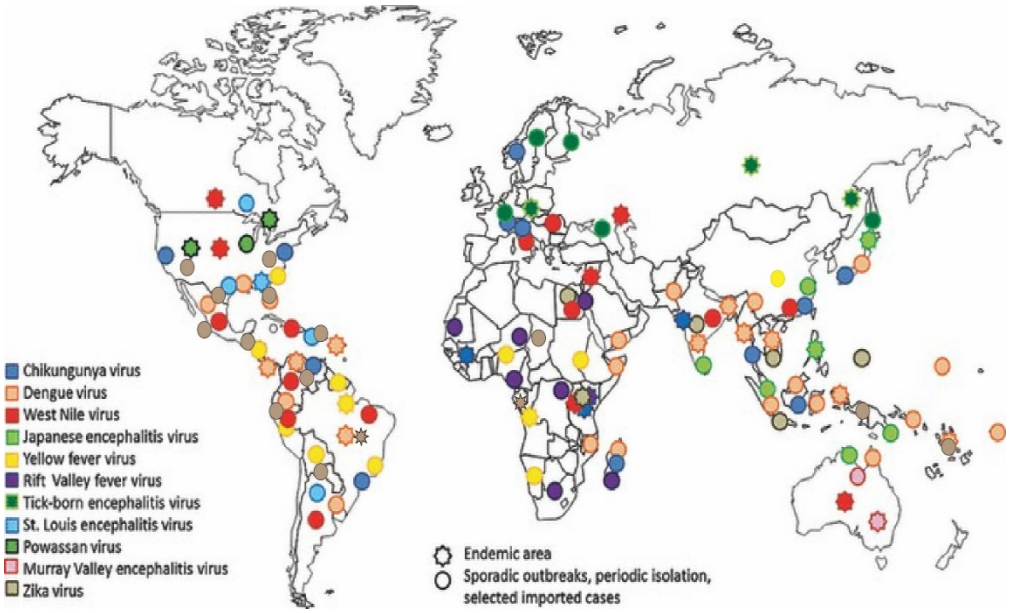

Figure 2. Geographic distribution of nine major human pathogenic flaviviruses. Map showing the extensive geographic distribution of nine flavivirus isolates, as well as co-circulating arthropod-borne viruses, Chikungunya virus and Rift Valley fever virus. The map was available from: (in document listed as "Figure 1") https://www.researchgate.net/publication/260870720_Dengue_virus_and_other_arboviruses_A_global_view_of_risks [accessed 1 Mar, 2018], and updated to include the rapid spread of ZIKV from 2012-2016, as well as the imported cases of YFV into China (Anez et al. 2012).

Mosquito-borne flaviviruses, JEV serogroup

Viruses within the JEV serogroup primarily circulate between *Culex* mosquitoes and birds, while in JEV outbreaks, pigs are a primary host for virus amplification. Humans, horses, and other livestock are readily infected with flaviviruses from this serogroup. JEV is endemic in 24 countries of Asia and the Western Pacific. Despite the availability of a licensed vaccine (SA 14-14-2) against JEV infections, there are approximately 68,000 clinical cases documented each year; with a case fatality rate as high as 30% among individuals with encephalitis ([WHO] World Health Organization 2015). JEV most often

affects young children, and is the primary cause of pediatric encephalitis in endemic areas ([CDC] Centers for Disease Control and Prevention 2013; Solomon et al. 2000).

While JEV has become fairly widespread, ROCV and MVEV have remained isolated to Brazil and Australia, respectively. Both viruses were responsible for large encephalitis outbreaks, and continue to be detected in both mosquitoes and reservoirs in endemic areas (Selvey *et al.* 2014; Silva *et al.* 2014). The geographic distribution of SLEV extends from Canada to Argentina, while the vast majority of human cases have occurred in the eastern and central U.S. ([CDC] Centers for Disease Control and Prevention 2017; Kopp et al. 2013). The largest U.S. epidemic of SLEV occurred in 1975, with 2,000 known infections, while major disease outbreaks may occur every five to 15 years ([CDC] Centers for Disease Control and Prevention 2017).

Although ROCV, MVEV, and SLEV outbreaks are sporadic, WNV is an example of the potential of an overlooked flavivirus to emerge rapidly in previously unaffected geographical areas and cause a significant number of disease cases. WNV was endemic to parts of Africa, Europe, Asia, and Australia; yet caused a low number of central nervous system disease outbreaks before its introduction into the U.S. in 1999 by migrating birds (Heinz and Stiasny 2012). After WNV appeared in New York City, it rapidly spread over the North American continent and subsequently to Central and South America. WNV is now the most widely distributed neurotropic flavivirus, as well as the primary source of vector-borne viral encephalitis in the U.S., with over 1,000 deaths occurring from WNV infection between the years 1999 to 2007 (Burakoff et al. 2018; Reimann et al. 2008). Unlike JEV, WNV most commonly affects the immunocompromised and elderly (Solomon and Winter 2004). Among patients who have developed severe neurological

symptoms due to WNV infection, more than half remain chronically infected and suffer from long-term sequelae (Murray *et al.* 2009). Due to the surge in the rate of infections and evidence of WNV transmission through blood transfusions in the U.S., blood collection agencies began screening measures for all blood donations in 2003 (Centers for Disease and Prevention 2003; Iwamoto *et al.* 2003). Despite research efforts and surveillance work, WNV continues to be a major global health concern. The most recent outbreak of WNV occurred in Greece from 2010 to 2011 and caused 197 human cases of West Nile neurovirulent disease with 17% of them leading to death (Danis et al. 2011a; Danis et al. 2011b).

Mosquito-borne flaviviruses, DENV serogroup

Viruses within the DENV serogroup circulate between *Aedes* mosquitoes and primates, but humans can also serve as primary amplifying host in urban outbreaks of DENV1-4, ZIKV, and YFV. Yellow fever virus was the first human pathogen that was confirmed to be transmitted by mosquitoes in the early 1900s (Reed et al. 1901). Despite the availability of an effective attenuated, live virus vaccine (17-D-204 or 17DD) since the 1930s, yellow fever remains a major public health problem for 47 countries in Africa, Central and South America. Vaccination is required for individuals over nine months of age who are living or traveling to areas where the risk of YFV transmission is high. Unfortunately, coverage in endemic areas is not high enough to prevent the continuation of outbreaks (Grobbelaar *et al.* 2016; Wasserman *et al.* 2016). In fact, there is only 1-40% coverage in Africa where yellow fever is most prominent, in comparison to 80-90%

vaccinations in South America (Monath 2001). Modeling studies based on data from Africa estimated that 127,000 persons annually on average become infected with symptomatic yellow fever leading to 44,500 deaths (Garske *et al.* 2014), and the number of yellow fever cases has recently increased. For example, severe outbreaks have occurred in regions of Africa and South America (Dec. 2016 - ongoing) that were relatively free of YFV for a number of years (Grobbelaar *et al.* 2016). There were over 3,000 reported cases from 2015-2016 and over 300 deaths reported in humans infected with YFV in Africa, with the vast majority of cases occurring in the capital of Angola. The ongoing YFV outbreak in Brazil has led to over 1,000 confirmed human cases, including over 400 deaths ([PAHO] Pan American Health Organization/[WHO] World Health Organization 2018). Further, the recent outbreaks in Angola and Brazil have renewed concerns about yellow fever disease, the production of the YFV vaccine, and the longevity of vaccine acquired immunity. More than 30 million doses of the yellow fever vaccine were distributed during the outbreaks in order to ensure protection and further transmission of the virus ([WHO] World Health Organization 2017c). However, emergency stockpiles were exhausted due to the number of vaccine doses that were dispatched, causing a global vaccine shortage (Gershman *et al.* 2017). There are continued concerns regarding replenishment of the vaccine stockpile before another large outbreak occurs due to the length of time (up to 6 months) it takes to produce the vaccine in pathogen-free embryonated chicken eggs ([UNICEF] United Nations International Children's Emergency Fund 2016; Barrett 2017; Monath et al. 2016). Furthermore, there are only four pre-qualified YFV vaccine manufacturers that are available and the vaccine can only be stored for two to three years ([UNICEF] United Nations International Children's Emergency Fund 2016). The vaccine shortage has also

raised questions about the longevity of acquired immunity to YFV and whether boosting may be necessary (Amanna and Slifka 2016). Furthermore, while the shortage prompted the World Health Organization (WHO) to permit fractional doses (ex. one fifth of standard dose) of the vaccine to be given in the interim, there are not sufficient data to ensure that the diluted dose will provide adequate lifelong protection ([WHO] World Health Organization 2016; Ahuka-Mundeke et al. 2018). Additionally, following the recent importation of 11 yellow fever cases into China there is a possibility that YFV could be introduced into new regions of Asia where competent vectors of disease exist and there are no current vaccination efforts (Agampodi and Wickramage 2013; Barrett 2017; Cui *et al.* 2017; Wasserman *et al.* 2016).

Dengue virus (DENV) is the leading cause of arthropod-borne viral disease in the world, infecting an estimated 390 million humans each year, with another 3.6 billion people at risk (Bhatt *et al.* 2013). Dengue disease is endemic in over one hundred countries within the equatorial zone of Asia, Africa, the Americas, and Australia ([CDC] Centers for Disease Control and Prevention 2014). Dengue virus is maintained in two distinct transmission cycles, an ancestral sylvatic cycle involving NHPs and mosquitoes and an urban cycle involving *Aedes* mosquitoes and humans. Although, the isolation of sylvatic strains in humans has been documented (Vasilakis et al. 2011), DENV is distinct from other flaviviruses in that the contribution of the sylvatic cycle in human viral infections is minimal since DENV is successfully maintained between mosquitoes and humans and does not require NHPs or other vertebrates for virus amplification (Whitehead et al. 2007). Though asymptomatic or dengue fever cases are more prevalent, there are four distinct DENV serotypes (DENV1-4) in circulation that can cause severe disease. Infection with

one serotype affords lifelong protection against the infecting serotype, while protection against heterologous DENV serotypes is temporary, only lasting a few months (Sabin 1952). Secondary dengue infection is a major risk factor for the more serious dengue hemorrhagic fever and dengue shock syndrome. Severe DENV infections can cause bleeding in the skin and gastrointestinal tract, capillary leakage, inability to form clots, liver damage, and death (Halstead 2007). The development of an effective vaccine against all four DENV serotypes has been complicated by the potential risk of enhancing the severity of disease. This is because the immune response following DENV infections has been hypothesize to both clear the virus, as well as enhance disease pathogenesis (Flipse and Smit 2015; Wan *et al.* 2013a; Wan *et al.* 2013b). One candidate, a live-attenuated tetravalent DENV vaccine (Dengvaxia ©) produced by Sanofi-Pasteur has been recently licensed in a few countries. However, variability in efficacy rates has been observed among serotypes and data has suggested that it seems to primarily benefit those with pre-existing DENV immunity (Aguiar *et al.* 2016; Guy *et al.* 2015; Hadinegoro *et al.* 2015).

ZIKV is closely related to both YFV and DENV, and was first isolated in 1947 from a non-human primate in Uganda (Dick *et al.* 1952). Since then, ZIKV was sporadically isolated from primates and *Aedes* mosquitoes, and was associated with a small number of human disease cases (<20 documented cases) in both Africa and Asia. Due to similar disease symptoms, ZIKV infections are commonly mistaken for DENV, malaria, or another mosquito-borne virus, chikungunya (Haddow *et al.* 2012). Recently ZIKV caused an extensive outbreak that spread to locations outside of Africa and Asia (Hayes 2009). The first large epidemic of ZIKV infection occurred on Yap Island of Micronesia in 2007 and then subsequently spread to French Polynesia and Oceania countries in 2013-

2014 where over 400 cases were confirmed through laboratory testing (Duffy *et al.* 2009; Lanciotti *et al.* 2008; Musso *et al.* 2014). ZIKV was reported in Brazil in 2015, causing a major epidemic that has since spread to surrounding countries in South America, as well as being introduced into the U.S. in 2016 (Florida and Texas) ([PAHO] Pan American Health Organization 2016; Barzon et al. 2016). The sudden emergence and rapid distribution of ZIKV to previously naïve regions, in combination with the urbanized *Aedes* vector highlights the reasons that ZIKV became a global public health emergency. ZIKV infection in humans usually manifests as a mild, febrile illness. However, deaths have been documented and autoimmune side effects such as Guillain-Barre syndrome, as well as congenital microcephaly via *in utero* infections have been observed in an unusually large percentage of those infected (Announcement: Guidance for u.S. Laboratory testing for zika virus infection: Implications for health care providers 2016; Cao-Lormeau et al. 2016; Cauchemez et al. 2016; Ioos et al. 2014; Mittal et al. 2017; Oehler et al. 2014; Weaver et al. 2016). Unlike DENV and YFV, hemorrhagic symptoms have not been seen in ZIKV infections, though co-infections with DENV have been documented (Dupont-Rouzeyrol *et al.* 2015; Lanciotti *et al.* 2008). Further, ZIKV can be sexually transmitted, whereas there is limited knowledge concerning sexual transmission of other flaviviruses. Guidelines for prevention of sexual prevention have been recommended for potential exposures due to the prolonged detection of ZIKV during infection, especially in semen (Foy *et al.* 2011; Mansuy *et al.* 2016; Paz-Bailey *et al.* 2017).

Tick-borne flaviviruses

Tick-borne flaviviruses circulate among small animals, mostly rodents, and are typically transmitted to humans after a bite from an infected *Ixodes* tick. Studies have shown that tick saliva contains active factors that aid in viral transmission and pathogenesis (Hermance and Thangamani 2015). Tick-borne flaviviruses can also be transmitted through the ingestion of infected milk or direct transmission from infected animals. Infection with tick-borne flaviviruses most commonly causes flu-like illness, with severe cases leading to encephalitis or death. Omsk hemorrhagic fever virus and Kyasanur forest disease virus are tick-borne flaviviruses that can cause hemorrhagic symptoms but have thus far been limited to areas of Siberia and south-western India, respectively (Yoshii *et al.* 2014). Despite the availability of an effective vaccine, TBEV is the most common and widespread tick-borne flavivirus in Europe and Asia, with an average 12,000 cases occurring annually (Dobler 2010). There are three subtypes of TBEV: European, Far Eastern, and Siberian. Although the three subtypes are genetically very similar, with less than 10% amino acid variability seen within the E protein, each one has a slight variation in disease phenotype (Ecker *et al.* 1999). Both the European subtype and the Far Eastern strains of TBEV are able to cause neurological disease, yet European TBEV disease is typically biphasic with a less than 2% fatality rate, whereas Far Eastern TBEV infection leads to a more gradual severe disease that causes up to 40% fatalities (Bogovic and Strle 2015). Less is known about the disease progression caused by the Siberian strain of TBEV; but it may be associated with a chronic form of disease with debilitating symptoms that include Parkinsonism, muscular dystrophy, and progressive nerve inflammation (Bogovic and Strle 2015). Another tick-borne flavivirus, POWV, also exists in eastern Russia and

is thought to have been introduced into this area recently from the U.S. where the virus is endemic (Leonova *et al.* 2009). Like TBEV, POWV circulates between *Ixodes* ticks and small mammals. POWV has an average of 10% case-fatality rate in individuals with neuroinvasive disease, while among those who have recovered, chronic symptoms such as muscle wasting, reoccurring severe headaches, memory loss, and paralysis are very common ([CDC] Centers for Disease Control and Prevention 2015; Gholam et al. 1999). Despite the low incidence of human infections, the severity of POWV infections along with the short amount of time it takes for ticks to transfer the virus, suggests that POWV may be an emerging disease of public health concern (Ebel and Kramer 2004; Hermance and Thangamani 2015).

Continued threat presented by flaviviruses

Birds and mammals are common reservoirs of most flaviviruses, while humans are typically considered dead-end hosts, since viremia levels are thought to be insufficient to infect feeding mosquitoes or ticks (Hollidge *et al.* 2010). Dengue virus is an exception to this as viremia levels are high enough in human infections that the virus can be efficiently transmitted between mosquitoes and humans without the need for an enzootic amplification host (Whitehead et al. 2007). Further, results from a recent study determined that asymptomatic DENV infected patients with low levels of virus were also able to transmit the virus to feeding mosquitoes (Duong *et al.* 2015). Additionally, mosquito and tick-borne flaviviruses can be maintained in nature through the overwintering of infected hibernating arthropods or through trans-ovarian transmission (Go *et al.* 2014). Flaviviruses

will continue to be dispersed into new geographic locations due to increasing human populations and travel, along with the changing environmental effects of global warming (Gould and Higgs 2009; Meltzer 2012; Weaver and Reisen 2010). Furthermore, viral mutations may lead to increased virulence, new strains, and vector-host transmission potentiality (Weaver and Reisen 2010).

Immune responses to flavivirus infection

The host immune defense mechanisms become activated by infection. Innate and cell-mediated immunity play critical roles in limiting and eradicating flavivirus infected cells, while antibodies are essential for restricting viral dissemination and host protection (Diamond 2003). Immediately after infection, flavivirus viral RNA is recognized by cellular pattern recognition receptors (PRRs) including Toll-like receptors. Recognition by the PRRs leads to the induction of the type I interferon system resulting in the expression of hundreds of interferon-stimulated genes (Elong Ngono and Shresta 2018). Interferon-stimulated genes directly affect steps involved in viral replication, as well as aid in T and B cell activation. In order to actively replicate and cause disease in vertebrate hosts, flaviviruses have evolved several mechanisms of immune evasion. For example, the DENV non-structural proteins NS2A/B, NS4, and NS5 have been found to mediate degradation of immune response transcription factors (STAT1/2) and cGAS-STING sensors that are vital to the proper functioning of the interferon signaling pathway (Elong Ngono and Shresta 2018). Other important contributors to the innate immune system include dendritic cells, monocytes, and macrophages that are sources of cytokines (ex. IL-6, IL-8, and TNF-α) and activators of adaptive immune response cells. Further, flavivirus

infected cells can be cleared from circulation by phagocytic cells and are detected by natural killer (NK) cells through antibody-dependent cellular cytotoxicity (ADCC).

Humoral immunity has an essential role in immunity to flavivirus infections. B cell deficient mice succumb to flavivirus infection despite other existing host immune mechanisms, whereas, passive transfer of flaviviral protein-specific polyclonal or monoclonal antibodies protected mice following flavivirus challenge (Diamond 2003; Diamond *et al.* 2003). Antibodies protect against flavivirus infections by direct blocking of receptor binding sites on the virus, antibody-dependent cell-mediated cytotoxicity (ADCC), antibody mediated complement activation, and Fc-receptor binding dependent phagocytosis.

Antibodies that bind to E and M virion surface proteins are a major source of virus neutralization and lifelong protective immunity (Barba-Spaeth *et al.* 2016; Colombage *et al.* 1998; Kaufman *et al.* 1989; Pincus *et al.* 1992). In particular for E, epitopes for antibody binding have been linked to each of the protein's domains (DI-III), and it is not clear if one domain is more critical than another in the protective antibody response to infection (Heinz and Stiasny 2012). Published results have suggested that while a large portion of antibodies are directed towards E-DII following infection, the majority are cross-reactive or poorly neutralizing (Beltramello *et al.* 2010). In contrast, antibodies against E-DIII were shown to be the most potent in mouse and *in vitro* studies (Beltramello *et al.* 2010; Chavez *et al.* 2010; Gromowski and Barrett 2007; Shrestha *et al.* 2010), but for unknown reasons lower populations of D-III specific antibodies have been observed in humans (Crill *et al.* 2009; Vratskikh *et al.* 2013; Wahala *et al.* 2009). Furthermore, other studies have suggested that some neutralizing human monoclonal antibodies do not bind to a single domain, but instead

bind to complex structure-dependent (expanding several domains, ex. hinge of D-I and D-II) epitopes on the virus surface (de Alwis *et al.* 2012; Fibriansah *et al.* 2015; Messer *et al.* 2014; Zhou *et al.* 2013). Protective antibodies are not only directed towards E or M, but may also involve NS1 and NS3 (Assenberg *et al.* 2009; Dai *et al.* 2016; Diamond 2003; Lazaro-Olan *et al.* 2008; Lindenbach 2007; Mackenzie *et al.* 1996; Matusan *et al.* 2001a; Matusan *et al.* 2001b; Roehrig 2003). Antibodies to the secreted protein NS1 (Avirutnan *et al.* 2007; Flamand *et al.* 1999) facilitate complement-mediated lysis and phagocytosis of infected cells, while antibodies to NS3 have been also detected (Avirutnan *et al.* 2010; Chuang *et al.* 2013; Churdboonchart *et al.* 1991; Diamond 2003; Fernandez *et al.* 2011; Muller and Young 2013; Valdes *et al.* 2000).

Flavivirus infections results in the production of both type-specific and cross-neutralizing antibodies. Additionally, the contribution of previous flavivirus infections to host responses towards new flavivirus infection is unclear. Some studies have shown that pre-existing flavivirus immunity aids in protection against future infections with antigenically related flaviviruses, while disease-enhancing activity of cross-reactive antibodies generated during previous infection with heterologous viruses has also been reported (Dejnirattisai *et al.* 2016; Saito *et al.* 2016; Tesh *et al.* 2002; Xiao *et al.* 2003). For DENV, which circulates in four serotypes, it is well established that secondary DENV infections with a heterologous serotype (different serotype of primary infection) can lead to severe disease (ex. hemorrhagic fever, capillary leakage, and dengue shock syndrome) as a consequence of adverse immune responses (Halstead *et al.* 1976; Halstead *et al.* 1983; Kliks *et al.* 1988; Russell *et al.* 1967). Several studies have suggested that the increased disease severity and viral load following secondary infection is due to antibody-dependent

enhancement (ADE) (Halstead 1979; 1988; Ng et al. 2014). This theory is based on the presence of poorly neutralizing or low levels of neutralizing antibodies following primary infection. Complexes of sub-neutralizing antibodies and flavivirus particles bind to Fcγ receptors on cells such as macrophages or dendritic cells facilitating viral uptake and subsequent replication. Antibody-dependent enhancement presumably leads to higher virus loads and longer duration of viremia, as well as consequential disease burden to host cells and tissues (Elong Ngono and Shresta 2018; Sun and Kochel 2013). However, several other studies have suggested that increased severity following secondary infection with a heterologous flavivirus is far more complicated and involves multiple immune interactions. For example, *in vitro* assays have shown that the addition of complement to non-neutralizing antibodies eliminated ADE, while immune complexes that trigger imbalanced innate immune responses have also led to increased disease severity (Laoprasopwattana et al. 2005; Mehlhop et al. 2007). Further, "original antigenic sin" has also been suggested to lead to increased disease severity following an active secondary infection. The original antigenic sin theory proposes that T or B cells that undergo clonal expansion following a primary infection can inappropriately dominate the response to secondary heterotypic infection, resulting in immune responses that have lower affinity to the current infecting virus leading to inadequate viral clearance and increased proportions of immune dysregulation (Halstead et al. 1983; Mangada and Rothman 2005). While there is a higher risk of more severe disease from secondary DENV infections, the extent of disease enhancement due to preexisting flavivirus immunity (disease or vaccination) in other human flavivirus diseases, such as ZIKV or YFV infections, is not well understood (Dejnirattisai *et al.* 2016; McCracken *et al.* 2017).

Serological assays for surveillance and diagnosis of flavivirus infection

Laboratory confirmation is essential to diagnosis, as similar clinical disease manifestations (ex. fever, rash, headache, and arthralgia) are not only seen amongst flaviviruses, but also in other febrile illnesses such as chikungunya (another mosquito-borne disease in the *Alphaviridae* family) and malaria that occur in flavivirus endemic locations. Detection of viral RNA based on real-time polymerase chain reaction (RT-PCR) is highly specific, but timing can be a limiting factor (Hobson-Peters 2012). Clinical symptoms of flavivirus infection usually appear 2 to 14 days after infection, starting as mild flu-like illness with fever, headache, and fatigue. Because many patients do not seek medical attention immediately, the detection of circulating virus or viral RNA in the blood can be extremely difficult since viremia levels in humans usually subside within 5 days after onset of disease symptoms (Gubler et al. 1981; Lanciotti et al. 2008; Vaughn et al. 2000). Following medical evaluation of symptoms, diagnosis is generally accomplished through the use of antibody-based serological assays, and confirmed by isolating circulating virus or detecting viral RNA (Guzman and Kouri 2004). Anti-flavivirus immunoglobulin M (IgM) antibody titers are most commonly observed in the acute phase of disease and are detectable by serological assays around day five (+/-two days) post symptom onset and decrease to undetectable levels around day 60-90 post disease onset (Busch et al. 2008). Similar to the kinetics observed with IgM, virus-specific immunoglobulin A (IgA, mostly isotype I) rises quickly after infection, but decreases to undetectable levels in patient serum within a few months (De Decker *et al.* 2015; Groen *et al.* 1999). Although IgA has been suggested to be a valuable serological marker of acute disease (De Decker *et al.* 2015), IgA is predominant in mucous membrane secretions and

is not routinely used for surveillance of flavivirus infections. While, the above mentioned antibody kinetics are common for the majority of flavivirus infections (Figure 3), the persistence of virus-specific IgM and IgA has been demonstrated in serum of WNV infected patients six months after disease onset (Prince *et al.* 2005; Roehrig *et al.* 2003). Immunoglobulin G (IgG) emerges after IgM and IgA about one week after onset of symptoms, peaks around days 14-28 days, and establishes lifelong titers following disease convalesce (Busch *et al.* 2008; Hobson-Peters 2012; Prince *et al.* 2005).

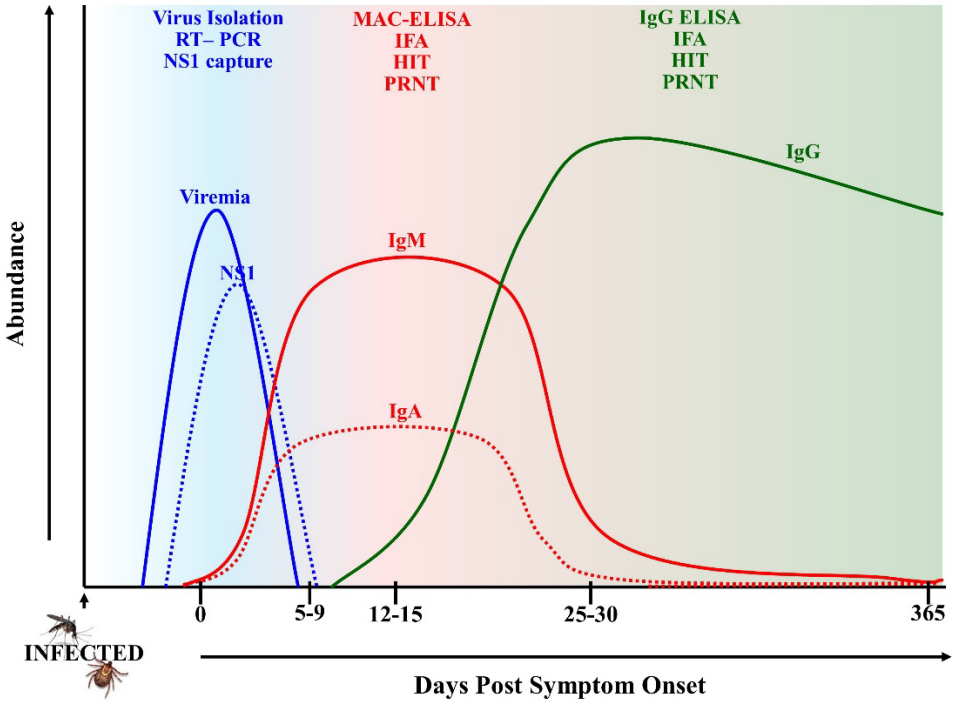

Figure 3. Immune response to a primary flavivirus infection with timing of diagnostic tests. Shortly after flavivirus infection, mature virions and secreted NS1 protein enter the bloodstream and peak around the time of symptom onset (ex. fever/rash). Virus can be directly isolated, but more commonly quantitative real-time PCR (RT-PCR) and NS1 capture assays are used in the acute phase of disease. Viral RNA (blue solid line) and secreted NS1 protein (blue dashed line) in the serum may be detected by real-time polymerase chain reaction (RT-PCR) and NS1 antigen capture assays, respectively, starting a few days before symptom onset until 5-9 days post-onset (ex. fever, rash). Anti-flavivirus IgM antibodies (red solid line) typically peak around 9-15 days post-symptom onset with a gradual decline thereafter. Commonly used assays for IgM detection include, IgM antibody capture-enzyme linked immunosorbent assay (MAC-ELISA), hemagglutination inhibition assay (HIT), or indirect immunofluorescent assay (IFA). Immunoglobulin A (IgA) capture ELISAs can be used to detect IgA antibodies (red dashed line) in the serum shortly after IgM, but are not commonly performed for the diagnosis of flavivirus infections. Flavivirus-specific IgG antibodies (green line) develop shortly after IgM and IgA and gradually rise, peaking at 20 to 30 days post-symptom onset with lifelong titers thereafter. Common methods for IgG detection include indirect-ELISAs, IFA, and HIT. Plaque reduction neutralization tests (PRNT) measure the amount of neutralizing antibody titers in patient serum and can be performed in either the acute or convalescent phase of disease.

It is important to note that antibody dynamics observed during primary flavivirus infections differs substantially from secondary infections (Figure 4). Specifically, virus-specific IgM titers are significantly lower in secondary infections, sometimes below detectable levels. In contrast, production of IgG is significantly more robust and can be measured within the first few days of disease onset to distinguish between primary and secondary infections (Guzman and Kouri 2004; Innis et al. 1989). Further, the concept of original antigenic sin is relevant in secondary infections in that IgG responses may become inappropriately elevated against the primary infecting strain (Halstead et al. 1983; Lanciotti et al. 2008).

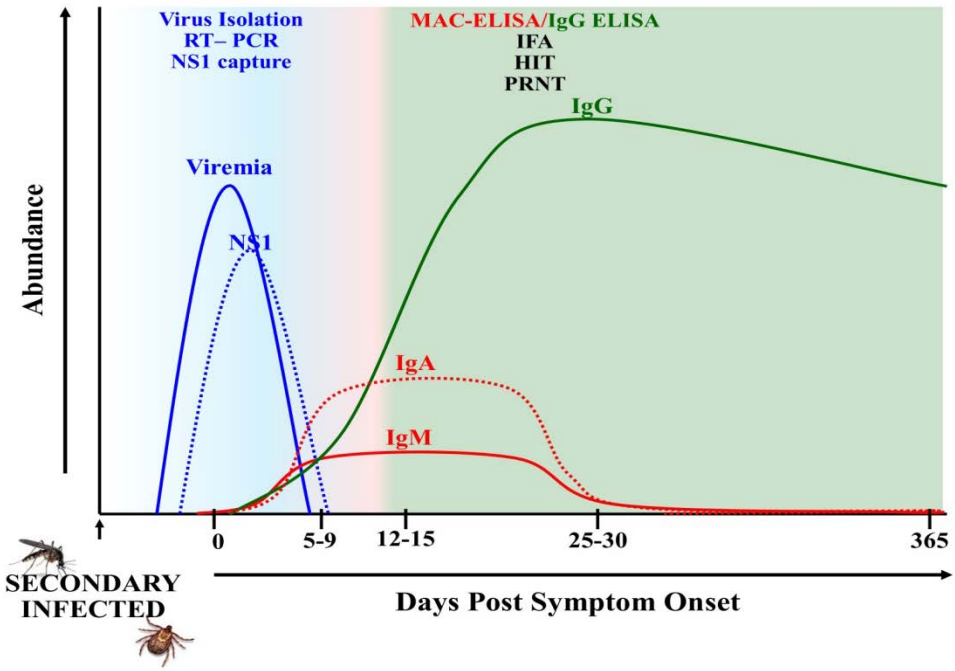

Figure 4. Immune response to a secondary flavivirus infection with timing of diagnostic tests. Infection with a heterologous flavivirus (secondary infection) leads to significant changes in antibody dynamics compared to primary infections. Specifically, IgM antibodies (solid red line) are significantly lower, sometimes undetectable in serological assays, whereas IgG antibodies (green line) are significantly higher and detected shortly after disease onset.

Viral plaque reduction neutralization tests (PRNT), enzyme-linked immunosorbent assays (ELISA) that detect IgM and IgG specific to flavivirus, and indirect fluorescence assays (IFA) are commonly used serological methods for detection and surveillance of flavivirus infections (Hobson-Peters 2012) (Figure 3 and 4). The PRNT measures the amount of neutralizing antibody against a specific flavivirus that may be present in a suspected patient's serum. Although commonly used in serological diagnosis, PRNTs are low throughput, require days for completion and multiple tests for various flaviviruses, and require handling of live virus that may require high level biosafety containment laboratories (Hobson-Peters 2012). While, ELISAs and IFA can differentiate IgM and IgG, neither are not suitable for rapid-point of care testing because of the difficulty in eliminating cross-reactivity between closely related and possibly co-circulating flaviviruses (Hobson-Peters 2012). In addition, prior flavivirus infection or vaccination against one or more flaviviruses (ex. JEV, YFV and TBEV vaccines) complicates the determination of serological specificity in diagnostic assays. A recent study showed that interpretation of virus neutralization assay is challenging for humans vaccinated with TBEV and JEV because of antibody cross-reactivity for DENV, WNV, and a species of the TBEV subgroup (Mansfield *et al.* 2011). Because timeliness, sensitivity, and specificity are critical in diagnosing flavivirus infections, a multiplex serological assay that takes into account the ability to test several viruses or flaviviral antigens simultaneously would be advantageous (Cleton *et al.* 2015; Kang *et al.* 2012). The use of recombinant flavivirus antigens rather than whole virus was shown to increase specificity in ELISA assays (Beasley *et al.* 2004; Kuno 2003). However, there has not been clear evidence to suggest that a single antigen can provide both the required specificity and sensitivity for every case.

The E protein was shown to be an immunodominant antigen in antibody neutralization studies, especially epitopes within domain III, but there is substantial amino acid homology between and within serogroups that may give rise to antibody cross-reactivity (Chabierski *et al.* 2014; Chavez *et al.* 2010; Kuno *et al.* 1998; Mansfield *et al.* 2011).

The NS1 protein is another important antigen that is produced in both membrane-associated and secreted forms (Akey *et al.* 2014; Muller and Young 2013). Due to high levels of secreted NS1 in the serum of flavivirus-infected subjects, serological assays have been developed for the detection of viral NS1 (Alcon et al. 2002; Chung and Diamond 2008; Gowri Sankar et al. 2014; Hermann et al. 2014; Singh et al. 2010). However, antibody-capture of soluble NS1 is limited to the acute phase of the disease (1-9 days after infection) due to the interference of NS1-immune complexes later in disease (Gowri Sankar *et al.* 2014; Hermann *et al.* 2014). Although, some studies have shown high antibody specificity to NS1 in serological assays, others have demonstrated problems with cross-reactivity and limited detection of anti-NS1 antibodies in late phase samples (Cleton *et al.* 2015). The specificities of antibodies interacting with NS1 are likely to be affected by a balance of surface features that are conserved among flaviviruses as well as the diverse electrostatic characteristics (Song *et al.* 2017).

While the pM protein acts as a chaperone for the proper folding of E, the precursor peptide is cleaved from M during virion maturation resulting in M and E on the surface of mature virus particles (Smit et al. 2011; Stadler et al. 1997). However, the proteolytic cleavage of furin is inefficient and a portion of non-cleaved protein remains on released virus particles (Rodenhuis-Zybert et al. 2011; van der Schaar et al. 2007). Some studies

have suggested a positive correlation of the abundance of anti-pM antibodies and the severity of flavivirus infection (Dejnirattisai et al. 2016; Rodenhuis-Zybert et al. 2010). Studies have also shown that pM may be used to distinguish DENV and JEV infections in humans by Western blot assays, but extensive serological testing of human sera samples has yet to be accomplished (Cardosa *et al.* 2002; Gowri Sankar *et al.* 2014; Hua *et al.* 2010). Further, past results have demonstrated that the detection of antibodies against multiple flavivirus proteins provide better differentiation between flaviviruses (Gowri Sankar *et al.* 2014). Due to these factors, the incorporation of multiple flaviviral antigens on a single platform would be beneficial in allowing a more precise profile of an individual's immune response to be observed in either acute or convalescent phase samples.

Protein Microarrays

Protein microarrays provide the surface area for thousands of different proteins to be immobilized onto a single slide. Due to this, numerous applications can be utilized for high-throughput discovery of novel biomarkers, detection of protein-protein interactions, and analysis of immune responses to infectious diseases or vaccination, and other interaction assessments with various protein binding analytes (ex. peptides, carbohydrates, etc.) (Chandra *et al.* 2011; Natesan and Ulrich 2010; Sundaresh *et al.* 2007; Tomizaki *et al.* 2010). In recent years scientists have strived to understand infectious diseases in a high-throughput, comprehensive, and accurate manner so that biomarkers of disease may be discovered. Biomarkers not only provide insight into the infectious disease of interest, but they also provide diagnostic capabilities and an understanding of immune responses.

Identifying proteins that are associated with immune responses is essential for the development or testing of vaccines and therapeutics (Natesan and Ulrich 2010; Sundaresh *et al.* 2007). Gene specific primers designed from genomic sequences can be used to amplify the gene of interest or create synthetic genes to perform molecular cloning techniques leading to the production of recombinant proteins for assembling microarrays. Once recombinant proteins are produced, they can be printed onto a protein microarray surface. Protein structures and function are often maintained for proteins that are immobilized on the microarray surface (Keasey et al. 2009; Natesan and Ulrich 2010; Tomizaki et al. 2010). Furthermore, high-throughput capabilities of protein microarrays have allowed for high reproducibility and decreased in production costs for assays that require only small amounts (1-2 µL) of serum analyte protein microarray development (Natesan and Ulrich 2010; Tomizaki et al. 2010). A microarray consisting of bacterial or viral proteomes can be probed with vaccinated or infected host serum to detect specific antibody binding events (Figure 5). Biomarkers of disease immunity can be discovered by detection of infected or vaccinated antigen-antibody interactions for comparison to non-infected or non-immune individuals allows for biomarkers of disease or immunity to be discovered. Reliable biomarkers are essential for the evaluation of vaccine and therapeutic efficacy, and can lead to new diagnostic tests (Natesan and Ulrich 2010; Sundaresh *et al.* 2007).

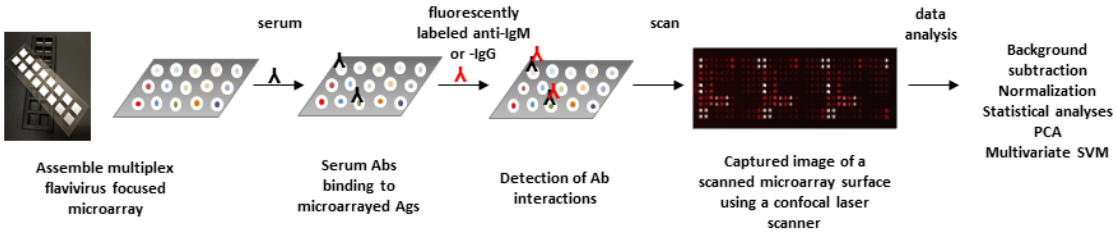

Figure 5. Schematic of a flavivirus-focused microarray used as an assay to detect disease-specific antibodies from sera of infected patients. Recombinant proteins and whole viruses were deposited by ink-jet printing on microarray surfaces coated with a thin layer of nitrocellulose. The interactions of antibodies from biological samples with the microarrayed antigens were quantified by probing with fluorescently-conjugated species-specific immunoglobulins, scanning the surface with a confocal laser scanner, and capturing the image for data processing. Statistical analysis of assay results allowed for identification of proteins that were significantly recognized by antibodies within and across study groups.

Antibody responses and protein microarrays

Results from protein microarray assays can be used to evaluate the efficiency of newly manufactured vaccines and therapeutics, as well as to greatly improve overall knowledge of infectious diseases. Previous studies from our laboratory have used protein microarrays to examine antibody responses to pathogenic bacteria and viruses. Keasey *et al.* (2009) developed a protein microarray that comprised approximately 70% of the proteome from the plaque bacterium, *Yersinia pestis (Y.pestis)* (Keasey *et al.* 2009). Results from the *Y. pestis* protein microarray assays identified plague-specific antibody interactions as well as those that were cross-reactive or specific towards other gram-negative pathogens such as *Burkholderia mallei*, *Pseudomonas aeruginosa*, *Salmonella typhimurium*, and *Escherichia coli (E.coli).* In addition, our laboratory group previously published a report that employed a vaccinia virus (VACV) protein microarray to compare immune responses of individuals to vaccination with the newly licensed smallpox vaccine,

ACAM2000, to the previously licensed Dryvax vaccine (Pugh *et al.* 2014). In the VACV study, I observed robust antibody responses to 21 individual VACV proteins in all smallpox vaccinated individuals, compared to the naive, while 11 proteins distinguished ACAM2000 vaccination from the polyclonal smallpox vaccine, Dryvax (Pugh *et al.* 2014). Other scientists have used protein microarrays to study infectious diseases by probing protein microarrays with serum from infected patients. For example, Sundaresh *et al.* (2007) developed a protein microarray that consisted of key antigens from the *Francisella tularensis* proteome, which was probed with sera from 46 individuals in the U.S. that were diagnosed with the disease tularemia as well as 54 healthy control patients to detect *F.tularensis* disease biomarkers (Sundaresh *et al.* 2007). In another example, Natesan *et al.* (2016) used a microarray that consisted of recombinant proteins and whole virions from six species of filoviruses in order to examine antibodies of humans that survived Ebola and Marburg virus infections. Results from the filovirus microarray detected robust antibody responses to the recombinant proteins of the infecting species 14 years after infection with some level of cross-reactivity observed to other filovirus antigens. Further, the results also suggested that recombinant proteins were better at distinguishing specific filovirus antibodies than whole virus preparations (Natesan *et al.* 2016).

My thesis

The research presented here involved the development of a protein microarray comprising whole virus preparations and recombinant proteins (E, E-DIII, pM/M, NS1, and NS3) from a large panel of human pathogenic flaviviruses. This platform was employed as a comprehensive serological assay to detect specific and cross-reactive antibody responses to DENV1-4, ZIKV, WNV, and YFV infections, as well as to evaluate vaccine induced antigen-specific immunity over time in YFV vaccinated subjects.

MATERIALS AND METHODS

Cloning and expression of recombinant proteins

Viral RNA for preparation of protein-expression plasmids were obtained from the following sources: American Type Culture Collection© (DENV1-4), Integrated BioTherapeutics, Inc. © (YFV and Japanese encephalitis virus (JEV)); NIAID-World Reference Center for Emerging Viruses and Arboviruses (Dr. Robert Tesh) (St. Louis encephalitis virus (SLEV), WNV, and rocio virus (ROCV)). The cDNA templates of E, NS1, and pM genes were produced by reverse transcription of full-length viral RNA by using 50 μM Oligo$(dT)_{20}$ primers and the SuperScript® III Reverse Transcriptase First-Strand Synthesis System (Life Technologies). ZIKV genes (E, NS1, pM) and E genes from Murray Valley encephalitis virus (MVEV), Powassan virus (POWV), and tick-borne encephalitis virus (TBEV) were synthesized (gblocks®, Integrated DNA Technologies, Inc; GeneStrings, Life Technologies), with codon optimization for expression in *Escherichia coli* (*E.coli*). Synthesized genes and cDNA were used as templates in PCR amplification reactions (50 μL total) with gene specific primers (final 2.5 μM conc.) and 2X Phusion High-Fidelity PCR master mix with HF buffer (New England BioLabs Inc.®) (Table 1). PCR amplified genes were purified using QIAquick spin column PCR purification kit (QIAGEN). NS1 and pM were produced as full-length open reading frames (ORFs), and E genes were truncated to exclude transmembrane domains, as predicted by analysis of amino acid sequences using TMHMM Server v.2.0 (Center for Biological Sequence analysis) (Krogh *et al.* 2001; Sonnhammer *et al.* 1998). Purified DNA were TOPO® cloned into the pENTR™/TEV/D-TOPO® vector (Gateway® Technology, Life Technologies™). Sequence-verified entry clones were shuttled into expression vectors by

recombination reactions using LR clonase II (Life Technologies). Specifically, the DENV 1-4 NS1, YFV-pM, JEV-pM, and ZIKV-MR766-pM ORFs were shuttled into an N-terminal His-maltose-binding protein (HisMBP) tagged vector (Nallamsetty *et al.* 2005), while all other flaviviral ORFs were shuttled into the N-terminal 6XHis tagged pDEST17 (Life Technologies). All flavivirus constructs were expressed in *E. coli* BL21 (DE3), propagating bacteria in media containing Luria broth (300 ml) supplemented with 100 μg/ml ampicillin and 0.1% glucose. Proteins were induced at mid-log phase with 1 mM isopropyl-beta-D-thiogalactopyranoside (IPTG, EMD Chemicals). Induction conditions were optimized for each protein, and bacteria were grown at either 30ºC (2-4 h) or 18ºC (12 h) prior to harvest by centrifugation. Bacterial pellets were lysed in B-PER reagent (Thermo Scientific) containing EDTA-free 3x Halt™ Protease Inhibitor Cocktail (Thermo Scientific), 0.2 mg/ml lysozyme, 250 U DNase I (Thermo Scientific), and 1 mM IPTG. Protein expression was analyzed by SDS-PAGE (Bio-Rad) followed by Coomassie stain, and Western blot using a mouse anti-His-HRP conjugated polyclonal antibody (Abcam).

Table 1. Sequence and primer information for the PCR amplified genes used for the production of recombinant flavivirus antigens.

Virus	Gene	GenBank Polyprotein Accession Number	Protein sequence	Forward primer (5'-3')	Reverse primer (5'-3')	Amino acid substitutions
ZIKV (str.SPH2015)	E	ALU33341	291-744	CACCATCCGGTGCATAGGTGTTTCG	TCATTTAAAGGCGGCTCCGAAGATTTG	
	NS1		796-1148	CACCGTGGGCTGTTCAGTCGAC	TTAAGAACCCGCTGTAACCATTGAACGCAC	
ZIKV_AS (str.YAP)	E	ACD75819	291-744	CACCATTCGTTGCATCGGCGTG	TTATTTAAAGGCTGCGCCAAAGATCTG	
	E-DIII		591-693	CACCAAAGGCGTAAGCTACTCA	TTAGCTGCGATGCCAATGATG	
	pM		126-290	CACCACGCGGCGCGGTTCAGCATA	TTAACTATACGCCGGAGCGATGAGCAG	
	NS1		796-1148	CACCGTGGGGTGTTCAGTTGAT	TTAAGAACCCGCCGTGACCAT	
ZIKV (str. ArD_41519)	E	AEN75266	291-744	CACCATTCGGTGCATAGGGGTCAGC	TCATTTAAACGCAGCTCCGAAAATCTGATG	
ZIKV (str. ARB7701)	E	AHF49785	291-744	CACCATTCGTTGCATTGGTGTTAG	TTATTTGAAGGCTGCACCAAAAATCTGATGCAC	
ZIKV_AFR (str.MR-766)	E	AAV34151	291-740	CACCAAAGGCGTTAGCTATAGT	TTATTTAAATGCGGCGCCGAAAATCTG	
	E-DIII		587-689	CACCAAGGGCGTGTCATATTCC	TTATGAACGATGCCAATGGTGCGT	
	pM		126-290	CACCACTCGCCGCGGGTCA	TTAGGAATACGCCGGTGCGATCAG	
	NS1		792-1144	CACCGTCGGCTGTAGCGTC	TTAAGAGCCAGCCGTAACCATACT	
DENV1	E	AIU47321	281-722	CACCATGCGGTGCGTGGGAATA	TTAAGTTCCAAAGATCTGGTGTAC	T441I, E483G,T506R,Q514E
	E-DIII		579-677	CACCTATGTGATGTGCACAGGCTCATTC	TTAGCTGCTTCCTTTCTTGAACCAGCT	
	M		206-279	TCCGTCGCACTGGCACCACAC	GGCCATGGATGGAGTTACCAG	T250I
	NS1		776-1126	GACTCGGGATGTGTAATCAAC	TGCAGAGACCATTGACTTAAC	G880R
	NS3		1476-2093	TCAGGAGTGCTATGGGACACACCC	TCTTCTTCCTGCTGCGAACTC	GSVEAF1796-1801RIGGGL, Q2081L
DENV2	E	AAC59275	281-722	CACCATGCGTTGCATAGGAATATCA	TTATGCTCCGAAAACTTGGTGGAG	P331S,E407K,V421I,V445I
	E-DIII		575-675	CACCAAAGGAATGTCATACTCTATGTGC	TTATCCTTTCTTAAACCAGTTGAGCTT	
	M		206-279	TCAGTGGCACTCGTTCCACATGTG	TGTCATTGAAGGAGTGACAGC	
	NS1		776-1127	GATAGTGGTTGCGTTGTGAGC	AGCTGTGACCAAGGAGTTGAC	A1127S
	NS3		1476-2092	GCCGGAGTATTGTGGGATGTT	CTTTCTTCCGGCTGCAAATTC	SIAA1768-1771GMGV, G1773R, GE1782-1783VK
DENV3	E	AAA99437	281-722	CACCATGAGATGTGTGGGAGTAGGA	TTAGTAAGCACTCCCAAATATTTGG	K571E
	E-DIII		574-672	CACCGGGATGAGCTATGCAATGTGC	TTACTTCTTGTACCAGTTGATTTTCAG	R671K
	M		206-279	TCAGTGGCGTTAGCTCCCCAT	TGTCATGGATGGGGTGACCAGCAT	
	NS1		774-1125	GACATGGGGTGTGTCATAAAC	CGCTGAGACTAAAGACTT	A1125S
	NS3		1474-2091	TCCGGCGTTTTATGGGACGTA	CTTTCTGCCAGCCGCAAA	T1593A, G1606R, M1709L, VP1749-1750GS, V1845D, I1892K,K1955N
DENV4	E	AAX48017	280-721	CACCATGCGATGCGTGGGAGTG	TTAACTACCAAAAACCTGGTGTAC	D374A,P436S,N437S,L681F
	E-DIII		574-676	CACCAAGGGAATGTCATACACGATGTGC	TTAGGAACTCCCTTTCCTGAACCAATG	F636L
	M		205-278	TCAGTAGCTTTAACACCACATTCA	TCCGTAGGATGGGGCGACCAG	
	NS1		775-1125	GACATGGGTTGTGTGGCG	GGCCGTCACCTGTGATTT	E825K
	NS3		1474-2091	TCAGGAGCCCTGTGGGAC	CTTCCTTCCACTGGCAAACTC	T1747N,F1787L,S1908L
WNV	E	YP_001527877	291-741	CACCTTCAACTGCCTTGGAATGAGCAAC	TTAGCGGAATGCTCCTCCGAACACTTG	L571F
	E-DIII		586-705	CACCCAGTTGAAGGGAACAACCTATGGC	TTACGCTCCTTTGAGGGTGGTTGT	
	pM		124-290	CACCGTTACCCTCTCTAACTTCCAAGGG	TTAGCTGTAAGCTGGGGCCACCAA	
	NS1		792-1143	CACCGACACTGGGTGTGCC	AGCATTCACTTGTGACTGCAC	V1076A
YFV	E	AFR54324	286-728	CACCGCTCACTGCATTGGAATT	TTACTGAAAGGCAGAGCCAAACAC	
	E-DIII		573-683	CACCTCAGCTTTGACACTCAAGGGG	TTACTTTCCTATTGAGCTTCCCTC	
	pM		122-285	CACCGTGACCTTGGTGCGGAAAAAC	TGAGTAGGCCGGACCAACAGC	
	NS1		779-1130	CACCGATCAAGGATGCGCCATCAAC	AGCTGTAACCCAGGAGCGCAC	
	NS3		1485-2107	AGTGGGGATGTCTTGTGGGAT	CCTCCTACCTTCAGCAAACTTAAT	
JEV	E	AAK11279	299-744	CACCTTTAATTGTCTGGGAATGGGC	TTATCTGAAGGCATCACCAAACACTTG	
	E-DIII		586-696	CACCGACAAACTGGCTCTGAAAGGC	TTACGTGCTTCCAGCTTTGTGCCAATG	
	pM		128-294	CACCATGAAGTTGTCGAATTTCCAG	TTAACTGTAAGCCGGAGCGACCAAC	
	NS1		795-1146	CACCGACACTGGATGTGCCATTGAC	AGCATGAACCTGTGATCTGACGAG	N876D
SLEV	E	ABN11832	289-739	CACCTTCAACTGTTTGGGAACATCA	TTACCTAAATGCTCCTCCAAAAAC	
	E-DIII		587-692	CACCGGAACGACATATGGTATGTGTGAC	TTAAATGCTGCTTCCCTCTTTGTG	
	pM		122-288	CACCTTGCAGTTATCAACCTATCAGGGG	TTAGCTGTATGCCGGAGCAATCAG	
	NS1		790-1145	CACCGATTCGGGATGTGCAATT	AGCTGTCACTCGAGATTTCAC	
MVEV	E	NP_051124	293-743	CACCTTTAATTGCCTGGGTATG	TTAACGAAATGCACCACCAAAAACCTG	
	E-DIII		590-698	CACCAAAGGAACCACTTATGGGATG	TTATTTGCCAATTGAACTACCCTC	
	M		218-292	CACCTTAAAGCTTTCCACCTTCCAGGGC	CTCGTTGCTCCTGCCTACAGTTAA	
	NS1		794-1145	CACCGATACCGGTTGTGC	TTATGCCTGAACACGGCTTTTAAC	
ROCV	E	ATG32103	286-736	CACCATCAACTGCTTGGGTGTGACC	TTATCTAAACGCTCCTCCGAAGAG	
	E-DIII		583-691	CACCAAAGGGTCAACATACCTGATGTGC	TTAGCTCCCGATCACACTACCAGA	
	pM		119-285	CACCCTGCGCCTGGGGACATATCAA	TTAGCTGTAGGCTGGGGCTATCAG	K165N
	NS1		788-1142	CACCACAGGATGCGCGATTGAC	TCCGGTCCCAGCTGTCACTTT	
	NS3		1498-2116	CACCGGTGGTGTTCTGTGG	GCGCTTCCCCGCCGCAAATTC	S1665H, T1722S
POWV	E	NP_620099	279-725	CACCACTCGCTGTACACACCT	TTAGTTAAATGCGCCGCCGAG	
	E-DIII		578-673	CACCAAAGGGACGACGTACAGTATG	TTATTGAAACCACTGCTGTGACAG	
	pM		111-278	CACCATGGCGATGGCTACCAC	TCACGCGTACACAGGACCCAG	
	NS1		776-1128	CACCGATTACGGCTGCGCAAT	TTACGCAACGACCATAGAACG	
TBEV_E (str. SOFJIN-HO)	E	BAB72162	281-726	CACCTCACGTTGCACACATCTG	TTAATTAAACGCACCACCGAGTAC	
	E-DIII		580-675	CACCAAGGGCCTGACGTATACG	TTATTTCTGAAACCACTGGTGGCT	
	pM		113-280	CACCATGACCTTGGCAGCGACG	TCAAGCGTATACCGGAGCCAGGCA	
	NS1		777-1128	CACCGATGTTGGTTGTGCG	TTACGCGACCACCATTGAGCG	
TBEV_EUR (str.NEUDOERFL)	E	NP_043135	281-726	CACCAGCCGTTGTACTCATCTG	TTAATTGAAAGCTCCGCCAAGCAC	
	E-DIII		580-675	CACCAAAGGCTTAACCTACACAATGTGT	TTATTTCTGAAACCACTGATGAGACAG	
	pM		113-280	CACCGTGACTCTGGCAGCG	TCATGCGTAGACCGGCGC	
	NS1		777-1128	CACCGACGTGGGTGGTGCCGTT	TTAAGCCACCACCATGCTCCGGAT	

Purification of viral recombinant proteins

With the exception of YFV-pM, all recombinant proteins expressed primarily in the insoluble protein pellet. Soluble expressed YFV-pM, was affinity purified on an NGC™ system (Bio-Rad) using immobilized metal affinity chromatography (IMAC), as previously described, with minor modifications (Kamata *et al.* 2014). Briefly, clarified supernatant containing expressed YFV-pM was loaded onto a 1mL nickel- charged, HisTrap HP column (GE Healthcare, Piscataway, NJ) that was pre-equilibrated with binding buffer (25mM HEPES, 200mM NaCl, 25mM imidazole, 2mM DTT, pH 7.5). Bound protein was washed with 11 column volumes (CV) of binding buffer and then eluted by applying an 8mL step gradient (0-100%) of binding buffer containing 500mM imidazole (elution buffer), followed by a final three CV isocratic elution step of 100% elution buffer. For the purification of insoluble proteins, except for DENV1-4 NS1, inclusion body pellets were washed as previously described, with minor modifications (Palmer and Wingfield 2012). Briefly, buffer containing 50 mM Tris-HCl pH 7.4, 1 M urea, and 1% Triton X-100 was used to wash pellets 3 times, followed by 2 washes with Tris-HCl pH 7.4. Centrifugation at 15,000 x *g* for 7 min was performed between each wash step. Purified inclusion body pellets were stored at -80^{o}C. Purified inclusion bodies were solubilized in 50 mM HEPES pH 7.3, 140 mM NaCl, 2 mM DTT, and 1% sodium dodecyl sulfate (SDS), followed by incubation at 99^{o}C with gentle mixing (5-15 min), and centrifugation to remove remaining insoluble protein. His-MBP tagged DENV1-4 NS1 proteins were purified using on-column refolding on His-Trap HP columns, as previously described (Kamata *et al.* 2014), with minor modifications. Briefly, DENV1-4 NS1 pellets were solubilized in buffer containing 25 mM HEPES, 0.2 M NaCl, 25 mM imidazole, 2 mM

DTT, and 6 M guanidine hydrochloride (pH 7.5). The pellets were gently agitated in solubilization buffer for 30 min at 4º C. Clarified supernatant containing the solubilized NS1 proteins were bound to HisTrap columns under denaturing conditions and refolded using decreasing proportions of 6M urea buffer (25 mM HEPES, 0.2 M NaCl, 25 mM imidazole, 2 mM DTT). Refolded DENV NS1 proteins were eluted using a step gradient of elution buffer that contained 500mM imidazole. All solubilized flavivirus proteins were analyzed by SDS-PAGE electrophoresis with Coomassie Blue staining, and by Western blotting using anti-His-HRP conjugated polyclonal antibody (1:5000, Abcam). Protein concentration and purity of flavivirus proteins were measured using the Agilent Protein 230 kit and Bioanalyzer 2100 instrument (Agilent Technologies). Purified proteins were stored at -20ºC in buffer containing 50 mM HEPES, 140 mM NaCl, 2 mM DTT, pH 7.3 with a final 25% glycerol concentration.

Microarrays of flavivirus antigens

Recombinant proteins that passed quality control criteria, along with controls, were diluted to 100-200µg/mL in microarray printing buffer (50 mM HEPES, 140 mM NaCl, 2 mM DTT, pH 7.3) with glycerol added to a final concentration of 40%. Flavivirus and control proteins were printed onto nitrocellulose-coated 4-pad slides (ONCYTE® SuperNOVA, Grace Bio-labs, Inc) in replicates (n = 6) using a non-contact inkjet microarray printer (ArrayJet, Glasgow, UK) with humidity inside the printer maintained between 60-70%. Control probes on the microarray included: IgGs (monkey, human, rabbit, goat, and mouse), IgMs (human, monkey, and rabbit), *E.coli* HisMBP (ProteinOne), BSA, influenza hemagglutinin antigens (HA, Immune Technology Corp.), hepatitis C antigen (ProSpec-Bio), and printing buffer. Additionally, whole virus preparations

consisting of DENV1-4 and various strains of ZIKV, as listed in Table 2, were produced by fellow colleague Stig Jensen and printed on separate microarrays at equivalent densities of the recombinant flavivirus proteins as previously described (Keasey *et al.* 2017). Printed microarrays were desiccated (12 h) under vacuum and stored frozen (-20^{o}C) until use.

The quality and deposition of the spotted antigens on the microarrays was evaluated using SYPRO®Ruby protein stain (Molecular Probes) and an anti-N-terminal 6X His monoclonal antibody (1:5000, Sigma Aldrich) specific for the detection of the protein fusion tag. The flavivirus E proteins on the microarrays were assessed further using a custom affinity purified rabbit polyclonal antibody (1:250, Covance) specific to an E-domain II peptide that was determined to be highly conserved based on multiple sequence alignments (ClustalW, DNASTAR® Lasergene v13, amino acids 98-111) amongst all 18 included E antigens. The peptide used for antibody production was synthesized (New England BioLabs, H2N-DRGWGNGSGLFGKGC-OH) to 90% purity with some modifications made to the native 14 amino acid peptide sequence. The internal cysteine was changed to a serine to avoid oxidation problems (p.C105S), while at the C-terminus a cysteine was added to allow conjugation to keyhole limpet hemocyanin (KLH) carrier protein. Lastly, specific and cross reactive antibody recognition of all spotted antigens was further evaluated with mouse anti-sera (dilutions ranged from 1:10-1:100) raised against each of the flaviviruses included in the multiplex microarray, except for ROCV since it was not available.

YFV propagation

The YFV vaccine strain 17D was obtained from BEI Resources, NIAID, NIH (NR-116, 8.9 x 10^7 $TCID_{50}$/mL) and propagated in Vero (CCL-81™, ATCC) cells. Vero cells were seeded in 2-T225 flasks and maintained in Dulbecco's Modification of Eagle's Medium (DMEM, Mediatech Inc., Manassas, VA), supplemented with 10% fetal bovine serum (FBS, GE Healthcare Life Sciences, Logan, UT), at 37ºC and 5% CO_2. At ~70% confluency, the cells were washed twice with cell culture grade 1X PBS (Mediatech Inc., Manassas, VA) then each seeded flask was infected with 15 mL of virus inoculum (50µl of suspended virus stock diluted in 30mL of DMEM with 2% FBS, approximate MOI 0.24) for 2h with gentle rocking every 30 min to evenly distribute the virus. After 2h, 35mL of fresh DMEM with 2% FBS was added. Viral supernatants were harvested on days 4 through 6 post-infection, with cytopathic effects (cell rounding and lysis) of the cells increasingly noted each day. Culture supernatants were centrifuged (1,200 x g, 20 min, and 4ºC) then filtered using pre-washed (DMEM media) 0.2 µm syringe filters (HT Tuffryn® Acrodisc®, Pall Life Sciences, Ann Arbor, MI). Aliquots of the propagated virus were snap-frozen in a dry-ice/ethanol bath prior to storage at -80ºC until use in neutralization assays, while approximately 90mL of the cell culture supernatants, combined from the 2 flasks, were concentrated for use in the microarray assays. Concentration of the virus was achieved by precipitating the supernatants for 12 h (4ºC) in 10% PEG8000 diluted in 1X PBS (v/v). Virus precipitates were pelleted by centrifugation (14,000 x *g*, 1 h 20 min., 4ºC), resuspended in 400 µl sterile 1X PBS (~225-fold concentration by volume), snap-frozen in a dry-ice/ethanol bath, and stored at -80ºC until use in printing of the YFV vaccine microarray.

YFV vaccine microarray

Dilutions of concentrated YFV (strain 17D), along with control proteins, were printed similarly to the flavivirus recombinant protein microarray. Control probes on the microarray included: IgGs (monkey, human, rabbit, goat, and mouse), IgMs (human, monkey, and rabbit), *E.coli* HisMBP (ProteinOne), BSA, influenza hemagglutinin antigens (HA, Immune Technology Corp.), cytomegalovirus glycoprotein B (CMV gB, ProSpec-Bio), and printing buffer. Whole virus preparation was diluted 1:2 (microarray printing buffer) and in ten subsequent 1:2 serial dilutions. The deposited virus was quantified against a dilution series of IgG capture-antibody standard by SYPRO®Ruby staining. Specific serum IgG binding to deposited spots of YFV were measured with mouse antisera (1:50) raised against vaccine-strain YFV, as well as antisera from NHPs (1:50) that were immunized by subcutaneous infection of 0.5ml of live, attenuated YFV vaccine (strain 17-D) as previously described in the flavivirus protein microarray methods (Figure 6). Printed microarrays were desiccated (12 h) and stored frozen (-20^{o}C) until use.

Microarray assays

All microarray processing steps were performed at 22^{o}C, protected from light. For IgM detection assays, serum IgG was inactivated using GullSORB^{TM} (Meridian) prior to performing microarray manipulations. NHP (1:50) and human (1:150) sera, diluted in probe buffer (1X PBS pH 7.4, 0.1% Tween 20, 1% BSA), were pre-cleared by incubating (1 mg/ml) with *E.coli* lysate (Promega) with gentle agitation, followed by centrifugation (17,000 x *g*, 5 min) to remove the pelleted immunoprecipitates. Microarrays were blocked with Super G blocking buffer (Grace Bio-labs) for 1.5 h and washed 3 times (5 min each) in wash buffer (1x PBS, 0.2 % Tween® 20, 1% BSA). The microarrays were incubated (2

h) with *E. coli*-cleared serum, washed (5x, 5 min each), and incubated for 1h with either goat anti-human γ-specific IgG (1:1000) or goat anti-human μ-specific IgM (1:250) Alexa Fluor 647-conjugated secondary antibody (Southern Biotech) diluted in probe buffer. Microarrays were washed 3 times with wash buffer (5 min each) followed by two washes in filtered deionized water to remove any residual salts, and then dried.

Data acquisition and analysis of microarray results

Microarray slides were scanned at 635 nm using a confocal laser scanner (GenePix® 4400A scanner; Molecular Devices) using settings below signal saturation. Background-subtracted pixel counts were determined with GenePix® Pro 7 software, and outliers among data replicates, identified using a modified Z-score (median absolute deviation >3.5), were removed. Pixel counts from replicate spots were averaged to obtain mean fluorescence intensity (MFI) and used for subsequent analyses. Relative binding (RB) was calculated as

$$RB = (x / x_i)100,$$

where x is MFI originating from microarrayed antigens, and i is the infecting virus species. Relative binding signals were used in hierarchical clustering analyses (average-linkage Pearson correlation) performed using MeV v4.8.1 within the TM4 software suite (Saeed *et al.* 2003). Student's t-tests, polynomial curve fitting, principal component analyses, and one-way analysis of variance (ANOVA) with Tukey's post-hoc honest significant difference (HSD) test were performed using OriginPro v9.0 (Origin Lab Corporation).[1]

For the study of antibody responses to YFV vaccination, microarrays were scanned and antibody binding results analyzed in GenePix® Pro 7 software, as previously

[1] Dr. Sarah L. Keasey performed the described analysis of results that I generated on the flavivirus-focused microarrays.

described. Following background subtraction, data was quantile normalized using preprocessCore package in R software (v3.3.3) (Bolstad *et al.* 2003). Outliers among data replicates were identified using a modified Z-score (median absolute deviation >3.5) and removed from data analysis. Graphs and statistical analyses including: student t-tests (two-tailed) with multiple comparisons, receiver operating characteristic (ROC) curves, linear regression, Pearson's correlation analysis, one- way analysis of variance (ANOVA) with Kruskal-Wallis (Dunn's) test to correct for multiple comparisons, and two-way analysis of variance (ANOVA) analyses with multiple comparison's corrected with Sidak's statistical hypothesis testing were performed using GraphPad Prism v7.03. Relative antibody binding values (%) for analysis of cross-reactive antibody responses was calculated as previously described, where x is MFI originating from microarrayed antigens, and i is the infecting virus species (YFV). Hierarchical clustering analyses (average-linkage Euclidean distance (MFI data) or Pearson correlation (relative binding data)) were performed using MeV v4.8.1 within the TM4 software suite (Saeed *et al.* 2003).

Machine learning[2]

The support vector machine (SVM) method LIBSVM (http://www.scie.ntu.edu.tw/~culin/libsvm/), available in the R package (Meyer D. *et al.* 2015), was used for predictions of infection histories with quantile normalized microarray data. An optimal separating hyperplane between data classes was determined with the SVM by maximizing the margin between closest points and minimizing the classification error. All binary sub classifiers were fitted to the model, and the correct class was identified

[2] Dr. Sarah L. Keasey developed the SVM (support vector machine) algorithm that was used for the classification of sera from unknown infection histories.

by a voting mechanism (i.e. the class with the highest probability). I used a radial basis function (RBF) as the kernel function, which is defined by

$$K(u,v) = \exp(-\gamma||u-v||^2),$$

where u and v are two data vectors and γ (set to 0.001) is a training parameter that makes the decision boundary smoother as the value becomes smaller. The regularization factor C, set to 100, controls trade-off between a low training error and a large margin. A grid search was used for selection of C (1 - 1000) and γ (0.0001 – 1) using 10-fold cross-validation of the training dataset and the built-in "tune" function of e1071. The final SVM model was generated using the optimal parameters with complete training datasets. To evaluate the model performance, a 10-fold cross validation was implemented on the training dataset, which consisted of a positive set of E-specific antibody binding signals from primary flavivirus infections (n = 32, human and NHP) and a negative set of background signals from flavivirus-naïve sera (n = 34, human and NHP). Based on one-way ANOVA followed by Tukey's range test, the overall antibody binding patterns of DENV2-challenged NHPs and humans were not statistically different ($p > 0.05$). Therefore, the positive training set consisted of data from both rDEN2Δ30-challenged humans and NHPs. The training dataset was randomly divided into ten equal parts, and each run of cross-validation was comprised of 1/10 as the independent test dataset and the remaining 9/10 as the training dataset. The performance of the model was calculated as *accuracy = (TP +TN) / (TP+FP+TN+FN).*

E protein molecular phylogeny[3]

A phylogenetic tree was generated based on E amino acid sequences (Asian-YAP/2007 and African-MR-766/1947 -lineage ZIKV selected as representative strains).

[3] Dr. Sarah L. Keasey completed the described phylogenetic analysis of the E proteins using the amino acid sequences I provided from my recombinant flavivirus clones.

CLUSTAL W2 (Larkin *et al.* 2007) was used to generate three multiple sequences alignments (MSAs), each with a different gap opening penalty (5, 10, 25), Blosum62 as the protein weight matrix, and all other options left as default. T-Coffee Combine (Di Tommaso *et al.* 2011; Notredame *et al.* 2000) was then used to generate a single alignment that had the best agreement of all three MSAs. Gblocks (Castresana 2000; Talavera and Castresana 2007), with relaxed settings (small blocks allowed, gap positions allowed within final blocks, and less strict flanking positions), was used to eliminate poorly aligned positions and divergent regions in the combined alignment, and 202 conserved columns within the alignment were retained. A molecular phylogeny was generated using the maximum likelihood method implemented in the PhyML program (v3.0 a LRT) (Guindon *et al.* 2010). The Blosum62 substitution model and 4 gamma-distributed rate categories were selected to account for rate heterogeneity across sites. The gamma shape parameter was estimated directly from the data (γ= 1.564). Tree topology and branch length were optimized for the starting tree and subtree pruning and regrafting selected for tree improvement.

YFV neutralization assays.

Both the length of infection and the amount of YFV (day 6 harvested) to use in neutralization assays were optimized prior to use in final neutralization assays. To optimize the length of infection that would allow for diluted YFV to be detected by a flow cytometry-based assay, two 12-well plates were seeded with 82,000 Vero cells per well in DMEM containing 10% FBS 24 h (cell media) before infection. Different dilutions of the YFV prepared in DMEM containing 2% heat-inactivated FBS (infection media), along with un-infected controls, were incubated (500µL) with the cells for 1.5h with gentle shaking every

20-30 min. The media containing the virus was removed by aspiration and the cells were washed 1 time with 500µL infection media. Fresh infection media was added and the cells were incubated at 37ºC, 5% CO_2 for either 24 or 48 h prior to harvest for cell staining. A similar infection protocol was used to determine the optimal concentration of virus to use in the neutralization assay with only slight modifications made to adapt to a 24 well plate. Briefly, 24-well plates were seeded with 38,500 Vero cells per well in cell media 24 h before infection. The virus stock was diluted in infection media starting at 1:25 in 2-fold serial dilutions to 1:3200 and was incubated (250µL) with the cells for 1.5h before washing and adding fresh infection media. The un-infected and YFV infected cells were incubated for 48h, since it was the determined optimum length of infection prior to harvesting for cell staining. To compare neutralizing antibody interactions with selected single and boosted vaccinated patient sera a flow cytometry-based infectivity assay (de Alwis and de Silva 2014) was used with modifications. Vero cells were seeded 24 h prior to infection (38,500 per well) in 24 well plates. Human sera from 3 single-YFV vaccinated patients and 3 boosted-YFV vaccinated patients, each with time points ranging from 1 to 6 years post final vaccination, as well as 3 non-vaccinated patients were heat-inactivated (55ºC, 30 min) prior to use in neutralization assay. Vaccinated sera were prepared in 4-fold serial dilutions (70µL volume) in infection media containing 1% penicillin/streptomycin with final dilutions ranging from 1:10 to 1:196,830, while non-vaccinated sera were prepared similarly but with dilutions of 1:10 and 1:100. An aliquot of day 6 harvested YFV was thawed in a 37ºC water bath and then diluted in infection media containing 1% penicillin/streptomycin for a targeted concentration (1:300) that should allow for the ideal range of 7-30% infection of the cells (de Alwis and de Silva 2014; Kraus *et al.* 2007). Pre-

incubation reactions comprised of samples containing an equal volume (70µL) of both diluted virus and human sera, as well as infection media containing no virus (Vero uninfected control), and diluted YFV alone was incubated in a 96-deep well PCR-clean/Lo-protein binding plate (Eppendorf) for 1 h at 37^{o}C, 5% CO_2. After an hour, the pre-incubation reactions were diluted 1:2 with infection media (140µL) containing penicillin-streptomycin (1%). Pre-incubation reactions (250µL) of human sera, along with media and virus-only controls, were added to Vero cells in the 24-well plates and incubated for 1.5 h (37^{o}C, 5% CO_2). Following incubation, supernatants were aspirated, cells were washed one time and incubated (~48 h, 37^{o}C, 5% CO_2) with 500µL fresh infection media containing penicillin-streptomycin (1%) prior to harvesting for flow cytometry.

Cell staining and flow cytometry.

YFV infected cells (~48 h) were washed (2 x, 500µL) with PBS (Mediatech, Inc, Manassas, VA) and removed from wells using 300µL of trypsin-EDTA (Sigma-Aldrich, St. Louis, MO). Trypsinization was inactivated by resuspension of the cells in 1ml PBS containing 10% FBS prior to transferring to 5ml round-bottom polystyrene tubes (Corning/Falcon™). The cells were incubated on ice for 10 min. and then centrifuged (500 x g, 7 min). Cells were washed in 1X PBS to remove any remaining trypsin or FBS, and then permeabilized by incubating in 300ul 1x BD FACS™ Permeabilizing Solution 2 (22^{o}C, 15 min). The cells were centrifuged (400 x g, 7 min), washed in 1X PBS, then blocked with 1X PBS containing 5% BSA (22^{o}C, 20 min). Following blocking, cells were washed in 1X PBS and resuspended in 50µL of mouse anti-flavivirus monoclonal antibody (clone D1-4G2-4-15) diluted to 20 µg/mL in 1X PBS prior to incubation (4^{o}C, 1h). Cells were washed with 1X PBS then incubated for 30 min. (4^{o}C) with (1:1000) goat anti-mouse

IgG (H+L) Alexa Fluor 488-conjugated secondary antibody (Life Technologies) diluted in 1X PBS, centrifuged, and stored in PBS containing 2% formaldehyde (ThermoFisher Scientific) at 4^{o}C prior to flow cytometry. Flow cytometry data was acquired on a BD FACSCalibur™ instrument with BD CellQuest^{TM} Pro software v 5.2.1 and then subsequently analyzed using FlowJo v10.3 software. Gating parameters were determined using the uninfected Vero cell controls (1.6 - 2.2% permitted for background % infection) and then applied to all experimental samples to determine the percentage of cells that were infected with YFV. The data was exported to Excel 2010 (Microsoft Office) and the percent infection values were background subtracted as follows:

$$I_{S-C} = I_S - I_C$$

where I_{s-c} is the percent YFV infection values, I_s is the percent infection values obtained from experimental samples, and I_c is the percent infection values obtained from the un-infected Vero cell used for initial gating. Following background subtraction, percent neutralization of single and boosted-vaccinated sera antibodies was calculated as follows:

$$\%\ N_{Ab} = 100 - \left[100\left(\frac{S}{NV_{avg.}}\right)\right]$$

, where S is the percent YFV infection values from the vaccinated patient samples following background subtraction and NV_{avg}. is the percent YFV infection values obtained from averaging the non-vaccinated control wells. The serum dilution that neutralized 50% of YFV was calculated by nonlinear, dose-response regression analysis (C constrained to 50) with Prism 7.0 software (GraphPad Software, Inc., San Diego, CA) following two independent experiments for each patient. Significant analysis of the mean neutralization titers between vaccinated cohorts was calculated with nonparametric Mann-Whitney-Wilcoxon test rank sum test (GraphPad Prism v7.03).

Animal and human sera used in the microarray assays (Figure 6)

Animal use statements

All macaque monkeys used in this study were cared for by the staff at the Wisconsin National Primate Research Center (WNPRC) in accordance with the regulations and guidelines outlined in the Animal Welfare Act and the Guide for the Care and Use of Laboratory Animals and the recommendations of the Weatherall report (http://royalsociety.org/topics-policy/publications/2006/weatherall-report/). This study was approved by the University of Wisconsin-Madison Graduate School Institutional Animal Care and Use Committee (Animal Care and Use Protocol Number G005401). For all procedures (i.e., physical examinations, virus inoculations, ultrasound examinations, blood and swab collection), animals were anesthetized with an intramuscular dose of ketamine (10 ml kg^{-1}). Blood samples were obtained using a vacutainer system or needle and syringe from the femoral or saphenous vein.

Human use statements

Research on human subjects was conducted in full compliance with DoD, NIH, federal, and state statutes and regulations relating to the protection of human subjects and adheres to principles identified in the Belmont Report (1979). All specimens, data, and human subject research were gathered and conducted for this publication under IRB-approved protocols.

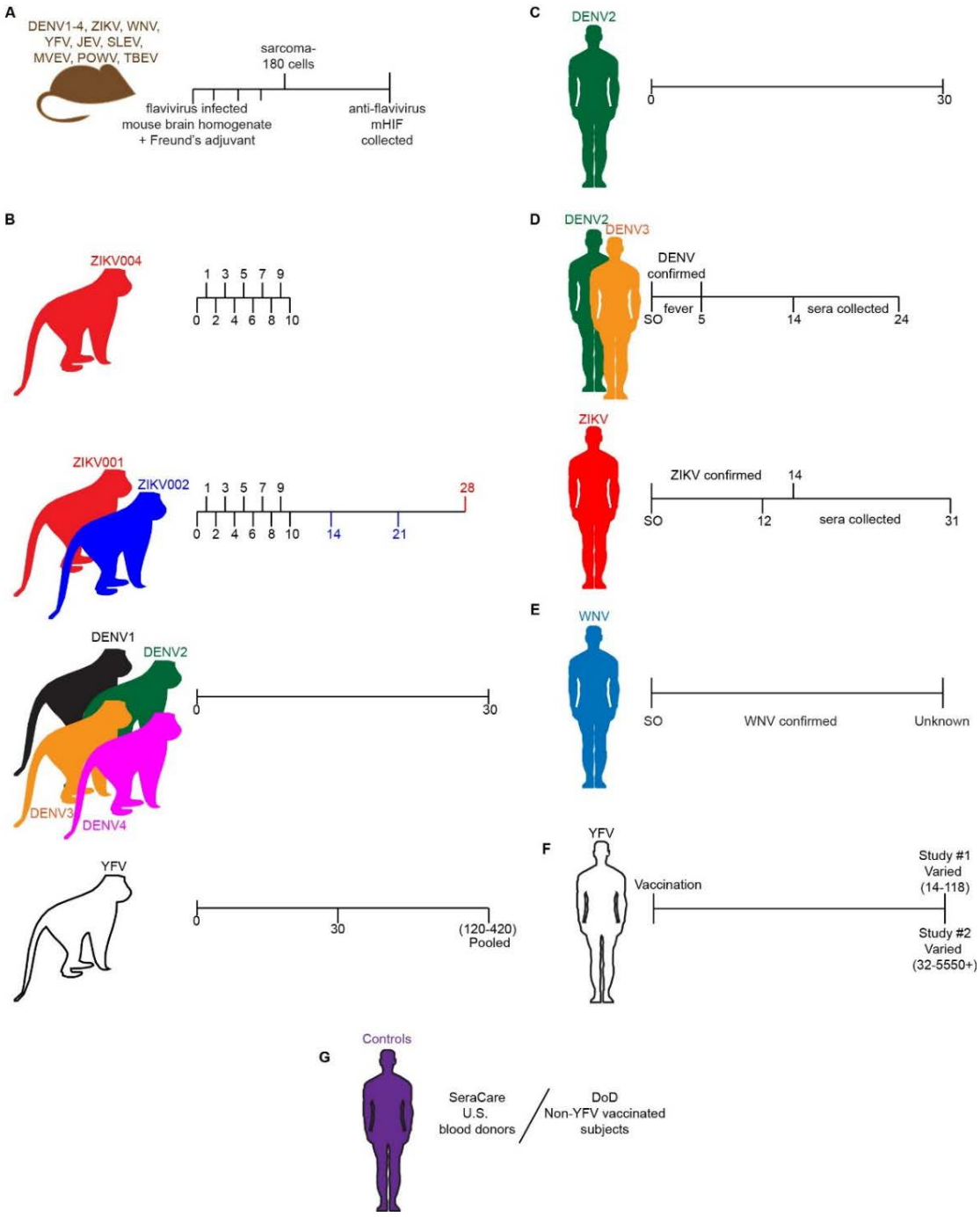
A
DENV1-4, ZIKV, WNV, YFV, JEV, SLEV, MVEV, POWV, TBEV
sarcoma-180 cells
flavivirus infected mouse brain homogenate + Freund's adjuvant
anti-flavivirus mHIF collected
B
ZIKV004
1 3 5 7 9
0 2 4 6 8 10
ZIKV001
ZIKV002
1 3 5 7 9 28
0 2 4 6 8 10 14 21
DENV1
DENV2
DENV3
DENV4
0 30
YFV
0 30 (120-420) Pooled
C
DENV2
0 30
D
DENV2
DENV3
DENV confirmed
SO fever 5 14 sera collected 24
ZIKV
ZIKV confirmed 14
SO 12 sera collected 31
E
WNV
SO WNV confirmed Unknown
F
YFV
Vaccination
Study #1 Varied (14-118)
Study #2 Varied (32-5550+)
G
Controls
SeraCare U.S. blood donors
DoD Non-YFV vaccinated subjects

Figure 6. Sera used for analysis of antibody responses to flavivirus antigens. Mouse hyper-immune ascetic fluid (mHIF) against 12 flavivirus isolates (DENV1-4, ZIKV, YFV, JEV, WNV, SLEV, MVEV, POWV, and TBEV) were used for the evaluation of antibody recognition to the deposited flavivirus antigens on the microarray (**A**). The horizontal lines give an indication of the study duration, while vertical hashes indicate the steps involved during the production of anti-flavivirus hyperimmune ascetic fluid in mice. Sera collected after flavivirus infection or vaccination from non-human primates (NHP), and humans will be used for measurement of antibody recognition to flavivirus antigens on the protein microarray. The horizontal lines indicate the study duration, while vertical hashes indicate the sera collection time points. (**B**) Primary flavivirus infection sera were collected from captive-raised NHPs prior to (day 0) and various time points after challenge with either an Asian-lineage (strain (str.) H/PF/2013) ZIKV (red, n = 3 each for Study ID ZIKV001 and ZIKV004), an African-lineage (str. MR-766) ZIKV (royal blue, n = 3, Study ID ZIKV002) (Dudley *et al.* 2016; ZIKV experimental science team 2016), a single DENV serotype (n = 4 each for DENV1 (str. West Pac 74), black; DENV2 (str. S16803), green; DENV3 (str. CH53489), orange; DENV4 (str. 341750), magenta) (Fernandez *et al.* 2011; Simmons *et al.* 2010), or were vaccinated with the str. 17D YFV vaccine (unfilled black, n = 3, BEI Resources, NIAID, NIH). (**C**) Sera from flavivirus-naïve humans (n = 10) were infected with rDEN2Δ30 (Kirkpatrick et al. 2016; Larsen et al. 2015). (**D**) Convalescent human ZIKV (red, n=4) or DENV (DENV2, green (n=5), DENV3, orange (n=2)) infection sera were collected from dengue-endemic regions in the Dominican Republic and Peru, respectively. (**E**) Confirmed WNV-infected sera (cyan, n = 20) were collected from blood donor locations (BioLINCC 2012; Ramos *et al.* 2012). **(F)** Human sera from subjects vaccinated with YFV vaccine (17D) (unfilled black, n = 13) were used in the study of the analysis of antibody responses to ZIKV in flavivirus-endemic environments (Keasey *et al.* 2017), as well as in the YFV-focused microarray study (unfilled black, n=87). (**G**) Sera from humans with no-known prior flavivirus infection or YFV vaccination history were used as controls in the microarray studies (purple, n=5; SeraCare, Milford, MA and n=14; DoD Serum Repository, Silver Springs, Maryland).

Flavivirus specific antibody standards.

Mouse hyper-immune ascitic fluid (mHIF) against 12 flavivirus isolates (DENV1-4, ZIKV, YFV, JEV, WNV, SLEV, MVEV, POWV, and TBEV) were obtained from NIAID-World Reference Center for Emerging Viruses and Arboviruses (WRCEVA, Dr. Robert B. Tesh) and used for the evaluation of antibody recognition to the deposited flavivirus antigens on the microarray (Figure 6A). Briefly, mice were injected intraperitoneally with flavivirus-infected mouse brain homogenate emulsified with Freund's adjuvant weekly for a total of 4 weeks. After the final antigen immunization, mice were given sarcoma-180 cells to induce ascites formation prior to the collection of the flavivirus-specific ascitic fluid.

ZIKV.

Three groups of Indian origin *Macaca mulatta* (3 individuals per group) were challenged subcutaneously with a different dose (10^6, 10^5, or 10^4 plaque forming units (PFU)) of either an Asian (Study ID ZIKV001 and ZIKV004) or African (Study ID ZIKV002)-lineage ZIKV (Table 2, Figure 6B). Sera were collected prior to ZIKV challenge (day 0) and daily for 10 days (all cohorts), followed by two to three times a week from 11 to 28 days post-infection (DPI) (ZIKV001 and ZIKV002 only) (Dudley *et al.* 2016; Zika open-research portal 2016) (https://zika.labkey.com). Human sera from ZIKV infections were collected from four female patients from the Dominican Republic that developed symptoms of ZIKV (fever, joint pain, headache, conjunctivitis, rash, and muscle pain) in January 2016 (Figure 6D). Three patients were PCR confirmed for ZIKV infection by the CDC within the first two weeks of symptom onset, whereas the remaining patient

tested positive for the presence of anti-ZIKV IgG by a microplate ELISA assay (EUROIMMUN, Inc.), as performed by BocaBiolistics (Pompano Beach, FL), and sera were collected at 12-31 days post-symptom onset.

DENV.

Sixteen healthy, flavivirus naïve rhesus macaques (*M. mulatta*) were subcutaneously injected with 10^5 PFU of either DENV1 (West Pac 74), DENV2 (S16803), DENV3 (CH53489), or DENV4 (341750) (n=4 per challenge group, Figure 6B), derived from low passage, near wild-type virus isolates. Sera were collected prior to and 30 DPI (Fernandez *et al.* 2011; Simmons *et al.* 2010). Sera from one NHP exhibited elevated binding to JEV, ROCV, and YFV- E with my assay prior to challenge with DENV4, and was excluded from further data analysis (Figure 7). Sera from human primary DENV2 infections (n = 10, Figure 6C) were collected as part of a DENV human challenge model originally developed by the Laboratory of Infectious Diseases at the U. S. National Institutes of Health. Sera from participants that had no prior history or serological evidence of flavivirus infection were collected before and after 28 days after challenge with 10^3 PFU of rDEN2Δ30, which is a genetically attenuated DENV2 strain (DENV2 Tonga/74) that had a 30 nucleotide deletion introduced in the 3' untranslated region (Kirkpatrick *et al.* 2016; Larsen *et al.* 2015). The rDEN2Δ30 challenge induced viremia in all participants by 5 DPI (Kirkpatrick *et al.* 2016; Larsen *et al.* 2015). Subjects that were included in the challenge studies were pre-screened with PRNT assays to include only dengue-naïves. Interestingly, the sera from two individuals exhibited elevated binding to flavivirus E with my assay prior to challenge with rDEN2Δ30 (Figure 7). Because these two subjects

presented evidence of prior exposure, their sera were excluded from further data analysis. Dengue disease sera (n=7) were also collected between February 2011 and November 2013 in Peru by our collaborators from the U.S. Naval Medical Research Unit No.6 (NAMRU-6). These subjects had febrile illness for five days or less and were confirmed to have DENV infections (DENV2, n=5; DENV3, n=2; Figure 6D) by PCR during the acute phase of infection. Sera were collected 14-24 days after confirmation of acute infection.

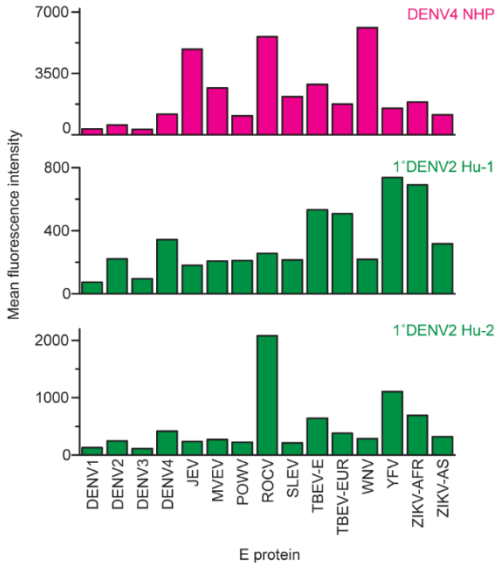

Figure 7. Human and non-human primate sera excluded from analysis. Pre-study sera from one DENV4-challenged non-human primate and two primary DENV2- challenged humans exhibited evidence of prior exposures to flaviviruses based on antibody interactions with E proteins.

YFV

Early-Immune Yellow Fever Virus Antisera from three NHPs (Figure 6B; NR-29335, 29337, 29338; BEI Resources, NIAID, NIH), immunized by subcutaneous injection of 0.5 mL of live, attenuated YFV vaccine (strain 17D), were collected 30 days after vaccination (Durieux 1956). Late-Immune Yellow Fever Virus antisera from the same

NHP cohort (Figure 6B; NR-42567, 42575, 42576; BEI Resources, NIAID, NIH), consisted of pooled time-point sera that were collected in approximate 30-day time intervals ranging from 120 to 420 days after vaccination for each animal.

Humoral immune responses of individuals living in environments of flavivirus endemicity were examined with the recombinant protein microarrays by probing with human sera from 17D-vaccinated individuals (seven primary and six boosted, Figure 6F), collected 14 – 118 after vaccination. For analysis of serum IgG responses over time, sera from subjects vaccinated once (n = 67) or multiple times (n = 20) with the YFV vaccine were collected 32 days to 15-plus years after vaccination, and compared to sera from non-vaccinated controls (n=17) (Figure 6F and Table4). Specimens used in both studies were archived by the U.S. Department of Defense Serum Repository (Silver Springs, Maryland).

WNV

Sera from confirmed WNV infection (n=20, Figure 6E) were collected between 2009 and 2011 by FDA approved blood donor locations within the U.S., in accordance with a surveillance protocol performed by the National Heart, Lung, and Blood Institute (NHLBI) Biologic Specimen and Data Repository Information Coordinating Center (BioLINCC) (Viral and immune parameters of dengue and wnv in donors: Blood safety implications 2012). Sera were identified as WNV positive by nucleic acid testing, indicating a current WNV infection at the time of blood donation. WNV positive donors were then contacted for study enrollment, at which point subjects completed symptom questionnaires and provided subsequent blood samples at several weekly and monthly

visits post-initial donation. Each specimen tested positive for the presence of WNV-specific IgM and IgG antibodies (Ramos *et al.* 2012).

Control Sera

Sera collected by SeraCare Life Sciences, Inc. from healthy U.S. donors (n=5) were used for negative controls (Figure 6G). These sera were selected based on no detectable antibodies to human immunodeficiency virus type 1 and type 2, Hepatitis A, B, and all flaviviruses used in the microarray.

Additionally, sera from the U.S. Department of Defense Serum Repository (Silver Springs, Maryland) subjects who were not recorded to have received a yellow fever vaccination (Figure 6G) were used for negative controls in the YFV-focused study (n=17).

RESULTS

Development of a flavivirus-focused microarray assay

I synthesized the structural proteins, membrane (pM/M) and envelope (trans-membrane domain truncated E and domain III of E (E-DIII), and non-structural proteins 1 and 3 (NS1 and NS3) from 18 species of human pathogenic flaviviruses (Table 2) (Keasey *et al.* 2017). These major antigenic targets of humoral immune responses to flavivirus infection and immunization were selected for inclusion in the microarray by analysis of immunological data from previous studies by our laboratory and others (Beasley et al. 2004; Cleton et al. 2015; Fernandez et al. 2011; Gowri Sankar et al. 2014; Kuno 2003).

As previously reported, we used microarrays of the entire DENV1-4 proteome to obtain a detailed analysis of non-human primate (NHP) antibody responses to DENV antigens following immunization with two different DENV vaccine candidates (tetravalent purified inactivated virus (TPIV) or tetravalent live, attenuated virus (TLAV) vaccine), as well as after challenge with live DENV virus (Fernandez et al. 2011; Simmons et al. 2010). Antibody binding to specific DENV proteins differed depending on the vaccination given, while a balanced response to both structural (E, M, and anchor capsid) and non-structural (NS) proteins (ex. NS1) was detected in antibody responses to DENV infection. Results from the DENV protein microarray demonstrated the importance of including multiple viral antigens in a serological assay for optimal detection of flavivirus specific antibody responses.

Table 2. Flavivirus strains included in the production of whole viruses and recombinant proteins.

Virus	Isolate	Country	Year	Targeted antigens					
				Virus	E	E-DIII	pM/M	NS1	NS3
ZIKV Asian lineage	SV0127/14	Thailand	2014	x					
	CPC-0740	Philippines	2012	x					
	VABC59	Puerto Rico	2015	x					
	SPH2015	Brazil	2015		x				
	YAP	Micronesia	2007		x	x	x	x	
ZIKV African lineage	MR-766	Uganda	1947	x	x	x	x	x	
	IBH30656	Nigeria	1968	x					
	DAKAR41525	Senegal	1984	x					
	DAKAR 41662	Senegal	1984	x					
	ARB7701	Central Africa	1976		x				
	ArD_41519	Senegal	1984		x				
DENV1	HAWAII	USA	1944	x	x	x	x	x	x
DENV2	NGC	New Guinea	1944	x	x	x	x	x	x
DENV3	H87	Philippines	1956	x	x	x	x	x	x
DENV4	H241	Philippines	1956	x	x	x	x	x	x
WNV	NY99	USA	1999		x	x	x	x	
YFV	17-D-204	USA	1985	x	x	x	x	x	x
JEV	SA14-14-2	South Korea	2006		x	x	x	x	
SLEV	PARTON	USA	1933		x	x	x	x	
MVEV	1-51	Australia	1952		x	x	x	x	
ROCV	SPH34675	Brazil	1975		x	x	x	x	x
POWV	LB	Canada	1958		x	x	x	x	
TBEV-E	SOFJIN-HO	Russia	1937		x	x	x	x	
TBEV-EUR	NEUDOERFL	Austria	1971		x	x	x	x	
		Total # of antigens produced:		12	18	15	15	15	6

The "x" indicates antigens that were produced, whereas unfilled squares are antigens that were not attempted for production.

[1]Virus abbreviations: Zika (ZIKV), dengue (DENV), West Nile (WNV), yellow fever (YFV), Japanese encephalitis (JEV), St. Louis encephalitis (SLEV), Murray Valley encephalitis (MVEV), rocio (ROCV), Powassan (POWV), eastern (E) and european (EUR) strains of tick-borne encephalitis (TBEV).

[2] Antigen abbreviations: Transmembrane domain truncated envelope protein (E), domain III of envelope protein (E-DIII), precursor membrane or membrane protein (pM/M), non-structural protein 1 (NS1), non-structural protein 3 (NS3).

Coding sequences for each antigen were amplified using cDNA or synthesized gene templates, gel purified, and then cloned into a pENTR™/TEV/D-TOPO® *E.coli* entry vector (Table 1, Figure 8A). Because the targeted viral antigens included membrane (E/M) or membrane-associated proteins (NS1/NS3) that may express poorly in *E.coli*, all sequence-confirmed plasmid clones were initially cloned as His-tagged maltose-binding

protein (MBP) fusion constructs. Maltose-binding protein is commonly used to increase solubility of the fusion partner, while the 6X histidine tag allows for purification using common metal-affinity strategies (Hewitt *et al.* 2011; Waugh 2016). As initially designed, all of the recombinant proteins with the exception of YFV-pM accumulated primarily as insoluble inclusion bodies regardless of changes in length and temperature of protein induction, or type of host cell used. The inclusion proteins were recovered by solubilizing the inclusion bodies in 6M guanidine hydrochloride and protein refolding by using decreasing concentrations of urea. Specifically, solubilized supernatants filtered to remove particles (syringe filter: 0.2uM) were added to nickel charged affinity columns (HisTrap HP) under denaturing conditions. Proteins that were bound to the column were refolded using a decreasing gradient of urea (6-0 M), and eluted from the column with an increasing imidazole concentrations from 25-500 mM. While this method worked for DENV1-4 NS1 proteins, the remaining proteins contained a substantial amount of truncated MBP protein rather than the targeted full-length viral protein (results not shown). I also attempted to obtain soluble expression of the recombinant proteins by implementing other expression systems, such as an *E.coli* cell-free *in-vitro* expression system specifically geared towards expression of non-native membrane proteins, as well as expression in baculovirus and mammalian cells (HEK293). Although improvements in solubility were noted with some of these systems, the quantity of expressed protein was so low that after purification steps the protein was no longer detectable. Additionally, I attempted to modify the protein-coding sequences by truncating the E protein to exclude the transmembrane domain in order to obtain soluble protein in *E.coli*. While truncated E in comparison to full-length protein led to higher amounts of expressed protein, the

protein remained in the insoluble protein pellet. Because of the difficulties in developing a consistent method for producing soluble recombinant proteins, I considered the advantages of using inclusion-sequestered products. The protein-encoding genes were recombined into an N-term 6X His tagged (pDEST17) vector and expressed in *E.coli* by using BL21-DE3 host cells and induction conditions of 30ºC for 2-4hrs or 18 ºC overnight. All of the remaining flavivirus proteins, except for pM from JEV and ZIKV (str.MR766) showed improved full-length expression with the pDEST17 vector, though still insoluble. Inclusion body aggregates primarily contain the over-expressed recombinant protein of interest, lending to the possibility of obtaining highly purified proteins with minimal purification steps needed (Ramon *et al.* 2014). Further, data has suggested that denatured antigens can be highly sensitive and specific in the detection of antibody responses following viral infection (Di Bonito *et al.* 2006; Ter Meulen *et al.* 1998). Therefore, inclusion bodies were washed and solubilized in HEPES buffer containing 1% sodium dodecyl sulfate (SDS). Soluble proteins obtained from either affinity purification or SDS solubilization steps were analyzed by SDS-PAGE electrophoresis with Coomassie Blue staining (Figure 8B), and by western blotting using an anti-HIS-HRP conjugated polyclonal antibody (1:5000, Abcam). Protein concentration and purity of the flavivirus proteins were measured using the Agilent Protein 230 assay (Figure 8C). Based on results from Agilent Protein 230, the median purity of all included flavivirus proteins was 73% (range 43-97%).

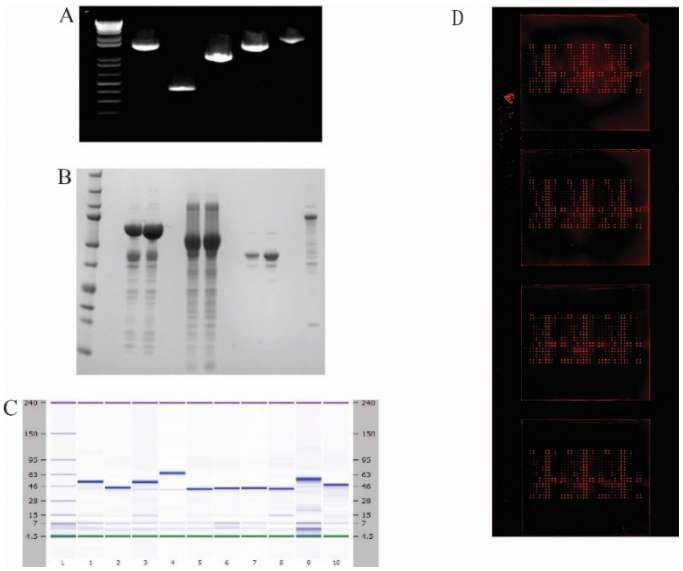

Figure 8. Production of flavivirus recombinant proteins. Targeted flavivirus coding sequences were cloned, sequence verified, expressed, purified, and arrayed onto nitrocellulose glass slides. (A) Representative PCR-amplified code determining sequences detected using ethidium bromide. (B) *E.coli* expressed recombinant proteins were visualized by SDS-PAGE electrophoresis with Coomassie Blue staining. Proteins were also verified using anti-His antibody after PAGE electrophoresis. (C) Purified recombinant proteins were analyzed and visualized by Agilent Protein230 chip. Recombinant flaviviral antigens that passed quality control criteria, along with control proteins, were printed in replicates of 6 onto SuperNOVA 4-pad nitrocellulose glass slides (Grace Bio-Labs). The array layout allowed for 4 different assays to be simultaneously performed on the same surface. (D) Representative confocal laser scanned image of flavivirus proteins spotted in replicates onto microarray slides (Grace Bio-Labs), visualized using 4 different human sera bound to Cy5-labeled anti-human IgG antibody.

Based on previously optimized microarray assay conditions (Fernandez et al. 2011; Kamata et al. 2014; Keasey et al. 2010; Pugh et al. 2014), protein concentrations of 100-200μg/mL were targeted for printing of the viral probes. Under these conditions, essentially all of the spotted proteins are non-covalently bound to the nitrocellulose surface of the microarray slides. The recombinant flavivirus antigens that passed quality control criteria were diluted to approximately 100-200 μg/mL in print buffer containing 40% glycerol into 384 well plates. Samples in the wells were drawn through capillary tubing into the print head of a non-contact inkjet printer (ArrayJet, Roslin, UK), and deposited (8 drops/spot,

~150 micron in size) in replicates of six onto glass slides containing four microporous nitrocellulose coated microarray surfaces (SuperNOVA 4-pad slides, Grace Bio-Labs, Inc.) (Figure 8D). The humidity inside the printer was maintained at 60-70% during the entire length of the print to optimize spot integrity. The following controls were also printed on the same surfaces: IgGs (monkey, human, rabbit, goat, and mouse), IgMs (human, monkey, and rabbit), HisMBP, bovine serum albumin (BSA), three hemagglutinin proteins (HA) from seasonal influenza, as well as buffer control spots. The spotted antigens of the microarrays were stained with SYPRO®Ruby to visualize all proteins (Figure 9A), and an anti-N-terminal 6X His monoclonal antibody (1:5000, Sigma Aldrich) to detect all His-tagged proteins. The coefficient of variance (CoV) or precision of the deposited protein replicates was 22%, as determined by results from the SYPRO®Ruby protein stain between all replicates across each of the four printed microarray surfaces. Probing with the anti-His antibody showed that all His-tagged proteins were successfully spotted and adsorbed onto the nitrocellulose-coated microarray surfaces (Figure 9B). Some variability in signal intensity was noted for the anti-His antibody due to varying accessibility of the fusion-tag on the recombinant proteins. I developed a rabbit polyclonal antibody (diluted 1:250) that was specific to a highly conserved E domain II fusion loop peptide to further assess the flavivirus E proteins on the microarrays. The E fusion loop sequence is conserved among flavivirus species because the peptide mediates fusion of the virus to host cell membranes, for transfer of viral RNA into the host cell cytoplasm (Allison et al. 2001; Seligman 2008). Based on multiple sequence alignments, I identified a 14 amino acid (aa) peptide (aa 98-111, DRGWGNGCGLFGKG) that was 98% conserved amongst recombinant E protein sequences of all 18 flavivirus species. The only sequence variations

were seen at aa104 (G104H) in sequences of tick-borne flavivirus E proteins and aa110 (K110F) in JEV and POWV-E. For peptide synthesis, the internal cysteine was replaced with serine in order to avoid possible problems of oxidation/internal cross-linking. The peptide was conjugated to a carrier protein (KLH) to increase the antigenicity for antibody production. Assessment of E antigens with the optimal dilution of rabbit anti-E domain II antibody (1:250) led to strong recognition of all tested flavivirus E proteins (Figure 10). Antibody recognition of all spotted antigens was further evaluated with mouse anti-sera (dilutions ranged from 1:10-1:100) raised against each of the flaviviruses included in the panel, except for ROCV (Figure 6A). The E antigens from all flaviviruses, except DENV3, were specifically detected by mouse antibodies (IgG) that were produced in response to the corresponding virus, as shown in (Figure 11). Significant E cross-reactivity for JEV anti-sera was noted. Specific and cross-reactive antibody recognition observed to flavivirus antigens was evaluated by using the phylogenetic relationship between E amino acid sequences (Figure 12). The NS1 proteins from all flaviviruses except DENV1-4 were detected by the mouse anti-virus sera, whereas the M antigen was only weakly recognized at best (Figure 11). I compared antibody responses to flavivirus antigens observed in mice to antibody responses of flavivirus infected human sera in order to determine which antigens demonstrated the greatest level of specificity. Mouse antibody responses to E-DIII showed some level of specificity, but were highly cross-reactive in human antibody responses. Further, though high levels of antibody bound to NS3 antigens, both human and mouse antibody responses were very cross-reactive for this antigen. Due to these factors, E-DIII and NS3 viral antigens were removed from analyses of human and NHP antibody responses. Combined, data from these control antibodies indicated that the flavivirus

protein microarrays could be used as to assess specific and cross-reactive antibody responses.

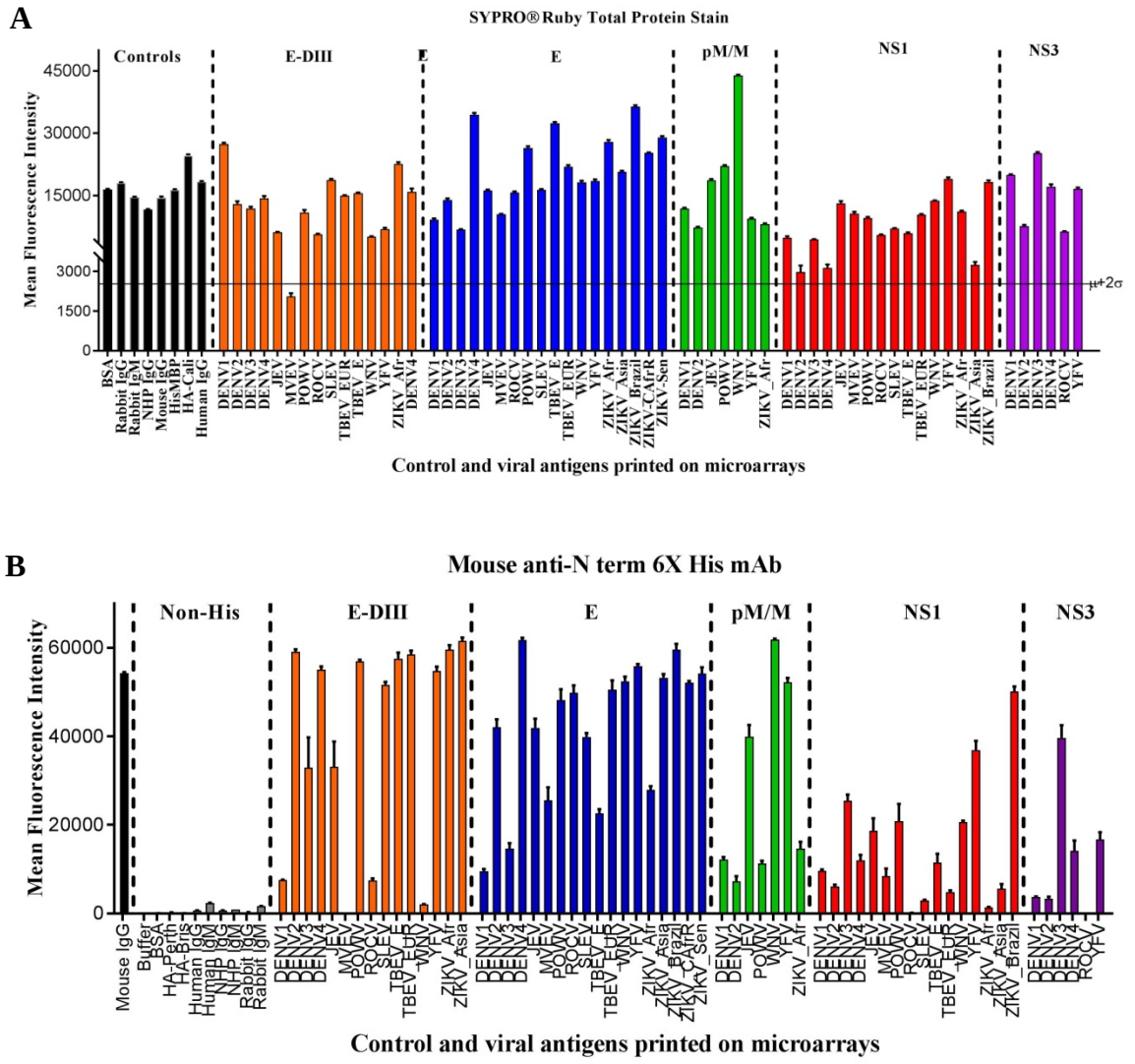

Figure 9. Validation of the antigens deposited on the microarrays. Recombinant proteins (E-DIII, orange bars; E, blue bars; pM/M, green bars; NS1, red bars; and NS3, purple bars) from 18 flavivirus isolates and several control antigens (black and gray bars) were deposited in replicates (n=6) onto microarrays covered in a thin layer of nitrocellulose. The deposition and quality of the printed antigens was evaluated by a (**A**) total protein stain and (**B**) monoclonal antibody directed towards the 6X His fusion tag on the N-terminus of the recombinant proteins. Error bars represent standard error of the mean between replicates.

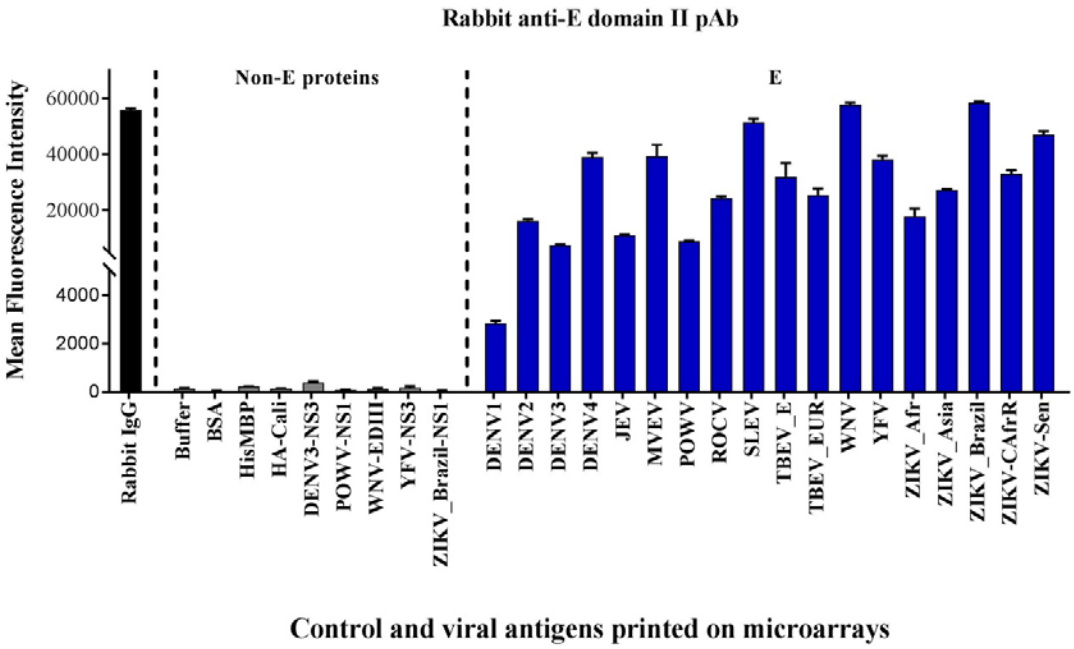

Figure 10. Recognition of flavivirus E proteins using an antibody directed to a highly conserved E-domain II fusion loop peptide. Deposited flavivirus envelope (E) proteins on microarray surfaces were evaluated using a rabbit polyclonal antibody directed to the E-domain II peptide that is highly conserved among all flavivirus species. Antibody recognition of the recombinant E proteins (blue bars) and control antigens (black and gray bars) was detected using an Alexa Fluor 647 conjugated goat-anti rabbit IgG secondary antibody. Error bars represent standard error of the mean between replicates (n=6).

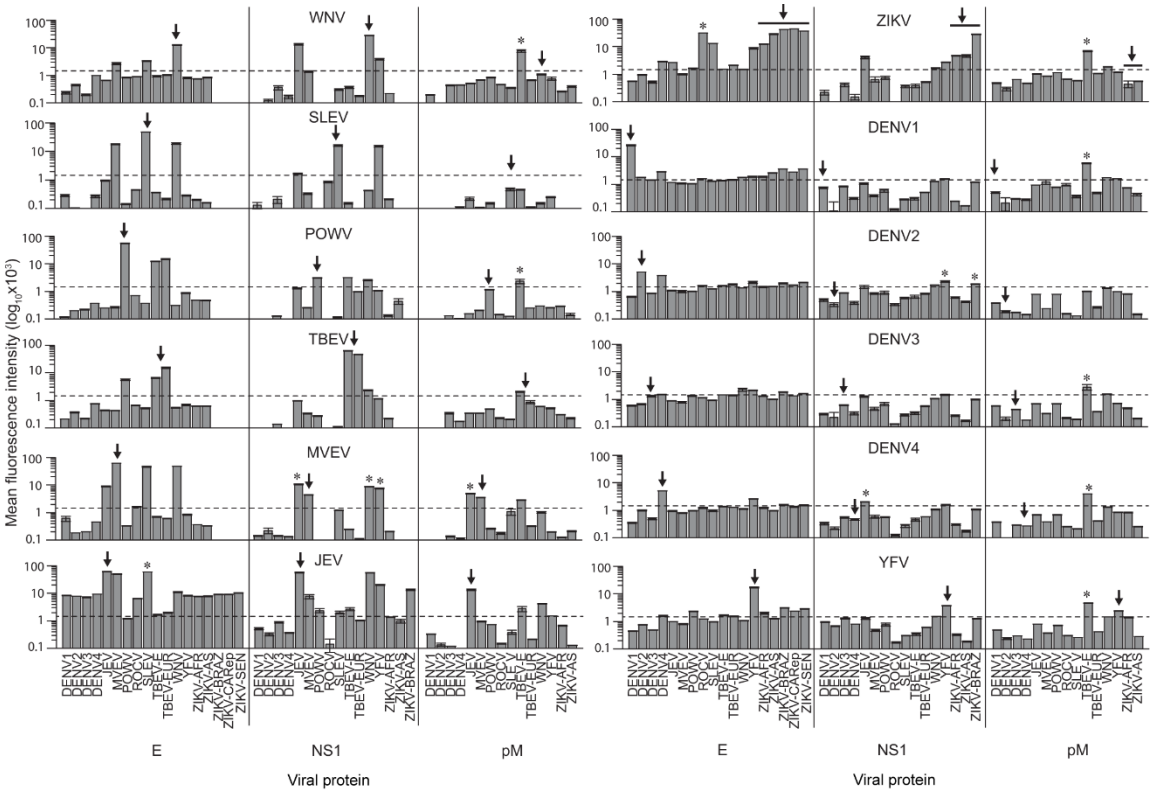

Figure 11. Recognition of deposited antigens by virus-specific antibody standards. Microarrays of E, non-structural 1 (NS1), and membrane (pM) proteins probed with mouse polyclonal antibodies (Figure 6A) generated against each virus shown (centered labels above each bar graph). Antibody binding data are shown as log10-transformed mean fluorescence intensity (± SEM), and arrows (↓) indicate the virus-specific antigens. Heterologous antigens that exhibit increased recognition compared to the virus-specific antigen are labeled with * ($p < 0.05$, one-way ANOVA with Tukey's range test). YFV, yellow fever virus; SLEV, St. Louis encephalitis virus; DENV (1-4), dengue virus; POWV, Powassan virus; TBEV, tick-borne encephalitis virus; MVEV, Murray Valley encephalitis virus; WNV, West Nile virus; ZIKV, Zika virus; JEV, Japanese encephalitis virus; ROCV, Rocio virus.

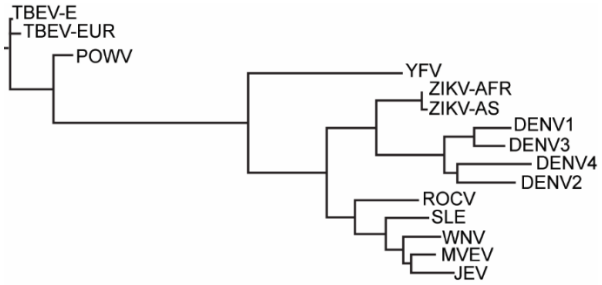

Figure 12. Phylogenetic relationship of flavivirus E proteins included on the microarray. The phylogenies of flaviviruses examined in this study were inferred from an alignment of amino acid sequences from the produced envelope (E) proteins.

Antibody responses to ZIKV[4]

I utilized the flavivirus-focused microarray to examine sera from NHPs (*M. mulatta*) that were challenged subcutaneously with either African or Asian isolates of ZIKV (Table 2; Figure 6B) (Dudley *et al.* 2016; Zika open-research portal 2016). The African and Asian lineages of ZIKV share ~95% of E protein amino-acid sequences (Haddow *et al.* 2012), or about the same level of similarity found among E proteins of individual DENV serotypes. Serum antibody binding to virus particles and E antigens of ZIKV, as measured by the microarray, was substantially elevated (Figure 13A, B) 21-28 days post-infection (DPI), while no antibody recognition was observed for NS1 or M proteins (Figure 13B), suggesting that anti-NS1 and -M antibodies represent a small proportion of the humoral immune response to infection during the time points examined. Antibody recognition was more robust for mature (~2-fold higher) compared to immature virus particles, which may display different conformations of E and M proteins (Kostyuchenko *et al.* 2016). Within the assay, the highest antibody interactions were detected to ZIKV E proteins in comparison to mature ZIKV (Figure 13A, B). However, a direct quantitative relationship between virus and recombinant protein cannot be determined by these results because the complex nature of the native virus precludes printing of equal molar amounts of available antigen. Only minor differences were observed in antibody responses to individual African and Asian-lineage ZIKV antigens for both virus and E (Figure 13), consistent with the conserved amino acid sequences and a single ZIKV serotype, as recently reported by others (Dowd *et al.* 2016). The E-specific IgM responses were detectable by 3 DPI, coinciding

[4] Data on pages 65- 77 was previously published in: Keasey SL, Pugh CL, Jensen SM, Smith JL, Hontz RD, Durbin AP, Dudley DM, O'Connor DH, Ulrich RG. 2017. Antibody responses to zika virus infections in environments of flavivirus endemicity. Clin Vaccine Immunol. 24(4).

with the rise of virus, peaked by 11 DPI, and subsided thereafter (Figure 13C). Corresponding IgG responses were delayed compared to IgM, consistent with a naïve immune response, and displayed increasing levels through 28 DPI (Figure 13C). Specific IgG interactions were greater with E than virus for these assay results (Figure 13C). Further, there were no apparent differences in the magnitude or kinetics of humoral immune responses to the different amounts of virus used for challenges (Figure 14), suggesting that levels of IgG and IgM were increasing in tandem with virus replication.

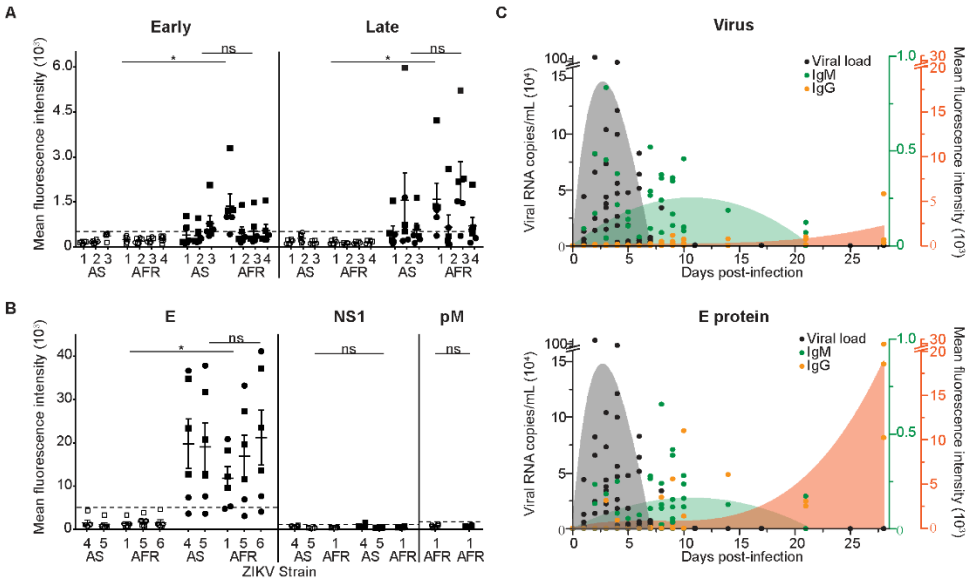

Figure 13. Virus particles and E antigens of ZIKV were significantly recognized post-infection, with the highest level of antibody interactions observed towards ZIKV E proteins as compared to mature virus. ZIKV-challenged non-human primate (NHP) IgG recognition of ZIKV particles harvested early (**A**, left, 48 h) or late (**A**, right, 144 h) post-infection of HEK293T cells, and ZIKV proteins (**B**; envelope, E; nonstructural protein 1, NS1; precursor membrane protein, pM), from five Asian (AS) and six African (AFR) lineages (Table 2). ZIKV-specific antibody responses are denoted by scatter plots with center horizontal lines representing the mean binding of serum antibodies from NHPs challenged with either an AFR- (n=3, circles) or AS- (n = 3, squares) lineage ZIKV at 0-2 days post-infection (DPI; open symbols) and 21-28 DPI (filled symbols). Error bars indicate ± SEM. Statistically significant differences between mean antibody binding of all ZIKV-challenged NHPs to ZIKV antigens at 0-2 DPI and 21-28 DPI were calculated using a one-tailed Student's t-test (*, $p < 7.5e\text{-}5$; ns, not significant), while no significant differences were observed between mean antibody binding of ZIKV-AS- and ZIKV-AFR-challenged groups to AS and AFR ZIKV antigens at 21-28 DPI (two-tailed Student's t-

test). (**C**) IgM (green) and IgG (orange) binding profiles to ZIKV particles (144 h harvest) (top) and ZIKV E protein (bottom) are compared to viral load (Zika open-research portal 2016) (black) from pre-infection (day 0) to 28 DPI for ZIKV-challenged NHPs (n = 9). Second- (IgM), third- (IgG) and fourth- (viral load) order polynomial curves were fitted to the data, with fitted lines and shading under the curve consistent with data point colors.

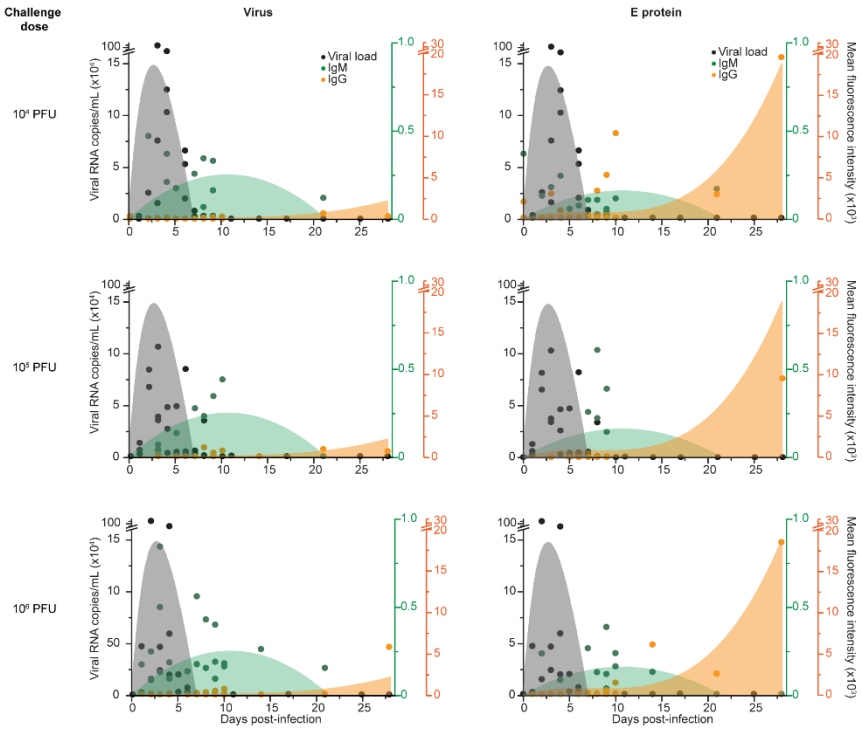

Figure 14. The kinetics and magnitude of humoral immune responses to ZIKV by non-human primates are not affected by challenge dose. IgM (green) and IgG (orange) binding profiles to ZIKV particles harvested at 144 h (left) and ZIKV E protein (right) are compared to viral load (black) from pre-infection (day 0) to 28 days post-infection for non-human primates challenged with either 10^4 (top), 10^5 (middle), or 10^6 (bottom) plaque forming units (PFU) of ZIKV. Second- (IgM), third- (IgG) and fourth- (viral load) order polynomial curves were fitted to the entire data set, as shown in Fig. 11C, and data from separate challenge doses (n = 3 for each dose) is overlaid on the fitted curves. Fitted lines and shading under the curves are consistent with data point colors.

Cross-reactivity of antibodies from primary flavivirus infections

The E proteins of ZIKV and DENV have a high degree of structural similarity that may contribute to shared antibody epitopes. I examined NHPs (*M. mulatta*) challenged independently with DENV1-4 (Figure 6B) (Fernandez *et al.* 2011). For virus, antibodies (30 DPI) from NHPs infected with any DENV serotype were highly cross-

reactive to heterologous DENV serotypes and ZIKV (Figure 15A, Table 2). Further, DENV2 and 3 antibodies displayed substantially higher reactivity with the heterologous ZIKV, while IgG from ZIKV-challenged NHPs was more specific for ZIKV at the virus level, with a lower overall level of cross-reactivity towards DENV1-4 (Figure 15A). In contrast with viruses, the E proteins presented antibody recognition profiles that were very specific for the challenge virus (Figure 15A), and minimal antibody recognition of E proteins from ten more distantly related flaviviruses (Figure 16A). DENV-challenged NHPs exhibited the highest antibody binding to the E protein from the DENV challenge serotype, and antibodies from ZIKV-challenged NHPs essentially bound only to ZIKV E antigens. To assess the similarity of antibody-antigen interactions within groups of infected NHPs, a principal component analysis (PCA) was performed. Principle component analysis can be used to visualize the covariance between pairs of data features that correspond to antibody binding to E or virus antigens in my analysis. The PCA based on antibody recognition of DENV and ZIKV E antigens differentiated serotype-specific DENV and ZIKV infection sera due to the higher degree of homotypic E recognition (Figure 14B). In contrast to the E antigen results, PCA based on IgG recognition of virus only enabled distinction of ZIKV- from DENV-challenged sera, whereas DENV serotype-specific clusters were not evident (Figure 14B). Furthermore, antibodies from NHPs challenged with African or Asian-lineage ZIKV were not differentiated by E or virus (Figure 13, 15B). I also considered YFV, both as a nearest neighbor of ZIKV and DENV (Figure 12), and because vaccination against yellow fever is common in many countries with high dengue prevalence. While serum antibodies from NHPs vaccinated with the 17D YFV strain (Figure 6B) (Durieux 1956) predominantly recognized the E

antigen of YFV (Figure 16A), a modest level of cross-reactivity was evident with several other E, including those of ZIKV and TBEV.

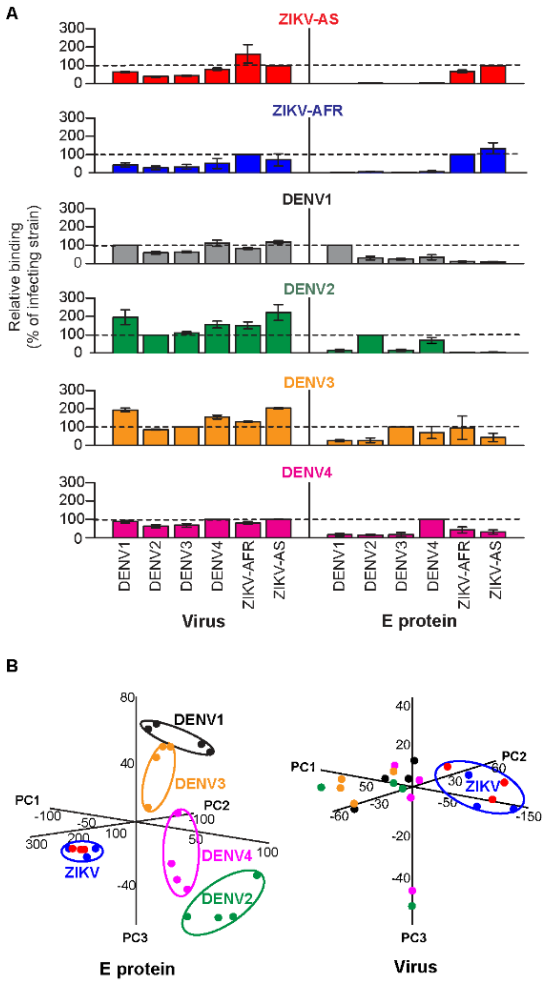

Figure 15. Highly specific antibody responses to E protein were detected in non-human primates infected with ZIKV and DENV, while a significant level of cross-reactivity was observed towards virus particles. (**A**) Binding of convalescent serum antibodies from non-human primates (NHP) challenged with either an Asian (H/PF, red, n = 3) or African (MR-766, royal blue, n = 3) –lineage ZIKV, or DENV (n = 4 each for DENV1, black; DENV2, green; DENV3, orange; and n = 3 for DENV4, magenta) to whole viruses (144 h, left) and E proteins (right). Values shown are antibody binding signals relative to the virus used for challenge (± SEM). (**B**) Principal component analyses of relative IgG binding to E proteins (left) and viruses (144 h, right) by NHP antibodies. Individual data points and virus-specific clusters are colored according to challenge virus as in **A**.

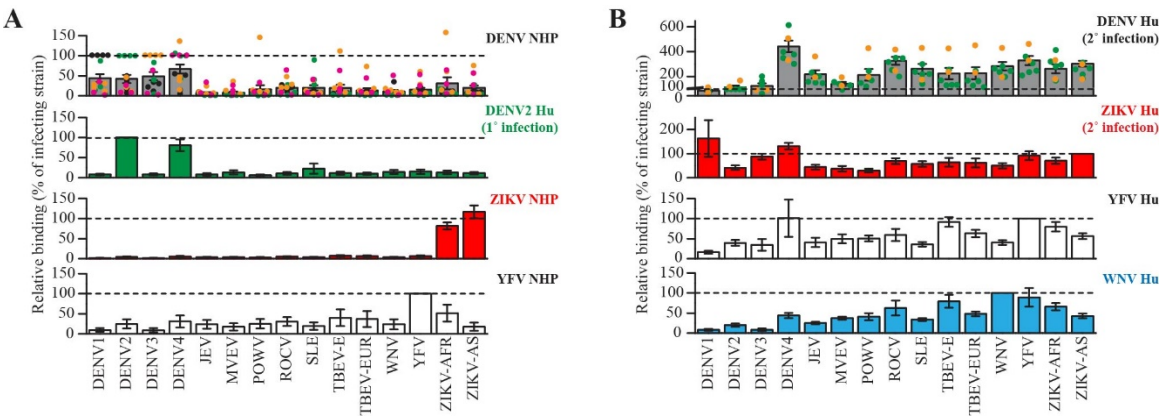

Figure 16. Antibody specificity of primary and secondary flavivirus infections. Relative binding (± SEM) of convalescent serum antibodies from non-human primate (NHP) and human flavivirus infections to fifteen flavivirus E proteins. (**A**) Sera from primary infections: grey, DENV-challenged NHPs (individual data from each NHP is overlaid in a scatter plot: n = 4 each for DENV1, black; DENV2, green; DENV3, orange; and n = 3 for DENV4, magenta); green, human rDEN2Δ30 (n = 8); red, pooled African and Asian-lineage ZIKV NHPs (n = 6); white, YFV-vaccinated NHPs (n = 3). (**B**) Sera from confirmed human flaviviral infections with unknown infection histories: grey, DENV (individual data is overlaid in a scatter plot and colors correspond to most recent DENV infection: DENV2, green (n = 5); DENV3, orange (n = 2)); red, ZIKV (n = 4); white, YFV vaccination (n = 13); cyan, WNV (n = 20). (**C**) Predicted infection histories of human secondary DENV (**B**, grey) and primary ZIKV (**B**, red) infections, based on a supervised SVM classifier. Individual human sera are shown at the bottom (Z, ZIKV; D2, DENV2; D3, DENV3; followed by sera identification (ID) number), with probability values for each viral class (left) gradient colored from low to high (white – royal blue, right). Predicted infection histories are designated by colored bar above sera ID (DENV1, black; DENV4, magenta; no prediction, unfilled).

The animals in the ZIKV, DENV, and YFV infection studies I examined were captive-raised in isolation from most infectious diseases. Therefore, it was important to compare results from the naïve backgrounds of animal disease models with primary infections of humans without documented prior exposures to flaviviruses. Human infection models of dengue were recently developed to assess the efficacy of live attenuated DENV vaccines (Larsen *et al.* 2015). Human challenges with the attenuated DENV2 strain rDEN2Δ30 (Kirkpatrick *et al.* 2016) result in a mild disease, with viremia, rash, and

neutropenia. I examined sera collected from flavivirus-naïve subjects 28 days after challenge (10^3 PFU) with rDEN2Δ30 by subcutaneous injection (Figure 6C) (Kirkpatrick *et al.* 2016). Among the extended panel of E proteins (Table 2), human antibody responses to rDEN2Δ30 resulted in specific recognition of the E protein from DENV2 and to a lesser degree DENV4 (Figure 16A, Figure 17A), which is most similar to DENV2 among all other flaviviruses (Figure 12). Low levels of neutralizing antibodies against other DENV serotypes were previously reported for individuals challenged with rDEN2Δ30 (VanBlargan *et al.* 2013). For viruses, extensive human antibody cross-reactivity was again noted for other DENV serotypes and ZIKV strains (Figure 17A). These results indicated that the NHP DENV challenge model replicated the antigen-specificity profile of human antibody responses to primary infection.

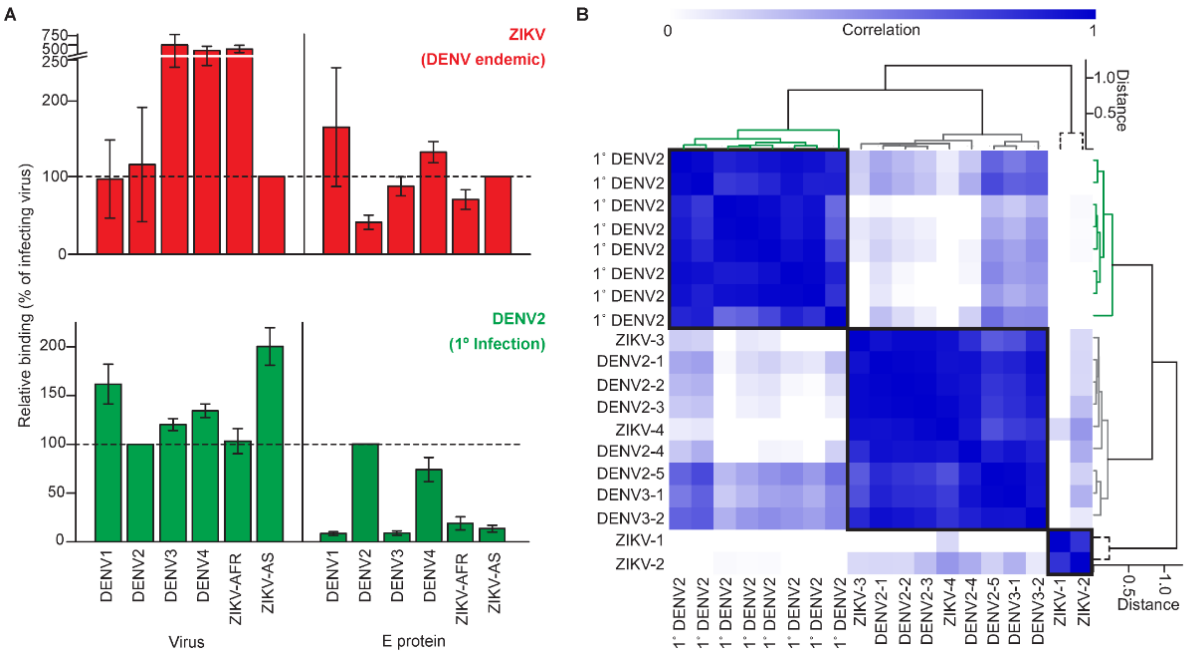

Figure 17. Antibody-E protein binding patterns are distinct for ZIKV- or DENV-infected humans. (**A**) Binding of convalescent serum antibodies from humans challenged with the attenuated rDEN2Δ30 strain (green, n = 8) or from primary ZIKV infections from a dengue-endemic country (red, n = 4) to viruses (144 h, left) and E proteins (right). Values shown are antibody binding signals (± SEM) relative to the infecting virus. (**B**) Correlation matrix of antibody binding patterns of all human infection samples to DENV and ZIKV E proteins, with Pearson correlation coefficients gradient colored from low (0, white) to high (1, royal blue), as indicated at the top of the matrix. Hierarchical clustering (Pearson correlation, average-linkage) reveals three distinct clusters (rDEN2Δ30, green; unknown prior history, grey and dashed black). Individual sera identification numbers follow the dash for DENV and ZIKV-infected humans and are consistent with labels in Fig. 17.

Antibody cross-reactivity between flaviviruses could be influenced by homology of sequences and structures, as well as the abundance and degree of cross-reactive antibodies in polyclonal sera. For example, cross-reactivity could be due to a small population of antibodies that exhibit high levels of specificity for heterologous E proteins, or may be due to a larger population of antibodies that exhibit broad cross-reactivity. Although the highest recognition of the homologous E protein was common for antibodies from primary infections, I observed differences in the amount of total antibody across virus

species (Figure 18). Comparing results obtained with all E proteins, cross-reactive antibodies were undetectable for ZIKV, while DENV1 and DENV2 antibodies recognized other DENV serotypes. Antibodies from DENV3-infected and YFV-vaccinated NHPs exhibited the lowest binding to the respective E proteins, while a high level of DENV2 E-specific antibodies interacted with the DENV2 E protein (Figure 18). The lower amount of DENV3 and YFV antibodies that were specific for the cognate E protein, compared to DENV2 for example, contributed to the appearance of an overall higher level of background cross-reactivity (Figure 15A and 16A). Vaccination with the live-attenuated 17D strain results in low levels of viremia that mimic a true YFV infection and lower titers of specific antibodies compared to wild-type YFV infections (Monath T 2008). In addition, antibodies from NHPs challenged with ZIKV (Dudley *et al.* 2016) and DENV (Simmons *et al.* 2010) exhibited neutralizing antibody titers (Dudley *et al.* 2016; Simmons *et al.* 2010) that directly correlated ($R^2 > 0.99$) with the E antibody recognition pattern I observed (Figure 18). I concluded from these results with E proteins that the humoral immune response to primary flavivirus infections is surprisingly specific.

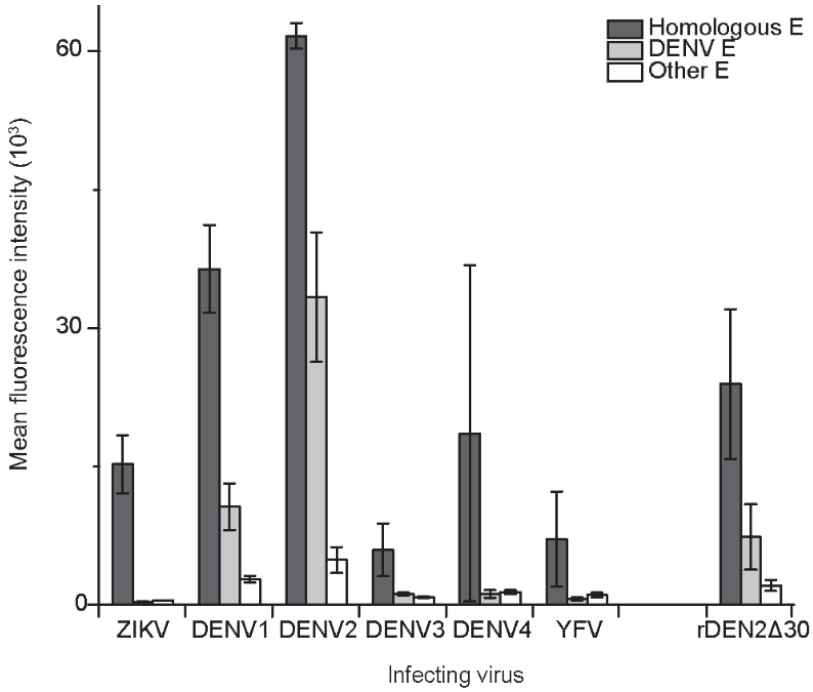

Figure 18. Quantitative comparisons of antibodies directed to the infecting virus versus all other flaviviruses. Antibody recognition of microarrayed E proteins displayed as mean fluorescence intensity (± SEM). Antibodies from primary flavivirus infections of NHPs (ZIKV, DENV1-4, YFV) and humans (rDEN2Δ30) exhibited significantly decreased recognition of heterologous E antigens compared to virus-specific E (dark grey) ($p < 0.05$, one-way ANOVA with Tukey's range test). DENV E proteins (light gray) are separated from all other flavivirus E proteins (white, inclusive of YFV, SLEV, POWV, TBEV, MVEV, WNV, JEV, and ROCV) to show DENV antibody cross-reactivity between serotypes.

Secondary flavivirus infections

The antibodies of flavivirus-naïve NHPs and humans to primary flavivirus infection were highly specific to the E protein of the challenge virus. Because increased levels of antibody cross-reactivity would be expected for flavivirus-primed individuals with secondary flavivirus infection, I next examined human sera after one or more flavivirus exposures. In contrast to results obtained with primary infections, IgG from DENV2 or DENV3 infections occurring in Peru prior to the Zika epidemic (here defined as secondary DENV infections; Figure 6D) collectively interacted with several E proteins, including those from ZIKV (Figure 16B), suggesting that antibodies from previous infections,

possibly DENV4 (based on the amount of IgG bound), dominated immune responses to other flaviviruses. Despite expectations, sera from secondary DENV2 infections did not correlate with primary DENV2 infections (Figure 17B), providing additional evidence of previous dengue infection in these samples. Moreover, although principally recognizing the E protein of YFV, antibodies from human 17D vaccinations (Figure 6F) were less specific compared to those from primary NHP vaccinations, as E from DENV4 and several other flaviviruses were also targeted (Figure 16B). It is possible that the less specific YFV responses were a result of declining antibody titers, as the sera were collected up to 118 days after vaccination. I further noted that serological responses from WNV infections that occurred in North America (Figure 6E), a region with only a small incidence of dengue, exhibited elevated antibody interactions with E from WNV and a few other flaviviruses, but only a low level of interactions with DENV antigens (Figure 16B). Finally, I examined primary ZIKV infections from the Dominican Republic (Figure 6D), a dengue-endemic Caribbean country. Antibodies from ZIKV infections interacted to a greater extent with E proteins from DENV compared to ZIKV (Figure 16B and Figure17A), and also recognized E proteins from several other flaviviruses. It is important to note that levels of total E-specific antibodies from all human flavivirus exposures were significantly reduced compared to levels observed in primary infections (Figure 18). While maximum E-specific antibody abundance never exceeded the low levels of binding observed for primary YFV and DENV3 exposures, these results suggested that serum levels of anti-E antibodies were predominantly driven by infection histories, and it is conceivable that at least one DENV infection preceded each clinical disease examined with sera from secondary infections.

Given the complexity of the human antibody response from primary ZIKV and secondary DENV infections (Figure 6D), I attempted to estimate both the probability of previous flavivirus exposures and to identify the likely antecedent virus. A supervised machine learning method was used (performed by Dr. Sarah L. Keasey) to classify sera by features of antibody binding to the extended panel of fifteen E proteins (Table 2). The support vector machine (SVM) classifier was trained on a positive set of E-specific antibody binding signals from primary flavivirus infections and a negative set of background signals from flavivirus-naïve sera. The performance of the SVM was evaluated using a 10-fold cross-validation re-sampling method, which readily differentiated infected from naïve sera and different primary infections, resulting in a total model accuracy of 98.5%. Using a probability cutoff value of ≥ 0.5, the classifier was used to predict flavivirus exposures that occurred prior to the secondary DENV and ZIKV infections. Four secondary DENV2 sera were predicted to have had a previous DENV4 infection, while high probability for two primary ZIKV sera suggested a previous DENV1 infection (Figure 19), which was consistent with clustering based on correlated antibody binding (Figure 17B). Lower overall probabilities for single virus infections were observed for the remaining secondary DENV and ZIKV samples, and classification to a single group was therefore not possible (Figure 19). For example, a secondary DENV3 serum had comparable probability values for DENV2 (0.28) and DENV4 (0.27), respectively, suggesting a previous infection with either virus. The inclusion of more extensive training data sets for primary ZIKV and other viral infections will be important for refining the predictive power of the described SVM method.

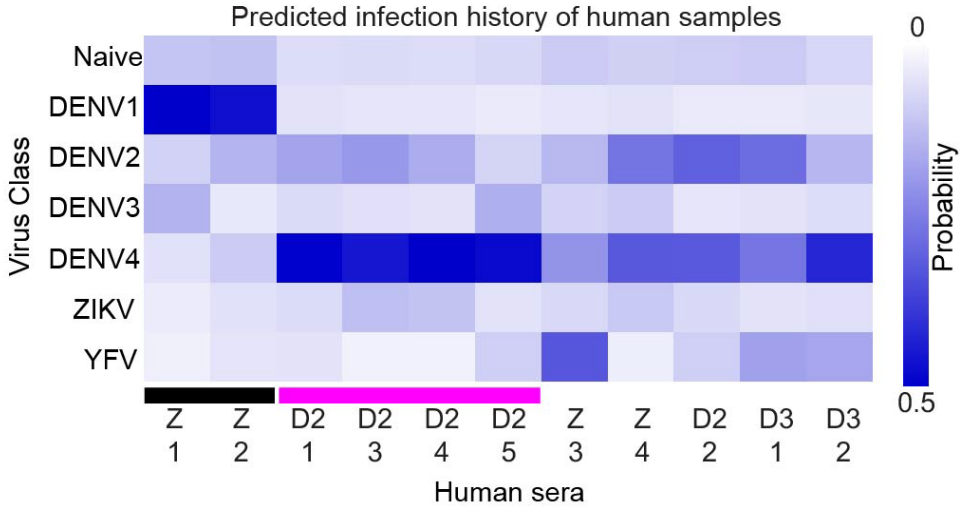

Figure 19. E-specific antibody recognition patterns can be used to predict previous flavivirus exposures. A supervised machine learning method (SVM classifier) was used to predict infection histories of human secondary DENV (shown in Fig. 14B, grey) and primary ZIKV (shown in Fig. 14B, red) infections, by features of antibody binding to the panel of 15 E proteins. Individual human sera are shown at the bottom (Z, ZIKV; D2, DENV2; D3, DENV3; followed by sera identification (ID) number), with probability values for each viral class (left) gradient colored from low to high (white – royal blue, right). Predicted infection histories are designated by colored bar above sera ID (DENV1, black; DENV4, magenta; no prediction, unfilled).

Development of an YFV focused microarray and serological assay.

The YFV strain 17D is a live attenuated virus that has been used for many years as an effective vaccine for prevention of yellow fever. However, due to recent yellow fever outbreaks in Africa and South America that are acerbated by insufficient vaccine coverage, there is a critical need to understand the longevity of antibody response to vaccination and the need for boosting. To examine serological immune responses to YFV vaccination, a yellow fever focused microarray of recombinant E, NS1, and pM protein antigens, as well as strain 17D whole virus. The recombinant proteins from YFV, along with closely related DENV1-4 antigens, were produced as previously described above. For the production of vaccine strain of YFV, Vero cells were infected with 17D virus (ATCC# NR-116) and harvested six days after infection, at a stage with a high amount of cytolysis. Viral

supernatants were filtered and concentrated ~225-fold, based on volume, by precipitation with polyethylene glycol (PEG 8000, Promega).

Following confirmation of the propagated YFV (str. 17D), the concentrated virus was printed in 2-fold serial dilutions in replicates (n=6) on nitrocellulose-coated microarray surfaces, to determine the optimal concentration of YFV that produced the best signal above background binding levels. The 17D virus preparations, control antigens, and recombinant proteins from YFV and DENV1-4, were printed in a combined microarray by using previously determined conditions on the same microarray surface (Table 3). The controls antigens included IgGs (monkey, human, rabbit, goat, and mouse), IgMs (human, monkey, and rabbit), HisMBP, bovine serum albumin (BSA), three hemagglutinin proteins (HA) from three strains of seasonal influenza, serial dilutions of anti-human IgG, human cytomegalovirus glycoprotein B (CMV-gB), and buffer control spots. The printed antigens were evaluated by SYPRO®Ruby protein stain to quantify total protein (Figure 20) and estimate precision for protein spotting. The overall mean CoV for all printed probes on the microarray was determined to be 14% between all replicates across each of the four printed microarrays. The deposited YFV and DENV1-4 recombinant proteins were visualized by antibody detection of the N-terminal 6X His fusion tag (Figure 21) to confirm placement on the microarray surface. While the deposition of all antigens was confirmed based on protein stain and anti-His antibody results, I observed higher binding to DENV4-E protein. This may indicate that DENV4-E was deposited in greater concentration than other heterologous flavivirus antigens. Further confirmation of the printed antigens was performed with mouse anti-sera raised against YFV, and with reference standard sera (ATCC) from non-human primates (NHP; rhesus macaques) that were vaccinated with

YFV strain 17D. Microarray assay results obtained with the mouse and NHP anti-sera confirmed predominant IgG recognition of E and whole YFV virus, while lower levels of IgG binding were detected for YFV- NS1 and pM (Figure 22A and C). Specific serum antibody binding to printed array spots of YFV was readily detected for 17D preparations that were serial diluted from 1:2 to 1:16 (Figure 22 B and D).

Table 3. Flavivirus and control antigens included in the YFV-focused microarray.

Virus[1]	Isolate	Country	Year	Targeted antigens[2]			
				Virus	E	pM/M	NS1
DENV1	**HAWAII**	**USA**	**1944**		**x**		**x**
DENV2	**NGC**	**New Guinea**	**1944**		**x**		**x**
DENV3	**H87**	**Philippines**	**1956**		**x**		**x**
DENV4	**H241**	**Philippines**	**1956**		**x**		**x**
YFV	**17-D-204**	**USA**	**1985**	**x**	**x**	**x**	**x**
Control Antigens							
IgGs: human, NHP, rabbit, goat, and mouse							
IgMs: human, NHP, and rabbit							
Anti-human IgG: dilution series ranging from 12.5-400 μg/mL							
Influenza hemagglutinin (HA) proteins: Brisbane, California, and Perth strains							
E.coli HisMBP							
Bovine serum albumin (BSA)							
Human cytomegalovirus glycoprotein B (gB)							
HEPES print buffer							

The "x" indicates antigens that were produced, whereas unfilled squares are antigens that were not attempted for production.

[1]Virus abbreviations: dengue (DENV) and yellow fever (YFV).

[2] Antigen abbreviations: Transmembrane domain truncated envelope protein (E), precursor membrane or membrane protein (pM/M), and non-structural protein 1 (NS1).

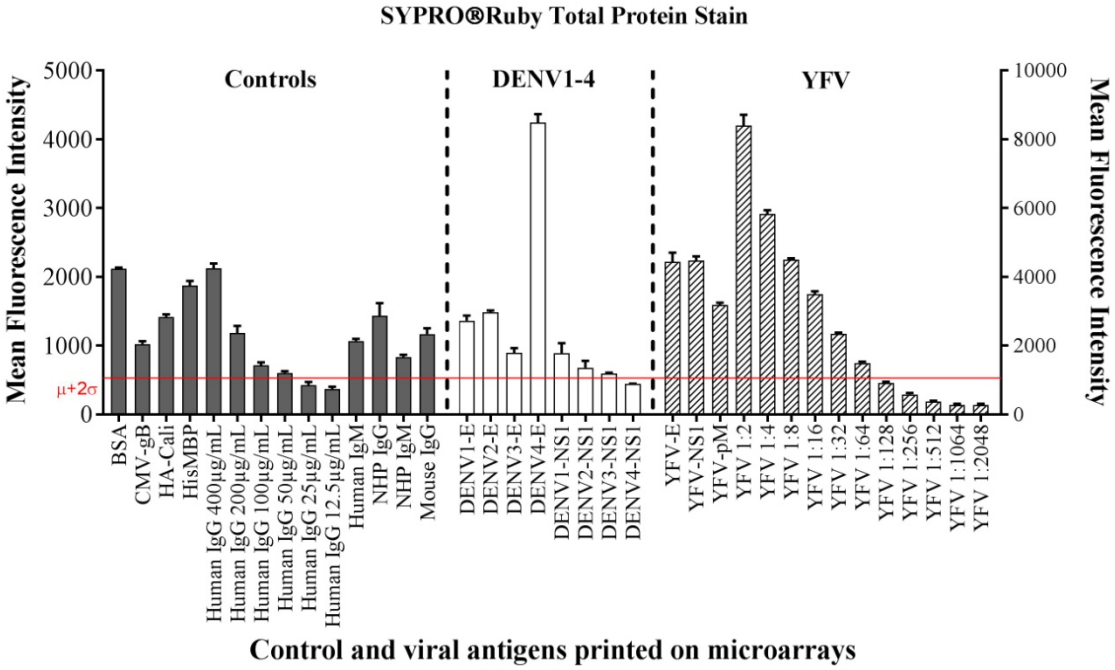

Figure 20. Protein and 17D virus printing precision. Bound antigens on the nitrocellulose microarrays were stained using SYPRO®Ruby total protein stain and then visualized fluorescently with a laser scanner at 488nm. Background-corrected fluorescence intensities of the detected total protein were averaged across technical replicates (n=6) on the microarrays. The bars represent mean fluorescence intensity ± standard error of the mean (SEM). Total protein measured by fluorescence intensity is represented on the left y-axis for control antigens (gray bars), while DENV1-4 E and NS1 proteins (unfilled bars), YFV proteins (E, NS1, and pM) and dilutions of whole virus (diagonal patterned bars) are represented by fluorescence signals on the right y-axis. The red horizontal line indicates the mean plus two standard deviations away from the mean (μ+2σ) fluorescence intensity of printing buffer control spots.

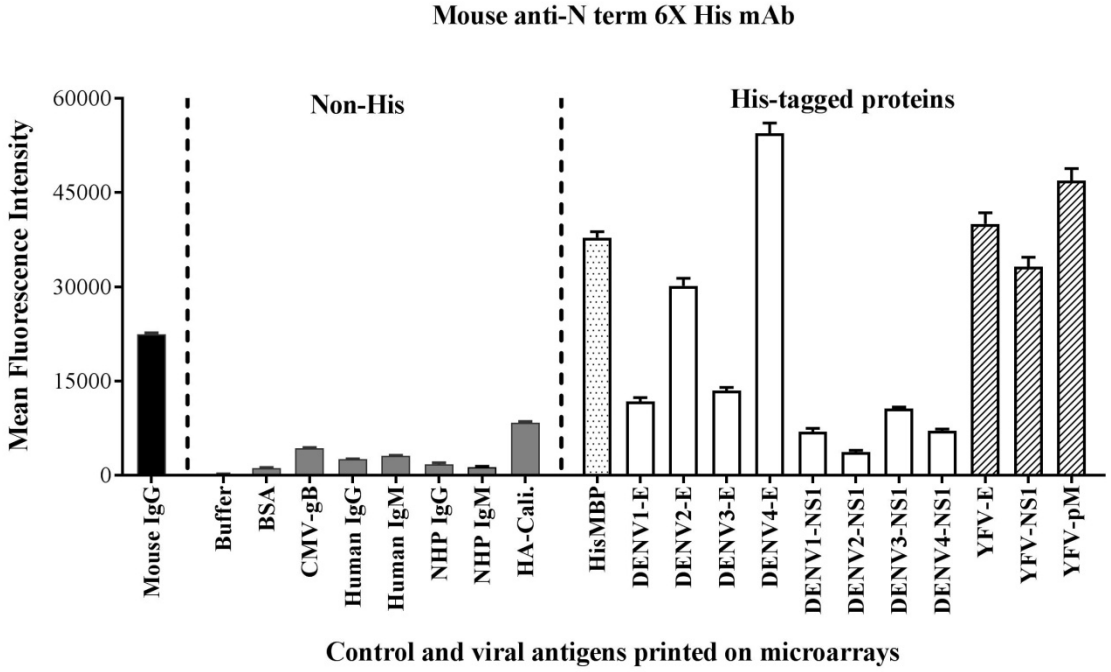

Figure 21. Characterization of recombinant proteins on the YFV microarrays by anti-His monoclonal antibody. Bound antigens on the nitrocellulose microarrays were probed with mouse anti-6X His monoclonal antibody (1:2000) in order to detect the N-terminal 6X fusion tag of the *E.coli* expressed recombinant DENV (unfilled bars) and YFV proteins (diagonal patterned bars). Antibody recognition of non-His tag proteins (gray) are also shown for comparison. Mouse IgG (black bar) was detected and shown to validate the quality of the anti-mouse Alexa647-conjugated secondary antibody. Background-corrected fluorescence intensities of the detected His tag were averaged across technical replicates (n=6) on the microarrays. The bars represent mean fluorescence intensity ± standard error of the mean (SEM).

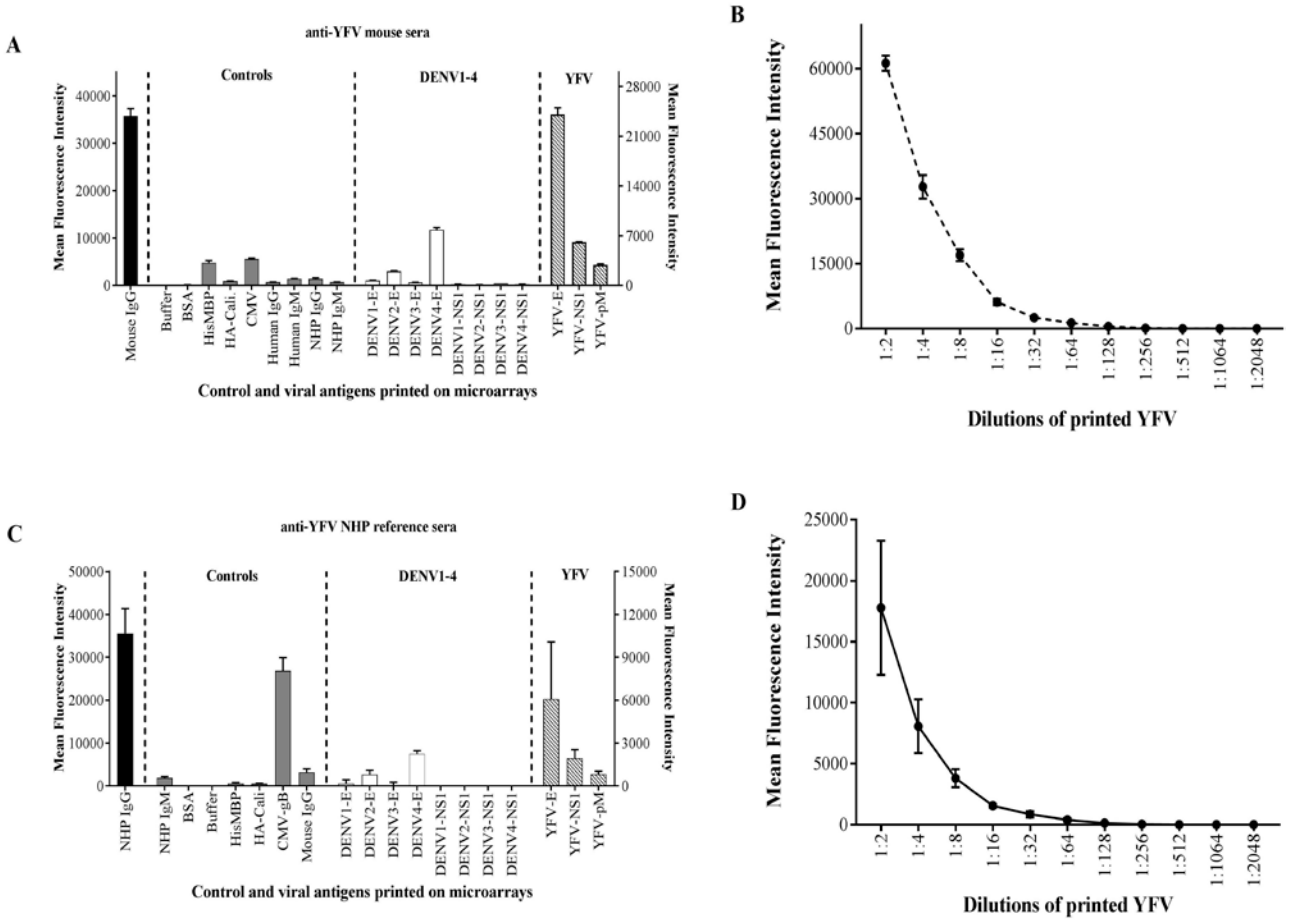

Figure 22. Specificity of polyclonal antibody standards for printed YFV antigens. Microarrays of YFV and DENV1-4 antigens (envelope (E), non-structural protein 1 (NS1), precursor membrane (pM), YFV virus (strain 17D) were probed with mouse polyclonal antibodies against YFV (**A** and **B**) or sera from YFV-vaccinated non-human primates (NHP, collected 30d post-immunization) (**C** and **D**). Antibody binding to viral proteins (**A** and **C**) or serial dilutions of whole YFV virus (**B** and **D**) is shown as the mean fluorescence intensity (MFI) of signals ± SEM of replicate protein spots (**A** and **B**, n=6) or sera samples (**C** and **D**, n=3). In **A** and **C**, antibody recognition of control probes (left axis; species-specific IgG, black; all others, gray) is compared to viral antigens (right axis; DENV, unfilled; YFV, patterned).

Analysis of YFV specific antibody responses to vaccination.

A search of the DoD Serum Repository identified subjects vaccinated with 17D, number of vaccinations, and lapsed time to blood collection. Sera obtained from this repository inquiry included 68 vaccinated individuals who were randomly selected to include time points of one month to sixteen years from the last day of vaccination (Table 4). The sera were employed to examine antibody responses to 17D in comparison to individuals (n=6) without a prior history of YFV immunity. I first examined spot densities for 17D virus deposited on the microarray, and observed a high background signal for antibodies from naïve subjects, which increased with greater density of virus. A 1:2 dilution of the virus was chosen for data analysis based on optimal signal to noise ratio (maximum signal difference between vaccinated and naïve) for antibody responses of all YFV vaccinated individuals in comparison with non-vaccinated subjects (Figure 23). Serum IgG binding to E and whole virus were significantly elevated (p 0.03 and <0.0001; respectively, Figure 24A) in vaccinated individuals as compared to non-vaccinated, while the relative amount of antibody bound to NS1 and pM was also elevated, but not statistically significant. The level of IgG binding to 17D whole virus was higher (>2.5 fold) than E, perhaps because the spot density of virus was much greater than the recombinant protein. A receiver-operator characteristics (ROC) curve was generated using the microarray antibody binding results of naïve and 17D vaccinated individuals to each YFV antigen in order to determine the strength of the antigen as a classifier of YFV immunity. Whole virus and E antigens had a greater ability to discriminate between antibody responses of naïve and YFV immune individuals than NS1 and pM, with area under the curve (AUC) values of 0.95 (p 0.0001) and 0.85 (p 0.0052) for virus and E, respectively (Figure 24B). Furthermore, strong positive correlation (Pearson's r=0.7, p<0.0001)

between antibody binding to whole virus and recombinant E was observed (Figure 25). Taking into consideration serum IgG recognition of both E and whole virus, it was determined that 98.3% of subjects that received either a single or multiple dose of the 17D vaccine had a significantly elevated ($\mu+2\sigma$) antibody response to the respective YFV antigen relative to non-vaccination individuals. In summary, these results indicated that antibody binding to E and whole virus discriminated immune responses of vaccinated from non-vaccinated individuals.

Table 4: Sera examined from naïve and YFV (17D) immunized subjects.

Vaccination cohort	Time cohort	Days post-vaccination	Total # patients
	30-90d	51[1] (32-82)[2]	19
	90-270d	196 (91-270)	18
Primary (n=62)	270-364d	302 (282-350)	11
	1-6yr	1106 (365-2151)	7
	6-16yr	3984 (2587-5810)	8
Boosted	1-6yr[3]	846.5 (385-1907)	6
Non-vaccinated	Naïve, d0	0	6

[1] median day post-vaccination
[2] minimum and maximum range of days post-vaccination
[3] time cohort represents year post most recent vaccination, days post-primary vaccination ranged from 4169-10,098d with 4849d as the median day post-primary vaccination

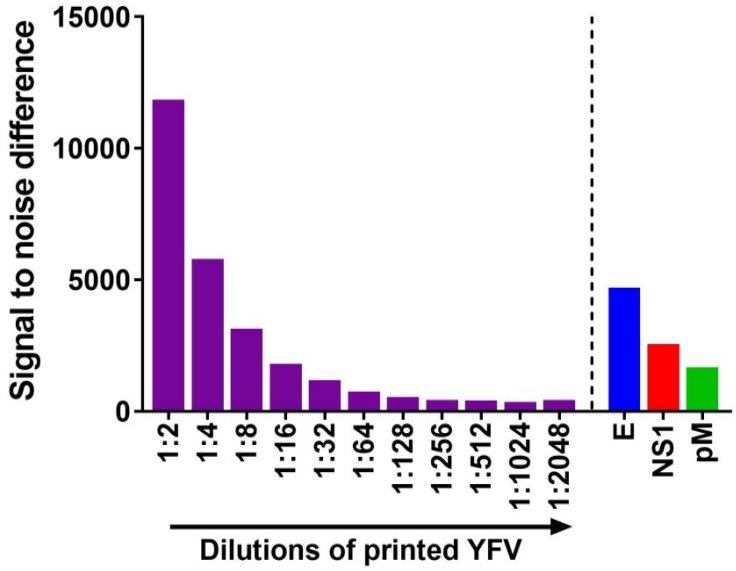

Figure 23. Evaluation of specific IgG binding to varying microarray spot densities of YFV and fixed concentrations of YFV proteins. Antibody responses to 11, two-fold serial dilutions of whole virus (strain 17D) and 200µg/mL dilutions of YFV proteins (envelope, E (blue), non-structural protein 1, NS1(red), and precursor membrane protein, pM (green) were assessed in YFV vaccinated subjects (n=68) and six YFV naïve individuals . In order to determine the optimal concentration of viral antigen that provided YFV-specific IgG recognition, mean relative fluorescence signals of naïve were subtracted from signals of vaccinated subjects (signal to noise difference).

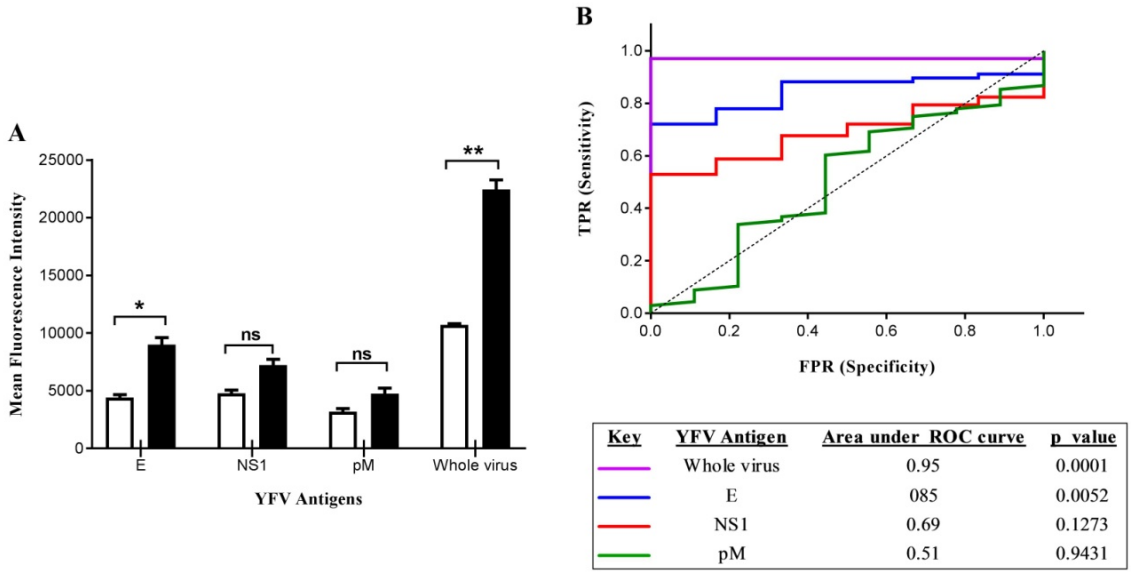

Key	YFV Antigen	Area under ROC curve	p value
	Whole virus	0.95	0.0001
	E	085	0.0052
	NS1	0.69	0.1273
	pM	0.51	0.9431

Figure 24. Antibody recognition of YFV-E and whole virus distinguish antibody responses between YFV vaccinated subjects and naïve. (A) Serum IgG binding to recombinant YFV proteins (envelope: E, non-structural protein1:NS1, and precursor membrane protein: pM) and whole virus (str.17D) were measured in 68 yellow fever immunized patients (filled bars) and compared to six non-vaccinated individuals (open bars). Error bars indicate standard error of the mean. Statistically significant differences between mean antibody binding to YFV antigens in vaccinees as compared to non-vaccinated controls were calculated using two-way analysis of variance (ANOVA) (*, p 0.03, **, p<0.0001, ns = not significant). **(B)** Receiver-operator characteristic (ROC) curves were generated for each YFV antigen to determine the strength of the antigen as a classifier of YFV immunity. The false positive rate (FPR) depicted on the x-axis is the fraction of antibody interactions that were misclassified (specificity), while the true positive rate (TPR) on the y-axis denotes the fraction of antibody interactions that were correctly classified by the specific antigen (sensitivity). The table indicates the color key for the different ROC curves with the area under the curve (AUC) values, along with p-values listed to the right of the individual YFV antigen.

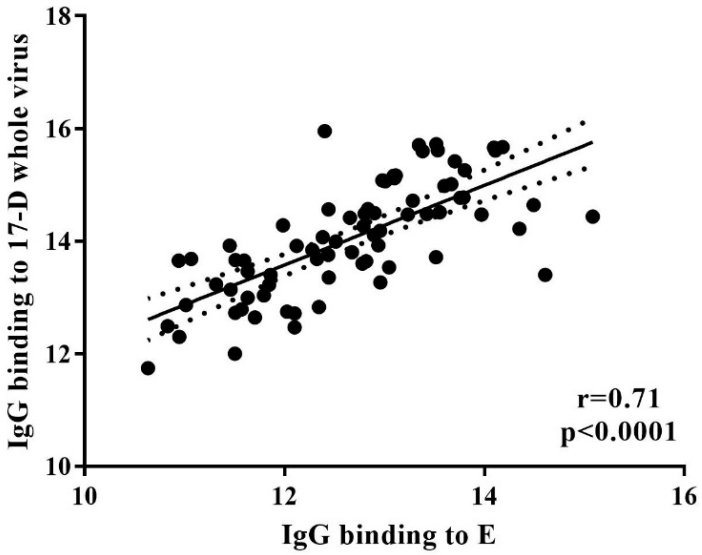

Figure 25. Correlation of antibody responses to YFV envelope (E) and whole virus. Pearson's correlation analysis was performed using results of serum IgG binding to YFV-E and whole virus as measured by microarray assays of all vaccinated (n=68) and non-vaccinated (n=6) subjects. Values shown are log_2 transformed mean fluorescence intensity of antibody binding (IgG) signal to E (x axis) and YFV whole virus (y-axis). The dotted lines indicate the 95% confidence bands of the best fit line. Pearson's rank r value and p value are displayed on the scatter plot.

Longevity of antibody responses to YFV

In order to examine immunological responses to YFV proteins and whole virus over time, serum IgG responses of primary vaccinated individuals (n=62) that ranged from 32 days to 15.9 years post-vaccination were examined (Table 4, Figure 6F). Because only specimens collected from one time point were available for each subject, the average polyclonal antibody response to YFV antigens was measured in six time intervals after vaccination (NV d0, 30-90d PV, 91-270d PV, 271-364d PV, 1-6yr PV, 6-16yr PV). Antibody responses to recombinant proteins (E, NS1, and pM) and whole virus increased progressively from 30-90d to 270-364d post-vaccination, and were significantly decreased for 1-6yr and 6-16yr post-vaccination in primary vaccinated individuals (Figure 26).

Compared to the 271-364d time interval, mean levels of antibody binding decreased substantially to all YFV antigens for vaccinated subjects from the 1-6yr and 6-16yr time intervals after vaccination, while serum IgG binding to 17D whole virus remained higher compared to non-vaccinated sera and was negligible for recombinant proteins. The total number of seropositive subjects to YFV vaccine, defined as those subjects having significantly elevated IgG responses to YFV antigens in comparison to naïve binding signals ($\mu + 2\sigma$), was determined for all vaccinated subjects (Table 5). A similar pattern to the kinetics of antibody responses to YFV vaccine was observed with percent seropositivity. The number of seropositive subjects increased from 30 to 271-364d after vaccination followed by a dramatic decline in the percent of patients that had a significant antibody recognition to recombinant antigens (Table 5). However, only a slight drop in seropositivity was seen towards whole virus over time. Furthermore, vaccinated subjects exhibited distinct levels of antibody binding to YFV proteins and whole virus antigens according to time post-vaccination (Figure 27). Hierarchical clustering was used to visualize the overall results for antibody interactions with the microarray YFV antigens. The majority of the 6-16yr post-vaccination subjects clustered with the non-vaccinated subjects, while the 30-90d and 270-364d along with a few patients from the 1-6yr time point blended together with higher antibody binding observed to E and whole virus (Figure 27). Interestingly, one subject from the 30-90d time point and two from the 91-270d time point had higher binding to NS1 and pM antigens than YFV-E or whole virus. Further, all patients from the 270-364d time point clustered separately due to distinctly high IgG recognition of all YFV antigens on the microarray.

Table 5. Longevity of IgG responses to YFV antigens for primary and boosted vaccinated subjects.

	Primary					Boosted
YFV Antigen	30-90d (n=19)	91-270d (n=17)	271-364d (n=11)	1-6yr (n=7)	6-16yr (n=8)	1-6yr[2] (n=6)
E	68.42[1]	88.24	100.00	28.57	0.00	100.00
NS1	31.58	58.82	100.00	14.29	0.00	83.33
pM	21.05	35.29	100.00	14.29	0.00	66.67
Whole virus	94.74	100.00	100.00	100.00	87.50	100.00

[1] Total % of patients that had significantly elevated IgG binding over the cutoff value to the given antigen relative to non-vaccinated individuals (cutoff= μ binding of YFV antigen in non-vaccinated controls+2σ).
[2] Time post-secondary YFV vaccination in boosted individuals.

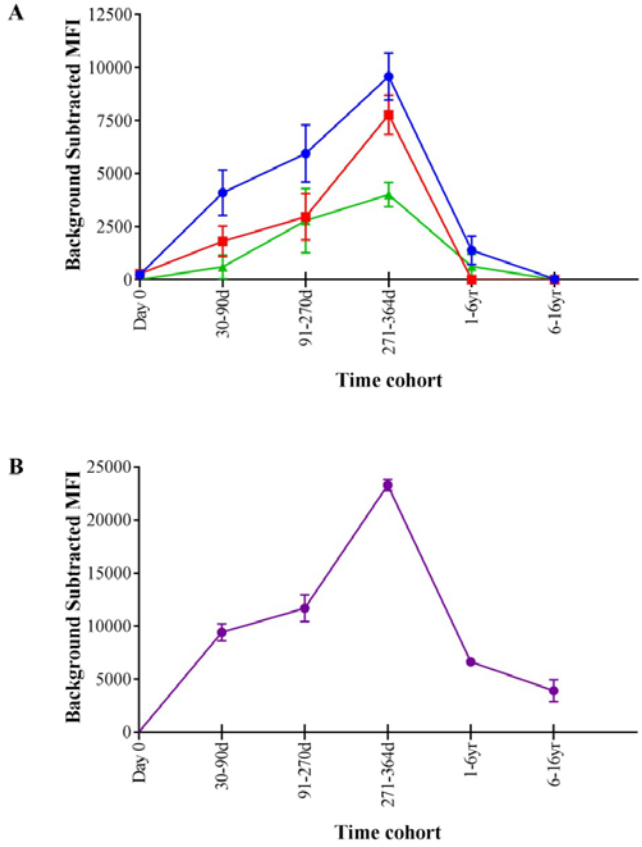

Figure 26. Kinetics of humoral immune response to YFV vaccination. Human IgG binding to (**A**) YFV proteins (envelope: E (blue), non-structural protein 1: NS1 (red), precursor membrane protein: pM (green) and (**B**) whole virus strain 17D (purple). 30-90d , n=19; 91-270d , n=17, 271-

364d, n=11; 1-6yr, n=7; 6-16yr, n=8: non-vaccinated individuals, n=6. Serum antibody binding to printed antigens was detected with Alexa647 conjugated anti-human IgG (γ specific) secondary antibody. The relative amount of antibody bound was measured as mean fluorescence intensity (MFI). The values shown are the MFI of the immunized antibody response after subtracting results for non-vaccinated MFI by antigen. Error bars indicate +/- standard error of the mean.

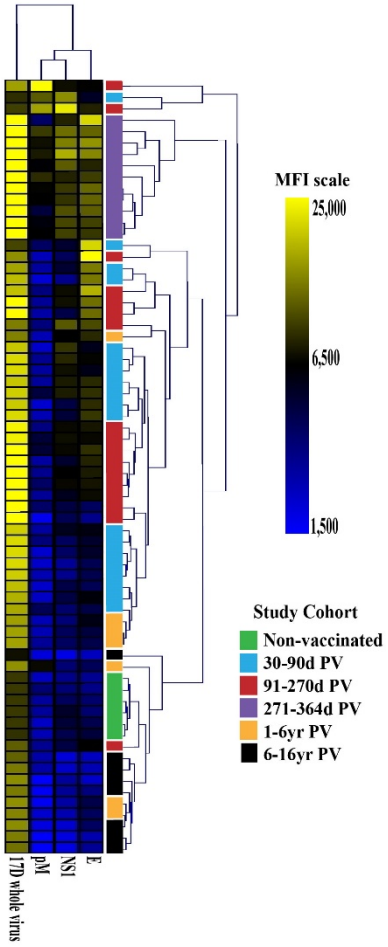

Figure 27. Relationship between IgG binding to YFV antigens and time from vaccination. Hierarchical clustering, using Euclidean distance- average linkage method with normalized mean fluorescence intensity data (MFI) of IgG binding to YFV proteins (E, NS1, and pM) and whole virus, was used to visualize protein microarray results. YFV vaccinated (n=62) and non-vaccinated (n=6) sera are listed in rows while yellow fever antigen-antibody interactions are listed in columns, with the YFV antigens listed on bottom of heat map. The gradient color key on the top right of the heat map shows the scale of signal intensity (1,500-25,000 MFI). The color blocks on the bottom right of the heat map represent the subject groups: non-vaccinated, green; and primary vaccinated subjects

separated based on time post-vaccination (PV) 30-90d PV, blue; 91-270d PV, red; 271-364d PV, purple; 1-6yr PV, orange; 6-16yr PV, black.

Comparison of antibody responses to primary and boosted YFV vaccination.

In the results presented above, levels of YFV specific antibodies in primary 17D vaccinated individuals were shown to decrease significantly by one year after vaccination, with an even greater decline observed 6 years later. Due to the observed decrease in primary immune responses at late time points (Figure 26) and the unknown benefit of boosts with a live, attenuated vaccine (17D), I examined antibody responses of subjects who received a boost 1-6yr before specimen collection. For subject sera examined 1-6yr after vaccine boost, there was a significant increase in mean antibody binding to E, NS1, and whole virus compared to antibody responses 1-6yr after primary vaccination ($p \leq 0.009$; E and NS1, $p < 0.0001$; whole virus by 2-way ANOVA) (Figure 28). Comparing time from primary vaccination, antibody responses to all protein antigens (E, NS1, and pM) as well as whole virus were significantly elevated (E, NS1, whole virus; $p < 0.0001$; pM $p < 0.01$ by 2-way ANOVA) in individuals that received multiple YFV vaccines (Figure 28). As noted above, total polyclonal antibody responses to both YFV proteins and whole virus decreased over time with primary vaccinations, but were elevated in individuals boosted within approximately the same length of time.

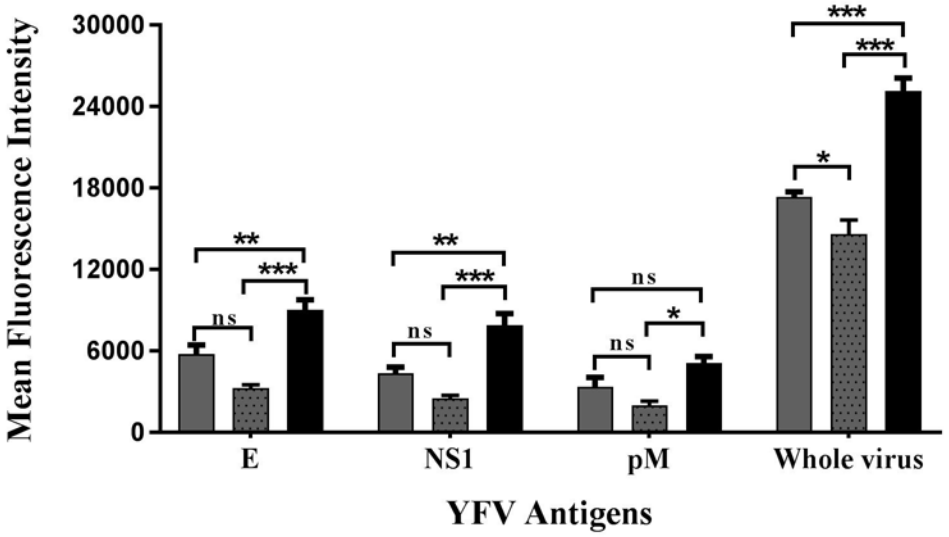

Figure 28. Comparison of antibody responses to 17D from primary and boosted vaccination. Antibody responses to YFV proteins (envelope: E, non-structural protein 1: NS1, and precursor membrane protein: pM) and vaccine strain whole virus in primary 17D vaccinees (gray bars, 1-6yr post-primary vaccination (n=7); gray pattern bars, 6-16yr post-primary vaccination (n=8)) compared to boosted (black bars, 1-6yr post-boost or 6-16yr post-primary before receiving boost (n=6)). Measurement of IgG binding to YFV antigens as measured by microarray analysis is shown as mean fluorescence intensity. Error bars indicate ± standard error of the mean. Statistically significant differences between mean antibody binding to YFV antigens of primary and boosted vaccinations were calculated by two-way analysis of variance (ANOVA) analyses, with multiple comparison's corrected with Sidak's statistical hypothesis testing (*, $p < 0.05$, **, $p \leq 0.009$, ***, $p<0.0001$, ns = not significant).

Because virus neutralization by serum antibodies is commonly used to assess functional immune responses to yellow fever vaccination, the levels of neutralizing antibodies for primary and boost vaccines were examined to provide a basis for comparison with the microarray results. Prior to measuring neutralizing antibodies in patient sera, I determined the optimal length of time for YFV infection, as well as the dilution of virus that would be within the optimal range (7-30% infectivity) suggested for neutralization assays. To do this, I measured infectivity of Vero cells that were incubated with different dilutions of virus for 24 and 48 hr, by flow cytometry method to a monoclonal antibody

(4G2) directed to the E domain II fusion loop peptide that is highly conserved among all flaviviruses. Intracellular virus accumulation was measured by 4G2 and a secondary antibody that was conjugated with Alexa Fluor 488 for detection of fluorescence by laser-excitation flow cytometry. While YFV antigens were not evident in Vero cells infected for 24hr, even at the highest dilution of virus, infected Vero cells were readily detected by 4G2 monoclonal antibody at 48hr (Figure 29), ranging from 5 to 76% for YFV dilutions from 1:3200 to 1:50 (Figure 30). A 1:300 dilution of YFV that led to ~21% infectivity was used for neutralization assay.

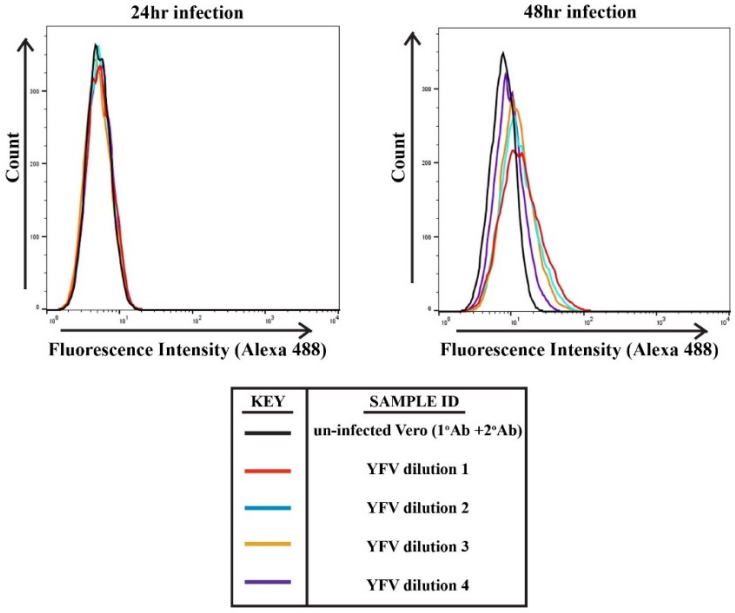

Figure 29. Comparison of 24 and 48hr YFV infected Vero cells using a 24 well plate cell cytometry based infection assay. Vero81 cells seeded in 24-well plates were incubated with media only (un-infected Vero) or infected with media containing different dilutions of YFV for 24 or 48hrs to determine the optimal length of infection that would facilitate detection of YFV infected cells by flow cytometry. Cells were intracellularly stained with 4G2 (pan-flavivirus) mouse monoclonal antibody followed by a goat anti-mouse Alexa488 conjugated secondary antibody for detection of bound primary. The histograms depict the number of cells in each sample that detected a shift in fluorescence intensity, while the table below provides the color key of the un-infected and YFV-infected Vero cell histograms.

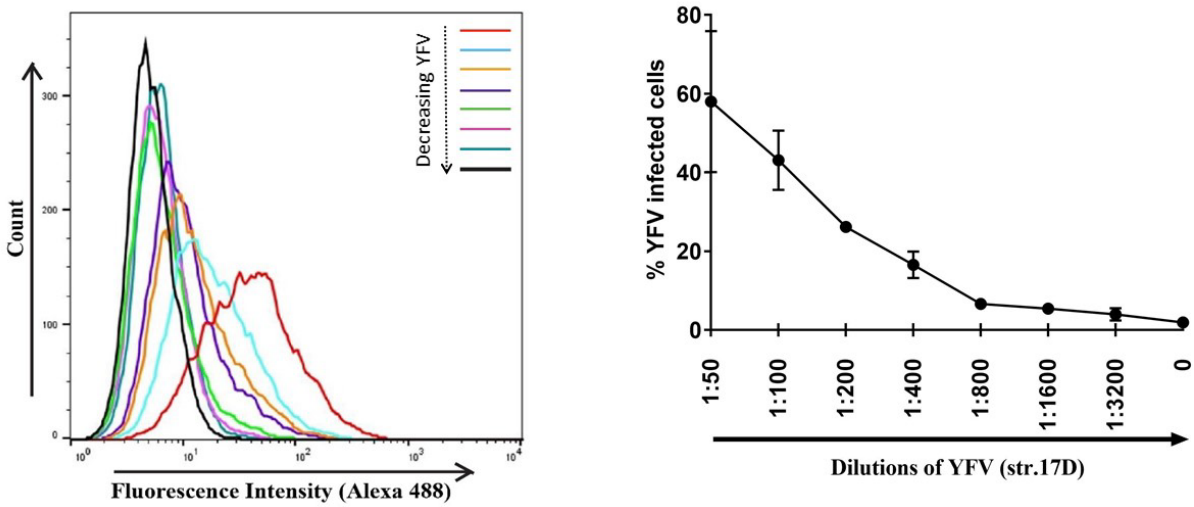

Figure 30. Titration of cell culture propagated yellow fever virus (17D vaccine strain). Seeded Vero81 cells were either cultured with media only (un-infected Vero) or infected with seven 2-fold serial dilutions of YFV for a total of 48hrs before being analyzed by flow cytometry to determine the dilution of virus that would be optimal for use in neutralization experiments. Cells were intracellularly stained with 4G2 (pan-flavivirus) mouse monoclonal antibody followed by a goat anti-mouse Alexa488 conjugated secondary antibody for detection of bound primary. The histograms depict the number of cells in each sample that detected a shift in fluorescence intensity (left), while the line graph (right) provides the average % of YFV infected cells based on the dilution of YFV used for infection. Error bars indicate ± standard error of the mean (n=2).

Using an assay that measured infectivity by flow cytometry, I measured neutralizing antibody titers of a subset of primary (n=3, 1-6yr post vaccination) and secondary (n=3, 1-6yr post-final vaccination) 17D-vaccinated subjects (Figure 31 and 32).

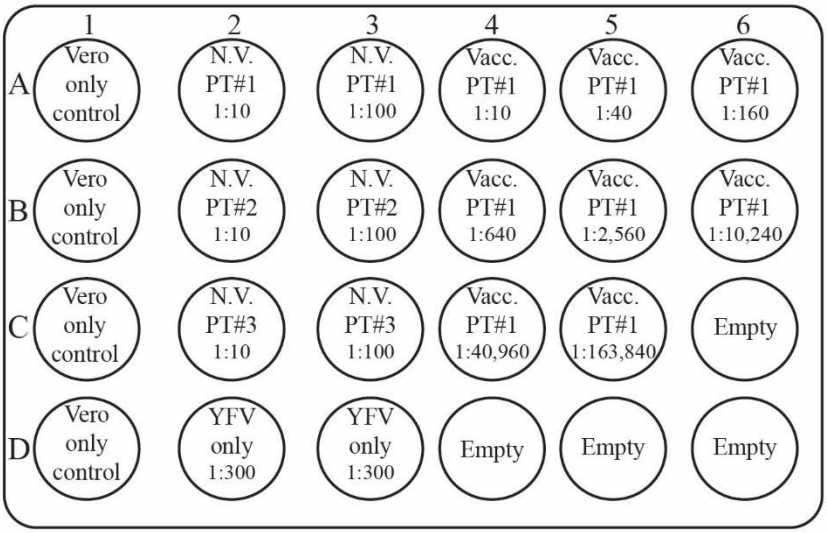

Figure 31. Example of experimental 24-well plate layout that was used in the flow cytometry based neutralization assay. A flow cytometry-based infectivity assay was used to measure neutralizing antibodies to YFV in sera of selected single (n=3) and boosted vaccinated subjects (n=3) in comparison to non-vaccinated subjects (n=3). Diluted sera of vaccinated (1-6yr post-vaccination) and non-vaccinated subjects were incubated with YFV for 1hr to allow for neutralizing antibodies to bind to the virus. Following antibody-virus incubations, sera were added to the Vero cells in the 24-well plates as shown and incubated for 48hr before analyzing by flow cytometry to measure the % of cells that were infected with YFV and not neutralized by antibodies of the patient sera. Controls were also included in the assay and included un-infected Vero cells (wells A1-D1), as well as YFV-infected Vero cells (wells D2-3) without the addition of patient sera.

Although an increase in mean antibody binding was observed in subjects who received multiple YFV vaccinations, the level of 50% neutralization titer was not significantly different between groups (p 0.7) (Figure 33). These results suggested that while the total polyclonal antibody response decreased 1-6 yr post-vaccination, the level of neutralizing antibody stayed the same. However, the number of sera tested was not

sufficient to reach a strong conclusion. A comparison of neutralizing antibody responses among 6-16yr post-primary and secondary vaccinations will also be important to determine if a boost would improve the level of YFV specific immunity after antibodies from the first immunization appear to wane.

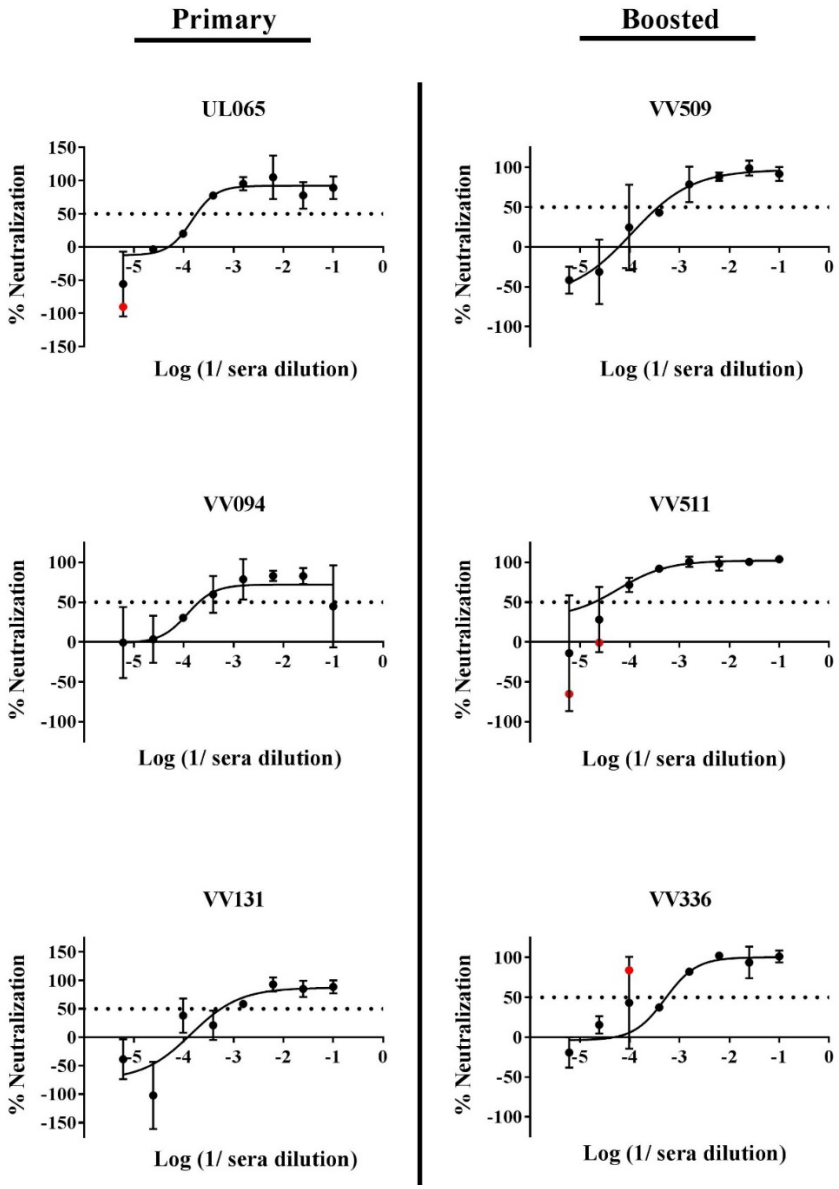

Figure 32. YFV neutralization by human immune serum from primary and boosted vaccinations. Neutralizing antibody to YFV (str. 17D) with selected primary and boosted vaccinated patient sera were measured using a flow cytometry based infectivity assay with Vero81 cells. Neutralization curves are depicted for three individuals who received a single

vaccine (left of line) and three boosted individuals (right of line). Sera were collected 1-6yr after the most recent vaccination. The neutralization curves were fitted using robust nonlinear, dose-response regression and outlier removal (ROUT) method. Identified outliers, shown as filled red symbols, were removed and ordinary least-squares regression analyses were performed on the remaining data with parameter F (percent between top and bottom of curve) constrained to 50. The horizontal dotted line represents 50% neutralization. Curves represent patient data acquired from two independent experiments.

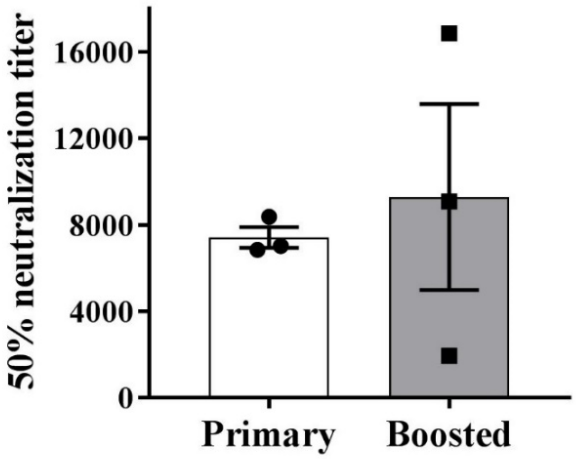

Figure 33: Comparison of 50% neutralization titers of YFV immunized cohorts. A flow cytometry infectivity assay was used to calculate the neutralization titers of YFV vaccinated subjects following two independent experiments. The serum dilution that neutralized 50% of YFV (strain 17D) was calculated for each primary (n=3) and secondary vaccinated individual (n=3), by nonlinear, dose-response regression analysis (F parameter constrained to 50). Bars indicate the mean 50% neutralization titer for each cohort (primary, non-filled bars; boosted, gray bars) with error bars indicating standard error of the mean. Individual data points are also shown for primary vaccinated subjects (filled circles) and boosted (filled squares). No significant difference in mean neutralizing antibody titer was found between groups using the Wilcoxon-Mann Whitney non-parametric test (p 0.7).

Antibody responses to heterologous flavivirus antigens resulting from YFV vaccination.

I concluded from the studies described above that sera from YFV vaccinations (n=13, 7 primary and 6 boosted dated from 14-118d post-vaccination) resulted in dominant antibody binding to recombinant YFV- E, with moderate cross-reactivity observed towards E antigens of DENV4, TBEV, and ZIKV (Keasey *et al.* 2017). Similar specificity towards homologous E was also observed in serum IgG responses of 30d post-YFV vaccinated non-human primates. However, total levels of YFV-specific antibody greatly decreased with time (Figure 34A). The E antigen of the infecting strain was predominantly detected with the pooled sera collected 120-420 days after vaccination, while higher levels of cross-reactive antibody responses were also directed towards E of the closely related flaviviruses ZIKV, JEV, and ROCV (Figure 34B). Lower overall levels of antibodies as well as specificity towards recombinant NS1 and pM antigens were observed in comparison to results with E at either time point examined (Figure 34C and D).

To examine antibody cross reactivity in greater detail, the analysis was expanded to include serological immune responses from 87 individuals at various time points after primary or boosted vaccination, ranging from 32d to 15.9yrs from vaccination (Figure 6F). These sera were collected from subjects serving in various branches of the U.S. military, including deployments to flavivirus-endemic locations. An examination of sera from primary (n=67) and boosted (n=20) vaccinations showed that antibodies principally recognized E and NS1 from YFV, with high levels of cross-reactive antibodies targeting heterologous pM antigens, especially DENV1 and WNV (Figure 35). Although antibody responses were primarily directed towards homologous E and NS1 among all vaccinees, there was also a high level of cross-reactivity to other flavivirus antigens. Over 70%

relative IgG binding to DENV4, TBEV, and ZIKV E antigens and WNV-NS1 was detected in sera of YFV vaccinated individuals. Because time from vaccination may influence the overall level of specificity as levels of antibody decline, I divided the subject sera into five different groups by time since vaccination: 30-90d, 91-270d, 271-364d, 1-6yr, and 6-16yr. Using the calculated relative binding values (%), hierarchical clustering visualized the protein-antibody interactions across time bins and number of vaccinations. The clustering analysis was performed with MeV software v4.9 (Saeed *et al.* 2003), using Pearson's correlation as the distance metric and average linkage method for pair-wise comparisons. Clustering of the relative antibody binding to E and NS1 distinguished two major groups and suggested that there were differences in cross-reactivity among vaccinated individuals, while antibody binding results from all groups were evenly scattered across clusters (Figure 36). The cluster on the top of heat map had a larger percentage of patients that had >50% relative binding (black to yellow color on the heat map) to heterologous flavivirus E antigens especially towards tick-borne flaviviruses (TBEV and POWV), DENV4, and ZIKV (Figure 36). However, the cluster shown on bottom of heat map had a larger percentage of patients with highest relative binding to YFV-E (<50% to heterologous flavivirus E; blue color on the heat map) with many individuals in this cluster having similar levels of relative binding to NS1 proteins of WNV. Two patients from the 271-364d group, denoted with * in Figure 36 had relatively low binding to YFV-E, but over 100% relative binding to E of multiple flaviviruses. Since time from vaccination and the number of vaccinations did not seem to have an effect on cross-reactive antibody binding, an analysis of antibody responses of individuals that had above average IgG binding to YFV antigens was performed to remove the possible influence of low assay signals from

some subject sera. Overall, the highest level of specificity was observed towards recombinant E of YFV with 50% relative binding measured towards DENV4, but <50% relative binding towards all other flavivirus E antigens (Figure 37A). Antibody responses to YFV-NS1 were predominant in sera of YFV vaccinated subjects, but more than 50% relative binding was measured to NS1 antigens of JEV and WNV (Figure 37B). Lastly, anti-YFV pM antibodies led to the highest observed level of cross-reactivity towards multiple flaviviruses. Greater than 50% reactivity was seen in M/pM antigens of DENV2, JEV, POWV, and ZIKV, while higher antibody binding was observed with DENV1 and WNV M/pM (Figure 37C). Collectively, these results suggest that total antibody recognition of E proteins may be best at distinguishing between infections caused by closely related species of flaviviruses, and that antibody cross-reactivity with heterologous E and NS1 does not correlate with time from YFV vaccination.

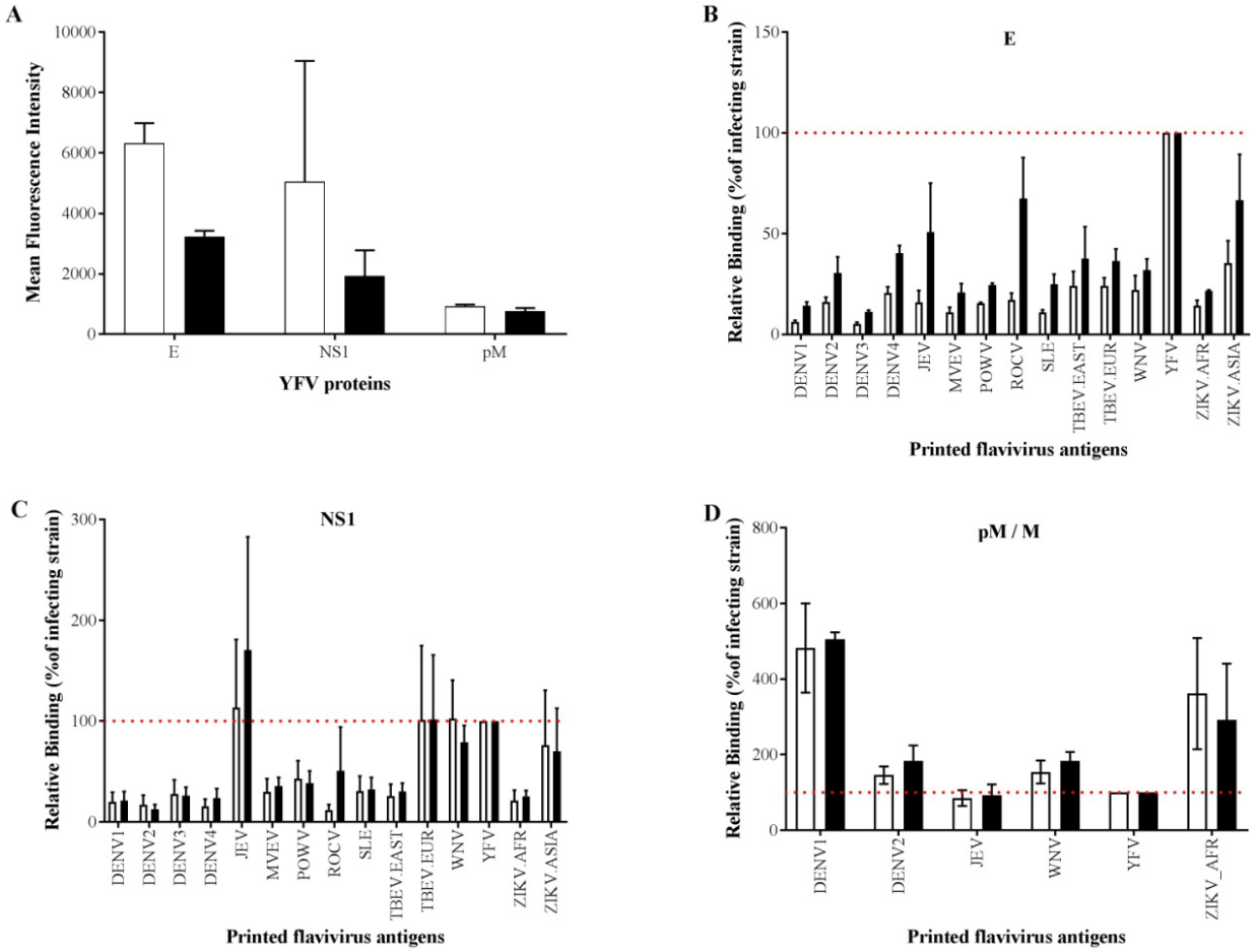

Figure 34. Comparison of antibody responses to flavivirus antigens in YFV immunized non-human primates based on time from vaccination. Yellow fever specific antibody recognition to envelope protein (E), non-structural protein 1 (NS1), and precursor membrane protein (pM) were evaluated in sera of non-human primates (NHPs) collected at 30d (unfilled bars) and a pooled later time point (~120-420d) post-17D vaccination (**A**). Measurement of serum IgG binding to flavivirus antigens was detected with an Alexa-647 conjugated anti-human IgG (γ specific) secondary antibody and is shown as mean fluorescence intensity. Error bars indicate standard error of the mean. The amount of relative antibody binding to non-YFV (heterologous) proteins was also assessed using the NHP sera. Relative binding, shown as % of YFV antigen, was calculated as antibody binding signals of the heterologous (non-YFV) antigen relative to the homologous YFV antigen. The horizontal red dashed line indicates 100% relative antibody binding.

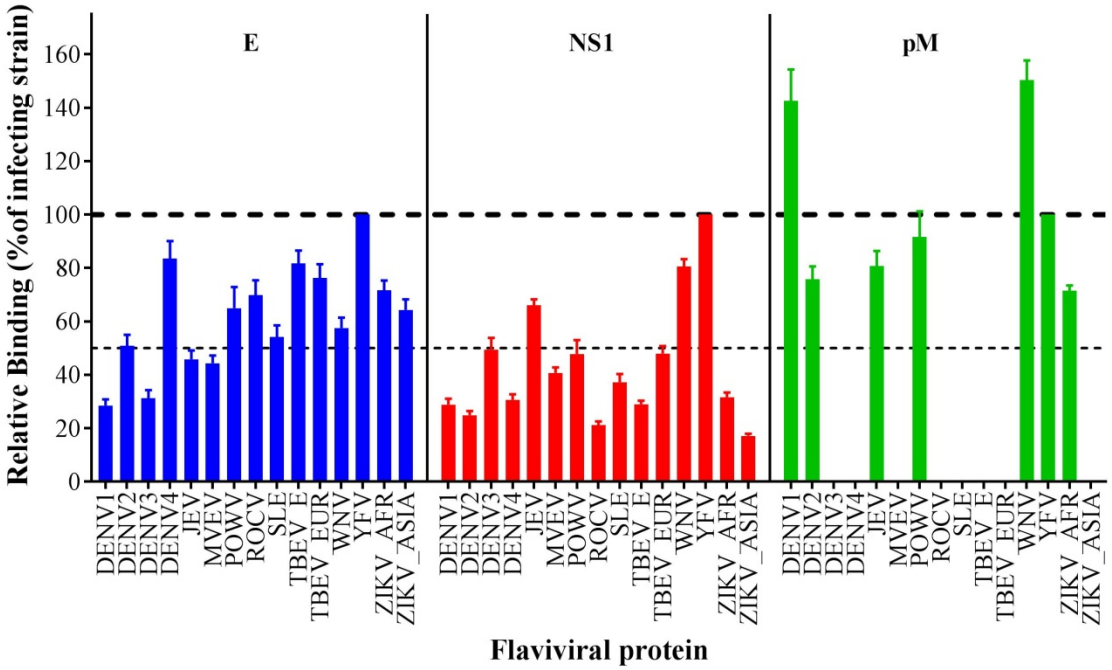

Figure 35. Recognition of non-YFV flaviviruses by 17D vaccination. Specific and cross-reactive antibody responses to flavivirus proteins (envelope, E (blue), non-structural protein 1, NS1 (red), and precursor membrane protein, pM (green) were measured in sera of 87 YFV vaccinated subjects. Relative binding values shown as % on the y-axis are antibody binding signals of the heterologous (non-YFV) antigen relative to YFV. Error bars indicate SEM. The dashed horizontal lines on the top and bottom of the graph indicate 100% and 50% relative binding, respectively.

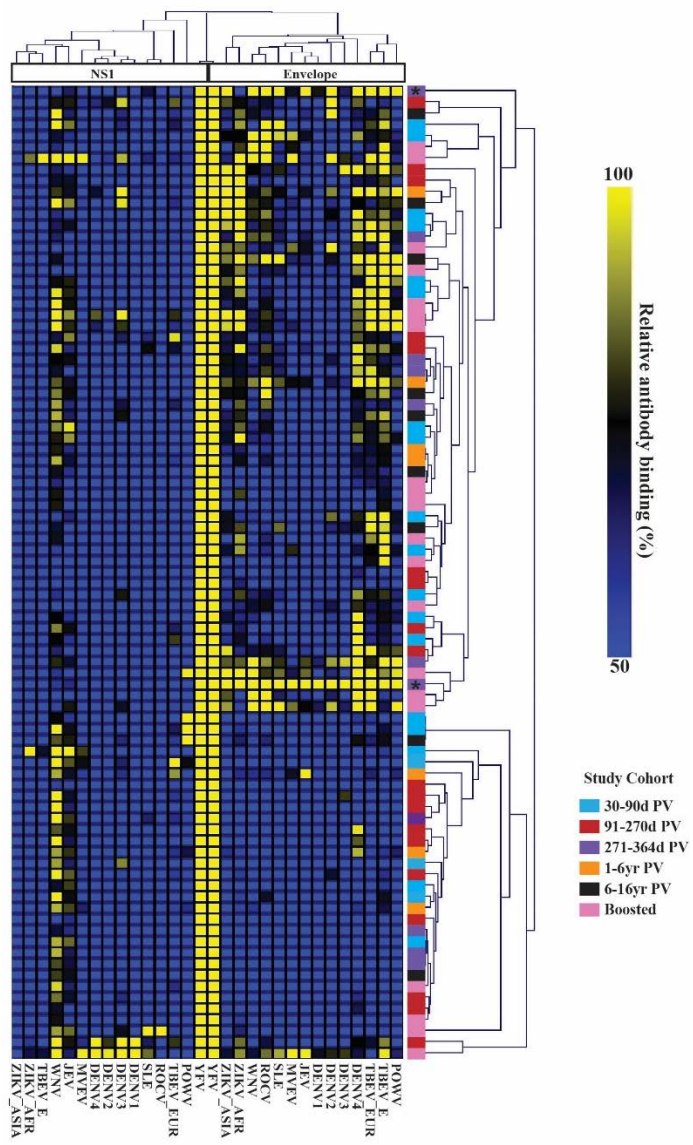

Figure 36. Antibody cross-reactivity to heterologous E and NS1 does not correlate with time from YFV vaccination. Hierarchical clustering, using Pearson's correlation-average linkage method with relative antibody binding percentages (% infecting strain), was used to visualize cross-reactive antibody responses to E and NS1 of 15 flavivirus isolates in relationship to number of YFV vaccinations and time post-vaccination. Sera of single YFV vaccinated subjects (n=67) and boosted (n=20) are listed in rows while flavivirus-envelope and non-structural protein 1 antibody interactions are listed in columns (top of heat map shows the protein, bottom of heat map shows the flavivirus species). The gradient color key on the top right of the heat map shows the scale of relative antibody binding (50-100%). The color blocks to the left of the heat map represent the subject groups: primary vaccinated subjects separated based on time post-vaccination (PV) 30-90d PV, blue; 91-270d PV, red; 271-364d PV, purple; 1-6yr PV, orange; 6-16yr PV; and boosted, pink.

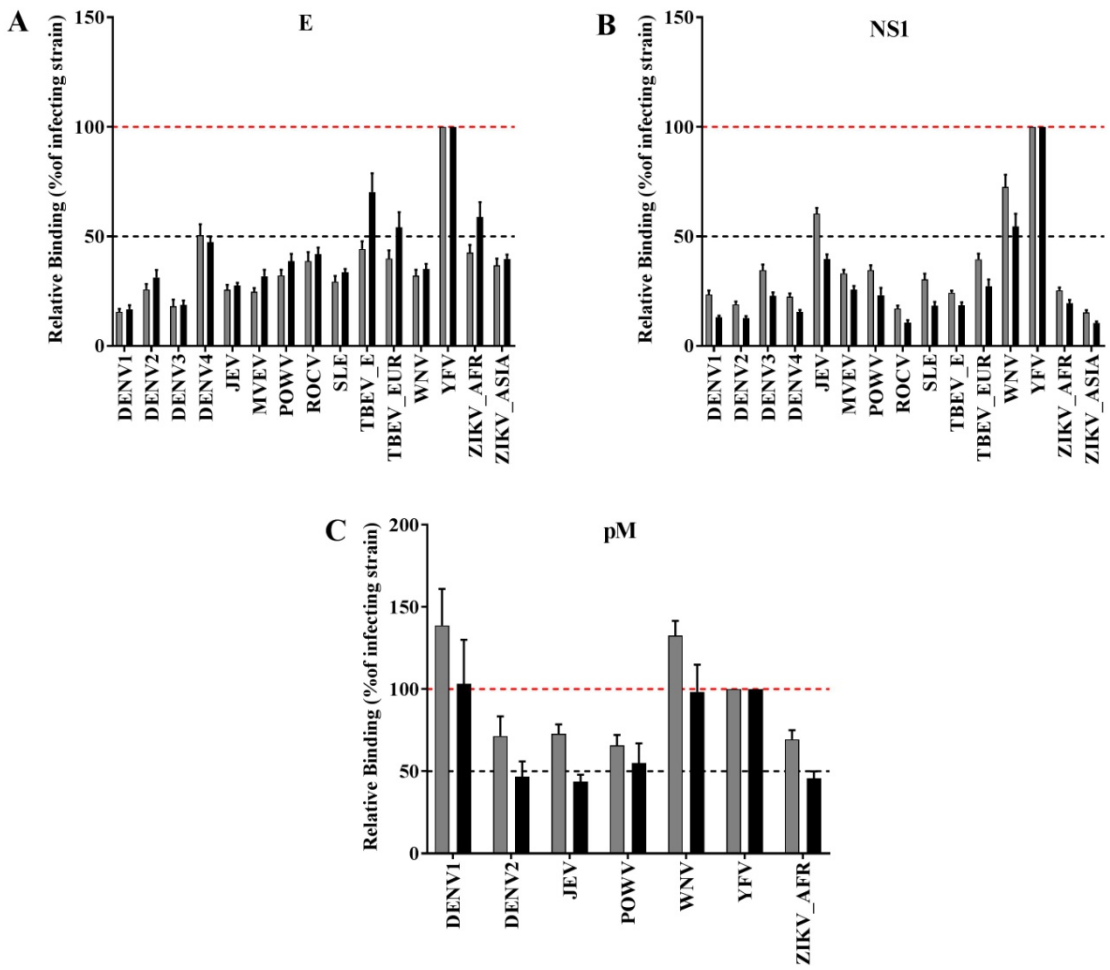

Figure 37. Elevated IgG recognition to YFV antigens is associated with decreased levels of cross-reactivity in YFV vaccinated subjects. Antibody (IgG) recognition to recombinant proteins (envelope, E; non-structural protein 1, NS1; and precursor membrane protein, pM) of YFV and 14 other closely related flaviviruses were measured in sera of primary (gray bars) and boosted (black bars) 17D vaccinated subjects. The vaccinated individuals chosen for analysis represent those that had above average antibody responses to YFV antigens following vaccination. Relative binding values shown as % on the y-axis are antibody binding signals of the heterologous (non-YFV) antigen relative to YFV. Error bars indicate SEM. The red dashed horizontal line indicates 100% relative binding, whereas the black dashed line denotes 50% relative binding.

DISCUSSION

The need for high-throughput serological assays that can detect and differentiate flavivirus infections has become critical due to the rapid spread of flaviviruses into new geographic regions and the high incidence of infectious diseases caused by these viruses. New methods for reliably evaluating the protective efficacy of vaccines and the implementation of vaccination programs are also needed. Towards this need, I developed a protein microarray comprised of native viruses and recombinant protein antigens from the major groups of pathogenic flaviviruses that can be used as a comprehensive serological assay. The microarray platform was employed in a comprehensive analysis of serum antibody responses to flavivirus infection and vaccination. My goals were to identify specific and cross-reactive antibody responses, and to characterize antibodies that result from complex infection histories involving more than one virus. A further aim of my project was to use the microarray results to provide insight into the level of cross-reactivity between viruses, the potential impact of subsequent flavivirus infections, as well as future considerations for the development of vaccines and diagnostics. The results presented here demonstrated that recombinant E antigens can be used to detect specific IgG response to primary infections, whereas off-target antibody recognition of flavivirus E proteins was noted with sera from ZIKV or DENV infections that occurred in areas where flavivirus disease are endemic. While microarrayed YFV-E and whole viruses distinguished vaccinated from naïve immune responses, the level of YFV antibodies decreased substantially from one to sixteen years post-vaccination. Antibody responses to YFV antigens were significantly higher for secondary compared to primary vaccination, and cross-reactive antibodies to other flaviviruses did not contribute to the boost in IgG levels.

The results demonstrated with the flavivirus protein microarray fulfilled my goal of developing a high-throughput platform for the analysis of serological immune responses to multiple flavivirus species and antigens in a single array. Further, the microarray results also fulfilled my objectives of providing a comprehensive analysis of immune responses to flavivirus infections and vaccinations, which may help guide public health responses to current flavivirus disease epidemics and future outbreaks.

Development of the protein microarray

Protein microarrays offer a high-throughput method for the analysis of antibody response to hundreds or thousands of antigens in one experiment (Natesan and Ulrich 2010; Tomizaki *et al.* 2010). This can be done with greatly reduced sample volume (1-5 μL) and processing time (minutes-hours), and highly specificity. The microarray that I developed should be compared to other published studies. A previously reported flavivirus-focused protein microarray was developed by Cleton *et al.* (2015) to examine human antibody responses to flavivirus infections and immunizations. In the reported study, His-V5 fusion-tagged NS1 proteins from eight different flaviviruses were expressed in mammalian cells, purified using a nickel-charged column, and spotted onto nitrocellulose coated glass slides. The array was then used to analyze serum IgG and IgM antibodies of humans infected with DENV, WNV, JEV, SLEV, and YFV (Cleton *et al.* 2015). While this study represented the development of a protein microarray for use as serological assay against eight flavivirus isolates, the microarray consisted of only recombinant NS1, rather than multiple viral antigens, therefore limiting the analysis of multiple host antibody-antigen interactions. Furthermore, the results from Cleton *et al.* microarray demonstrated flavivirus-specific human antibody binding to homotypic NS1 in most cases, but was unable to distinguish

between DENV1-4 infections. In order to achieve this level of specificity with the flavivirus NS1 microarray, a high concentration of protein (0.5mg/mL) was deposited on the array and the biological samples were highly concentrated (1:20) (Cleton *et al.* 2015). In contrast, the flavivirus protein microarray developed as part of this thesis contained multiple viral antigens from 18 species of clinical relevant flaviviruses, thus providing a more complete platform for detection of antibody binding patterns.

My first aim was to develop a flavivirus protein microarray that could be used as a multiplexed serological assay for the detection of immune responses to flavivirus infection or immunization. This required cloning, expression, purification, and printing of a minimum of 45 flavivirus antigens (E, E-DIII, pM/M, NS1, and NS3) representing 15 significant human pathogenic flavivirus on a single platform. The well-established Gateway-cloning system was used for directionally cloning plasmids into an *E.coli* entry vector. Initially, cDNA reverse-transcribed from isolated virus RNA was used as templates for amplification of the gene of interest, but this often led to poor amplifications or high mutation rates due to not knowing the exact virus strain sequence or the inherent quasi-species that exist among RNA viruses. Improvement of this initial step was achieved by using synthesized genes as templates. Synthesized genes served as higher quality templates that improved cloning efficiency, led to a decrease in the number of spurious mutations, avoided handling of live virus, and allowed for new genes of interest from emerging flaviviruses to be quickly added. Sequence-verified clones were recombined into a fusion-tagged expression vector and expressed in *E.coli.* Due to the large number of unique viral protein targets to be expressed, protein expression in *E.coli* was favored, as it is a highly established system with many choices of vectors and host cells, which aid in project

timeliness and expense. However, the majority of expressed recombinant proteins were sequestered into cytoplasmic inclusions despite considerable efforts to generate soluble products.

Inclusion bodies primarily contain the expressed protein of interest (Ramon *et al.* 2014), which is often biologically active (Garcia-Fruitos *et al.* 2005). Using this observation to my advantage, the inclusion body aggregates were washed to remove *E.coli* membrane and cell wall material, and solubilized in a HEPES based buffer containing 1% SDS. Altogether, the use of inclusion body pellets proved to be advantageous as it was cost effective and allowed for quicker processing time without compromising the quantity or quality of the protein. The purity and size of each His-tagged protein was characterized using Agilent Protein 230 chip and SDS-PAGE analysis followed by Coomassie staining. The purity of the recombinant proteins based on Agilent Protein230 assay ranged from 43 to 97% (median was 73%). Western blotting using an antibody directed towards the fusion tag confirmed protein identity. Only proteins that were determined to be within 10% of their expected size and detected by anti-His antibody were included on the microarray. The recombinant and control proteins were printed onto the nitrocellulose-coated microarray surface.

Characterization of the protein microarray

Several quality control measures were performed to evaluate the antigens deposited on the microarrays. All proteins were quantified by using a SYPRO®Ruby total protein stain, while probing with the anti-His antibody showed that all fusion-tagged proteins were successfully spotted and adsorbed onto the nitrocellulose-coated microarray surfaces. Further, precision of the replicates was determined have a CoV of 22%. The quality of the

recombinant flavivirus E proteins was further validated with a rabbit polyclonal antibody binding that detected the conserved fusion loop peptide. Lastly, evaluation of specific and cross-reactive antibodies to antigens on the microarray was established by mouse anti-sera produced against 12 different flaviviruses. Highly specific antibody responses to recombinant E was detected by all flavivirus mouse anti-sera except for DENV3. It is likely that the DENV3 mouse antibody was low titer, because the antibody against the highly conserved E-domain II fusion loop peptide detected the protein, as did subsequent flavivirus infected biological samples. The NS1 proteins from all flaviviruses except DENV1-4 were detected by the mouse anti-virus sera, whereas the M antigen was only weakly recognized at best. Combined, data from these quality control steps indicated that the flavivirus protein microarrays performed properly and could be used as a serological assay to assess specific and cross-reactive antibody responses.

In the work described, I demonstrated the successful development of a flavivirus protein microarray for use as a serological assay, but there are still limitations that should be addressed. In assessing antibody recognition of the proteins using the mouse anti-sera against the different flaviviruses, high cross-reactivity was observed for JEV anti-sera. It may be that the serum dilution was not optimal for the detection of JEV-specific antibodies, or perhaps the JEV antigens may require further optimization of design. While fusion-tags allow for a reliable way to assess the quality of the recombinant proteins, it is possible that antibody recognition may be inhibited by the fusion-tag found at the N-terminus of a particular protein. This is possibly the case with N-term HIS-MBP tagged proteins, such as DENV1-4 NS1, because of the large size of the MBP protein tag (~42kDa). The epitopes are located at or near the N-terminus of the protein may not be recognized due to the tag,

thus inhibiting the detection of an antibody response. This problem could be addressed by producing the DENV1-4 NS1 as N-term 6X His tagged proteins in order to examine if differences in antibody recognition occur. However, it should be mentioned that the DENV1-4 NS1 recombinant proteins were also detected at low levels with the protein stain and anti-His antibody, which may indicate that a lower amount of protein was deposited on the microarray. Further, mouse antibody responses to E-DIII showed some level of specificity, but human antibody responses were highly cross-reactive. The difference in anti-E-DIII specificity was also noted in other studies (Crill et al. 2009; Vratskikh et al. 2013; Wahala et al. 2012; Wahala et al. 2009; Williams et al. 2012). Although high levels of antibody bound to NS3 antigens, the mouse and human antibody responses were highly cross-reactive. It is important to note that other studies have suggested higher level of antibody specificity to non-structural proteins compared to structural proteins. However, additional studies have shown that T-cell responses to flavivirus infections predominantly target non-structural proteins (Weiskopf et al. 2013). Further, a strong correlation between T-cell responses, NS3, and disease severity were noted (Duangchinda et al. 2010). Several pM/M proteins were not included in my analysis of serological immune responses due to reduced purities and unacceptable background antibody binding. Other NS proteins, besides the NS3 that was examined here, may also be useful assay probes that should be explored in future studies.

Detection of antibody responses from primary flavivirus infections.

A major goal was to use the protein microarray as a platform for the analysis of serum antibody responses to common flavivirus infections. I first measured antibody

recognition to flavivirus antigens in primary infections by using sera from DENV, YFV, and ZIKV-challenged (NHPs) that were raised in isolation from most infectious diseases, and the human subjects had no prior documentation of flavivirus exposure. This allowed me to examine polyclonal antibody responses that were characteristic of each disease challenge strain without the interference of other flavivirus infections. Because printed microarrays also allow the performance of many test antigens to be evaluated in the same assay, I was also able to compare antibody responses to individual proteins from DENV1-4 and ZIKV with antibody responses to produced viruses of DENV1-4 and seven ZIKV isolates.[5] The microarray results demonstrated that antibodies from first exposures of non-human primates and humans to ZIKV, DENV, WNV, and YFV were predominantly directed towards the E surface antigen from the infecting virus, and enabled differentiation of infections. Whereas isolated human monoclonal antibodies that were cross-reactive for E antigens have been described (Dejnirattisai *et al.* 2016), our results with polyclonal antibodies present a global analysis of the composite B-cell response. In contrast to the high specificity observed with E antigens, whole viruses exhibited significant levels of cross-reactivity with serum antibodies from primary ZIKV and DENV infections. This is in agreement with previous reports that used antigen preparations from whole virus (Duffy *et al.* 2009; Lanciotti *et al.* 2008; Priyamvada *et al.* 2016). Although the precise reason for high cross-reactivity between viruses is unknown, possible mechanisms may include antibodies that interact with additional quaternary and glycosylated epitopes that were not present on the recombinant antigens, or other indeterminate factors (Dejnirattisai *et al.* 2015; Sirohi *et al.* 2016). Further, the results presented here emphasize the value of

[5] Dr. Stig M.R. Jensen propagated the DENV1-4 and ZIKV strains that were used for development of microarrays consisting of whole virus preparations. Further details are included in the manuscript: ibid.

determining total antibody recognition of E proteins for distinguishing between infections caused by different species of flaviviruses. While virus neutralization assays measure a functional subset of antibodies and provide an important indicator of anti-viral immunity, the best correlate of protection against viremia in DENV infection may be total polyclonal antibodies rather than neutralizing antibody titers (Simmons *et al.* 2010). Antibodies that are weakly neutralizing in cell culture assays can contribute to physiologically important non-ADE mechanisms of virus clearance that are facilitated by receptor-mediated uptake and effector cells (Klasse 2014).

Detection of antibody responses from secondary flavivirus infections.

I used the microarray-based serological assay to examine the impact that prior flavivirus exposure may have on the immune responses to flavivirus antigens. To accomplish this goal, I measured antibody responses of individuals with recent ZIKV, DENV, WNV, and YFV infections. Antibodies from human ZIKV or DENV infections that occurred in dengue-endemic regions recognized heterotypic E antigens, and decreased recognition of the homotypic E, consistent with higher levels of IgG from previous flavivirus exposures compared to the most recent infection. The high degree of antibody specificity for E with sera from primary DENV and ZIKV exposures suggests that the apparent cross-reactivity observed in many assays may result from an overlap in rising and waning antibody responses to independent infections, as modeled in Figure 38.

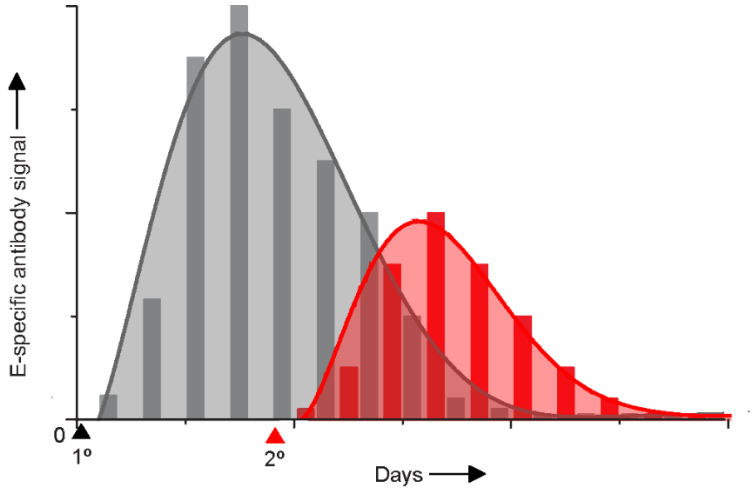

Figure 38. Overlap in rising and waning antibody responses to independent infections. The primary infection of a flavivirus-naïve individual with dengue virus occurs at day 0 (solid black arrowhead). Levels of virus-specific antibody (gray bars and shading) begin to increase shortly after the acute phase of infection, peak after convalescence, and subside thereafter. A second infection with Zika virus (solid red arrowhead) is followed by an increase in virus-specific antibody (red bars and shading), resulting in detection of a mixture of anti-dengue and anti-Zika virus antibodies that will vary with time from infections. The ratio of dengue: Zika virus antibodies, as shown, will be further increased if the secondary infection results in a less potent activation of serological immune responses.

A more detailed understanding of the interrelationships of antibody responses across flaviviruses is imperative because infections by one species or serotype are known to influence disease susceptibility and severity for infections caused by other related viruses (Anderson *et al.* 2011; Halstead *et al.* 1976; Kliks *et al.* 1988; Reisen *et al.* 2008). New techniques are also needed to guide accurate diagnosis of emerging infections, especially for flavivirus-immune individuals, as antibodies persist at levels that are detectable long after disease resolution (Durieux 1956; Monath T 2008; Prince *et al.* 2007; Roehrig *et al.* 2003). Although the lapse of time from previous exposures may influence detection of responses to new infections, my results demonstrate that antibody recognition patterns from secondary infections can be used to estimate infection histories. Importantly, since

severe dengue is linked to secondary infections with a heterotypic DENV (Anderson *et al.* 2011; Halstead *et al.* 1976; Kliks *et al.* 1988; Reisen *et al.* 2008), it is possible that dengue-primed populations are more prone to ZIKV infections, and perhaps the associated severe neurological disorders of Guillain-Barré syndrome (Cao-Lormeau *et al.* 2016) and microcephaly (Cauchemez *et al.* 2016; Rasmussen *et al.* 2016; Schuler-Faccini *et al.* 2016). However, there is currently no evidence of enhanced severity, increased ZIKV loads, or increased incidence of Zika disease in countries with widespread immunity to dengue. The microarray results presented here indicate that it should be possible to develop protein-based serological assays that are sensitive enough to differentiate flavivirus infections in individuals with preexisting immunity. Based on the assumption that multiple independent antibody-binding events were measured for each clinical specimen collected from a dengue-endemic region, data from primary infections can be used to train machine-learning methods for classification of sera from unknown infection histories. The predictive algorithm that was developed by my lab[6] for E recognition patterns may find useful applications in disease surveillance for inference of infection histories in both primary and secondary flavivirus encounters. As diagnostic methods by necessity focus only on the current disease, the general approach described here will also be important for addressing any causal relationships between current flavivirus diseases, like ZIKV and previous infections.

[6] Dr. Sarah L. Keasey developed the SVM (support vector machine) algorithm that was used for the classification of sera from unknown infection histories.

Development of a yellow fever focused microarray.

Because the flavivirus protein microarray served as an improved platform for the analysis of antibody responses of closely related flaviviruses, I wanted to further employ the microarray approach for the examination of both proteome-level and whole-virus antibody interactions that are involved in the YFV vaccine antibody response over time. In order to do this, I developed a yellow-fever focused microarray of recombinant proteins (E, NS1, and pM) from YFV and DENV, as well as live, attenuated vaccine strain (17D) whole-virus. The recombinant proteins, E, NS1, and pM were produced and validated as previously described. I used a flow-cytometry based infectivity assay for detection of antibody recognition of my cell-culture produced virus. Intracellular accumulation of YFV antigens during infection of Vero cells was confirmed by using a monoclonal antibody (4G2) directed towards the pan-flavivirus E domain II fusion loop peptide, as well as with mouse anti-sera raised against vaccine strain YFV. Following antibody confirmation of the YFV whole virus antigen, the preparation could be used for deposition onto the microarray surfaces. Because the whole virus preparation was not as pure as the recombinant proteins, and I had experienced issues of auto fluorescence with microarray printed virus preparations in the past (Pugh *et al.* 2016), the concentrated virus was spotted in 2-fold serial dilutions to determine the optimal concentration. The overall CoV of the printed probes on the microarray surfaces was very low at 14% and within the instrument specifications of 20% variance. Detection of the deposited fusion-tagged YFV and DENV1-4 recombinant proteins was demonstrated using the anti-His monoclonal antibody. Specific serum antibody binding was detected predominantly towards YFV- E and whole virus antigens (dilutions 1:2 – 1:16) in comparison to DENV and control

antigens, whereas lower levels of YFV IgG antibodies were detected to YFV-NS1 and pM. Prior to in-depth analysis of antibody responses to YFV vaccination, I had to determine which concentration of whole virus antigen was optimal for providing detection of YFV-specific antibodies relative to binding to non-specific virus components. To do this, I compared antibody binding results of all yellow fever vaccinated subjects to dilutions of whole virus in comparison to YFV naïve. Non-specific binding to whole virus was quite high, with an average relative fluorescence antibody binding signal of 10,000 among non-vaccinated subjects. The highest concentration of the virus (1:2) provided the best signal to noise ratio to be used for data analysis.

Detection of antibody responses to YFV antigens in 17D vaccinated subjects.

I used the microarray in a study that provided detailed information on both protein-level and whole-virus interactions of antibodies that were tracked for up to 15 years after YFV vaccination. IgG recognition of YFV-E and whole virus was significantly higher in vaccinated subjects in comparison to non-vaccinated, and lower levels of specific antibodies were directed to YFV- NS1 and pM antigens. Previously reported studies have also suggested that anti-NS1 and anti-pM antibodies represent a smaller proportion of the humoral immune response against YFV (Vratskikh et al. 2013). While E and whole virus YFV demonstrated a better ability to distinguish overall YFV seropositivity (i.e. $\mu+2\sigma$ above non-vaccinated antibody binding), this was not the case for all vaccinated subjects. Specifically, for three vaccinated patients, the level of IgG antibodies directed towards E and whole virus were much lower than of those detected towards NS1 and pM. These results emphasize the need for multiple antigens to be included in serological assay platforms, because patients with atypical immune responses might be missed. Furthermore,

the microarray assay detected increasing levels of IgG antibodies to YFV antigens from 30-90d after primary vaccination with the highest level of antibodies detected at 271-364d in our assay followed by a sharp decline in antibody binding levels a year after vaccination. Human IgG levels to YFV-E, NS1, and pM were indistinguishable from responses of non-vaccinated at both the 1-6yr and 6-16yr time points, whereas antibodies to whole virus remained slightly elevated, though not significantly higher at the latest time points post-vaccination. These results corroborate with other reports that showed humoral immunity decreased progressively with time (Collaborative group for studies on yellow fever 2014; Miyaji *et al.* 2017). Further support for differences in antibody binding levels across time were demonstrated by the changes in the percentage of seropositive vaccinated individuals (significantly elevated IgG levels compared to non-immune) based on time post-vaccination, as well as distinct clusters that were observed based on IgG interactions to YFV antigens over time. In contrast to past studies from our laboratory, the results from this microarray assay indicated that antibody recognition of whole virus antigen was better (~2.5 fold higher) at discriminating virus-specific antibody responses (Keasey et al. 2017; Natesan et al. 2016). However, it is important to point out that it is difficult to print equal molar amounts of whole virus and recombinant protein due to the complex nature of the native virus. Although, it is not entirely an accurate measurement due to the complexity of the whole virus preparation, the SyproRuby results indicated that the amount of deposited whole virus antigen for the 1:2 dilution used in the microarray was approximately five-fold higher than the amount of deposited YFV-E protein. Perhaps the higher concentration of virus allowed a better ability to detect antibody responses of YFV immune individuals even at the late time intervals. Only one YFV vaccinated subject in the 6-16yr time interval did

not have a significant level of antibody binding to whole virus compared to non-vaccinated sera. The dilution of deposited virus that was used for analysis of antibody responses was chosen based on having the best ratio of specific signal to background binding levels (Figure 23), and it is possible that further optimization of the amount of recombinant protein may improve sensitivity.

A comparison of antibody responses of primary and secondary YFV vaccinated subjects.

Although my study, along with a number of others, demonstrates the decrease in YFV-specific antibodies over time (Collaborative group for studies on yellow fever 2014; Miyaji et al. 2017), the requirement of a boost is still debated (Amanna and Slifka 2016; Hepburn et al. 2006; Miyaji et al. 2017; Wieten et al. 2016). Due to the need for additional information towards this matter, I examined antibody responses to YFV antigens in primary and secondary vaccinated subjects at both 1-6 year and 6-16 year post-vaccination time intervals. Since antibody responses to YFV antigens was shown to decrease 1-6yr post-vaccination with a progressive decline thereafter in primary vaccines, antibody responses of individuals that received a boost 1-6 years ago (6-16yr from their primary vaccine) (n=6) were also examined to determine if re-exposure of YFV antigen altered the observed kinetics. Serum IgG levels to E, NS1 ($p<0.005$), and whole virus ($p<0.0001$) were significantly elevated in secondary YFV vaccinees when compared to antibody responses of primary vaccinated individuals dated 1-6yr post-vaccination. This difference in antibody recognition of recombinant proteins and whole virus ($p<0.0001$ for all YFV antigens including pM) was even more significant when antibody responses were compared between 6-16yr post-primary vaccinated and boosted cohorts. Further, when neutralizing

antibody responses were analyzed in primary (1-6yr) and secondary vaccines (n=3), the observed 50% neutralization titer was higher, though not significantly significant, possibly due to the limited number of samples that were run (n=3 for each). This suggested that while the total polyclonal antibody response decreased at 1-6yr post vaccination, the level of viral neutralizing antibody did not. This suggested that further neutralization studies with additional patients need to be performed in order to complete the comparison of total polyclonal and neutralizing antibody responses in primary and secondary vaccinated subjects. It is plausible that a greater difference in both total polyclonal antibody response and viral neutralizing titers would be seen when antibody responses of boosted was compared to those of the 6-16yr post-primary vaccinees. While neutralization tests measure an important functional subset of antibodies that are involved in clearance of the virus, our test measures total antibody recognition of YFV antigens that may provide a better indication of protective immune correlates. Additional factors may play a role in the observed increase in YFV specific antibodies among the boosted cohort. Perhaps those individuals received a natural boost in immunity due to exposure of YFV in endemic areas or possible enhancement due to cross-reactive antibodies from other flavivirus infections or vaccinations (Muyanja et al. 2014). The YFV vaccinated cohort consisted of individuals in the U.S. military and therefore may have a higher likelihood that they were exposed to multiple flaviviruses such as TBEV, JEV, and WNV. Furthermore, it has been previously reported that patients that have a low baseline titer following initial vaccination benefit more from a boost than those whose initial vaccination already produced a high reactivity to YFV (Hepburn *et al.* 2006). Microarray analysis of serum antibody responses over time

in individuals, rather than group time intervals, would allow me to determine if baseline titers were a factor in the responses observed in this study.

Detection of cross-reactive antibody responses amongst YFV vaccinated subjects

The plaque reduction neutralization test (PRNT) is the standard assay used to assess protective efficacy of YFV vaccine. However, interpretation of results from PRNTs may be complicated in areas where YFV vaccine programs coincide with DENV, ZIKV, JEV, and other flavivirus infections. A recently published study by the CDC analyzed virus neutralizing antibody responses of patients who received fractional doses of the YFV vaccine in Africa (Ahuka-Mundeke *et al.* 2018). The results suggested that 98% of vaccinated subjects had 50% PRNT titers that were suggestive of seropositivity rates similar to those seen in standard vaccine doses. However, the authors could not rule out that the measured protective titers were not mediated by cross-reactive antibodies from other flaviviruses (Ahuka-Mundeke et al. 2018). Antibody cross-reactivity between flaviviruses could be influenced by homology of sequences and structures, as well as the abundance and degree of cross-reactive antibodies in polyclonal sera. In order to evaluate cross-reactive antibody responses involved in YFV immune individuals at different time points post-vaccination, I took advantage of our developed flavivirus focused microarray that was used in the analysis of antibody responses to ZIKV in areas of flavivirus endemicity (Keasey *et al.* 2017). The multiplexed flavivirus protein microarray comprised of recombinant antigens (E, NS1, and pM/M) from YFV and 14 other clinical flavivirus isolates were utilized for the analysis of IgG responses in sera from primary (n=67) and secondary (n=20) vaccinated individuals. Total serum IgG recognition to homologous E and NS1 antigens was observed among all vaccinees, with high amount of cross-reactive

antibodies to heterologous pM proteins. Neither time from vaccination, nor number of YFV vaccinations were determined to be factors in the level of cross-reactive antibodies. Hierarchical clustering of antibody binding interactions to E and NS1 flavivirus proteins were not distinguishable based on early or late time points nor primary or secondary vaccinations, but rather was based on an individual's immune response (unique levels of cross-reactive antibodies in polyclonal sera). This is not the case for natural DENV that exhibit significantly higher amounts of cross-reactive flavivirus antibodies early in infection, with more specificity directed towards the homologous DENV serotype later in immunity (Sabin 1952). Because lower levels of YFV antibodies complicate analysis of cross-reactivity due to the overall higher level of non-specific signals, I reasoned that subjects that had above average binding to YFV antigens would be most useful for analysis. Antibody recognition of YFV- pM resulted in the highest observed level of cross-reactivity, with over 50% relative binding towards six other flaviviruses. Notably, IgG binding to YFV-E resulted in the lowest level of observed cross-reactivity with only moderate levels of relative IgG binding noted to DENV4. YFV antibodies directed towards NS1 also demonstrated a high degree of specificity, but over half of mean antibody binding was directed towards heterologous JEV and WNV antigens. Future studies on cross-reactive antibodies in YFV immunized individuals should also include whole virus preparations to better understand the contribution of antigen specificity. Reasoning that a secondary flavivirus exposure occurring either through natural infection or vaccination could alter YFV immune response levels, I examined antibody responses of JEV vaccinated individuals (n=6). Among the six subjects who were immunized with both vaccines, five were among the YFV boosted cohort. For JEV-vaccinated subjects who received a YFV

vaccine boost, little to no antibody response was observed towards antigens of JEV, likely due to the lapse in time from vaccination (median 8.2 yr post-vaccination, range 370d – 18.1 yrs), which suggests that the increase in antibody binding to YFV antigens was not influenced by JEV vaccination. Of significance, the one subject that did not have significant antibody responses to any YFV antigen demonstrated robust antibody recognition to DENV2-E in both microarray platforms, indicating history of DENV infection. Altogether, the results from this microarray study indicate that the microarray assay was sensitive enough to differentiate YFV immunity among vaccinated individuals that likely have preexisting antibodies to other flavivirus pathogens. Further assessment of the influence of antibody responses to YFV vaccination and flavivirus infections should be explored with serum samples of individual vaccinated subjects over time. Future studies of natural yellow fever infections in comparison to 17D by using the flavivirus protein microarray will also be informative for better understanding of the protective mechanisms behind the highly successful live-attenuated viral vaccine.

Future research

While, this study primary focused on analyzing IgG recognition of the viral antigens in convalescence phase of disease, except for IgM responses of ZIKV infected NHPs, it would be of great value to expand the analysis of IgM responses in order to determine specificity and cross-reactivity of flaviviruses during the acute phase of disease. Future research should focus on optimizing antigens that were unsatisfactory for use in the current serological assays, as well as including additional antigens on the microarray that will encompass newly emerging flaviviruses (ex. Usutu virus), as well other human pathogenic viruses that co-circulate in flavivirus endemic areas and cause similar early

clinical disease symptoms as flaviviruses. This may include chikungunya and Mayaro alphaviruses, the bunyaviruses of Crimean-Congo hemorrhagic fever and Rift valley fever, Lassa fever virus (an arenavirus), and the filoviruses of Ebola and Marburg disease. All proteins have already been produced by our lab (Kamata et al. 2014; Smith 2018) so the incorporation of the viral antigens into a single platform allows the very unique ability to analyze antibody responses across a wide-variety of human infectious diseases. Further, the protein microarray platform could also be used as a comprehensive serological assay for disease surveillance, perhaps by transitioning to a rapid, point of care diagnostic device.

REFERENCES

Japanese encephalitis surveillance and immunization-asia and the western pacific, 2012. 2013. [accessed 2016 1 Feb]. https://www.cdc.gov/mmwr/preview/mmwrhtml/mm6233a2.htm?s_cid=mm6233a2_e .

[CDC] Centers for Disease Control and Prevention. 2014. Epidemiology-dengue virus.

Powassan virus: Symptoms and treatment. 2015. [accessed 2016 1 Feb]. https://www.cdc.gov/powassan/symptoms.html.

Powassan virus statistics and maps. 2016. [accessed 2017 1 Nov]. https://www.cdc.gov/powassan/statistics.html.

Saint louis encephalitis: Epidemiology and geographic distribution. 2017. [accessed 2018 1 Mar]. https://www.cdc.gov/sle/technical/epi.html.

[PAHO] Pan American Health Organization. 2016. Zika-epidemiological update, 29 december 2016.

[PAHO] Pan American Health Organization/[WHO] World Health Organization. 2018. Epidemiological update:Yellow fever.

Flavivirus. 2016. [accessed 2016 1 Feb]. https://viralzone.expasy.org/24?outline=all_by_species.

[UNICEF] United Nations International Children's Emergency Fund. 2016. Yellow fever vaccine: Current supply outlook.

Japanese encephalitis fast sheet no386. 2015. [accessed 2016 1 Feb]. http://www.who.int/mediacentre/factsheets/fs386/en/.

Lower doses of yellow fever vaccine could be used in emergencies. 2016. [accessed 2017 1 Nov]. http://www.who.int/mediacentre/news/statements/2016/yellow-fever-vaccine/en/.

Hepatitis c fact sheet. 2017a. [accessed 2018 1 March]. http://www.who.int/mediacentre/factsheets/fs164/en/.

Update questions and answers related to the dengue vaccine dengvaxia and its use. 2017b. [accessed 2018 1 March]. http://www.who.int/immunization/diseases/dengue/q_and_a_dengue_vaccine_dengvaxia_use/en/.

Who dispatched 3.5 million doses of yellow fever vaccine for outbreak response in brazil. 2017c. [accessed 2018 1 Feb]. http://www.who.int/csr/disease/yellowfev/vaccination-in-Brazil/en/.

Agampodi SB, Wickramage K. 2013. Is there a risk of yellow fever virus transmission in south asian countries with hyperendemic dengue? Biomed Res Int. 2013:905043.

Aguiar M, Stollenwerk N, Halstead SB. 2016. The impact of the newly licensed dengue vaccine in endemic countries. PLoS Negl Trop Dis. 10(12):e0005179.

Ahuka-Mundeke S, Casey RM, Harris JB, Dixon MG, Nsele PM, Kizito GM, Umutesi G, Laven J, Paluku G, Gueye AS et al. 2018. Immunogenicity of fractional-dose vaccine during a yellow fever outbreak - preliminary report. N Engl J Med.

Akey DL, Brown WC, Dutta S, Konwerski J, Jose J, Jurkiw TJ, DelProposto J, Ogata CM, Skiniotis G, Kuhn RJ et al. 2014. Flavivirus ns1 structures reveal surfaces for associations with membranes and the immune system. Science. 343(6173):881-885.

Alcon S, Talarmin A, Debruyne M, Falconar A, Deubel V, Flamand M. 2002. Enzyme-linked immunosorbent assay specific to dengue virus type 1 nonstructural protein ns1 reveals circulation of the antigen in the blood during the acute phase of disease in patients experiencing primary or secondary infections. J Clin Microbiol. 40(2):376-381.

Allison SL, Schalich J, Stiasny K, Mandl CW, Heinz FX. 2001. Mutational evidence for an internal fusion peptide in flavivirus envelope protein e. J Virol. 75(9):4268-4275.

Amanna IJ, Slifka MK. 2016. Questions regarding the safety and duration of immunity following live yellow fever vaccination. Expert Rev Vaccines. 15(12):1519-1533.

Anderson KB, Gibbons RV, Thomas SJ, Rothman AL, Nisalak A, Berkelman RL, Libraty DH, Endy TP. 2011. Preexisting japanese encephalitis virus neutralizing antibodies and increased symptomatic dengue illness in a school-based cohort in thailand. PLoS Negl Trop Dis. 5(10):e1311.

Anez G, Chancey C, Grinev A, Rios M. 2012. Dengue virus and other arboviruses: A global view of risks. ISBT Science Series. 7(1):274-282.

Announcement: Guidance for u.S. Laboratory testing for zika virus infection: Implications for health care providers. 2016. MMWR Morb Mortal Wkly Rep. 65(46):1304.

Assenberg R, Mastrangelo E, Walter TS, Verma A, Milani M, Owens RJ, Stuart DI, Grimes JM, Mancini EJ. 2009. Crystal structure of a novel conformational state of the flavivirus ns3 protein: Implications for polyprotein processing and viral replication. J Virol. 83(24):12895-12906.

Avirutnan P, Fuchs A, Hauhart RE, Somnuke P, Youn S, Diamond MS, Atkinson JP. 2010. Antagonism of the complement component c4 by flavivirus nonstructural protein ns1. J Exp Med. 207(4):793-806.

Avirutnan P, Zhang L, Punyadee N, Manuyakorn A, Puttikhunt C, Kasinrerk W, Malasit P, Atkinson JP, Diamond MS. 2007. Secreted ns1 of dengue virus attaches to the surface of cells via interactions with heparan sulfate and chondroitin sulfate e. PLoS Pathog. 3(11):e183.

Barba-Spaeth G, Dejnirattisai W, Rouvinski A, Vaney MC, Medits I, Sharma A, Simon-Loriere E, Sakuntabhai A, Cao-Lormeau VM, Haouz A et al. 2016. Structural basis of potent zika-dengue virus antibody cross-neutralization. Nature. 536(7614):48-53.

Barrett ADT. 2017. Yellow fever live attenuated vaccine: A very successful live attenuated vaccine but still we have problems controlling the disease. Vaccine. 35(44):5951-5955.

Barzon L, Trevisan M, Sinigaglia A, Lavezzo E, Palu G. 2016. Zika virus: From pathogenesis to disease control. FEMS Microbiol Lett. 363(18).

Beasley DW, Holbrook MR, Travassos Da Rosa AP, Coffey L, Carrara AS, Phillippi-Falkenstein K, Bohm RP, Jr., Ratterree MS, Lillibridge KM, Ludwig GV et al. 2004. Use of a recombinant envelope protein subunit antigen for specific serological diagnosis of west nile virus infection. J Clin Microbiol. 42(6):2759-2765.

Beltramello M, Williams KL, Simmons CP, Macagno A, Simonelli L, Quyen NT, Sukupolvi-Petty S, Navarro-Sanchez E, Young PR, de Silva AM et al. 2010. The human immune response to dengue virus is dominated by highly cross-reactive antibodies endowed with neutralizing and enhancing activity. Cell Host Microbe. 8(3):271-283.

Berg MG, Lee D, Coller K, Frankel M, Aronsohn A, Cheng K, Forberg K, Marcinkus M, Naccache SN, Dawson G et al. 2015. Discovery of a novel human pegivirus in blood associated with hepatitis c virus co-infection. PLoS Pathog. 11(12):e1005325.

Bhatt S, Gething PW, Brady OJ, Messina JP, Farlow AW, Moyes CL, Drake JM, Brownstein JS, Hoen AG, Sankoh O et al. 2013. The global distribution and burden of dengue. Nature. 496(7446):504-507.

Blitvich BJ, Firth AE. 2015. Insect-specific flaviviruses: A systematic review of their discovery, host range, mode of transmission, superinfection exclusion potential and genomic organization. Viruses. 7(4):1927-1959.
Bogovic P, Strle F. 2015. Tick-borne encephalitis: A review of epidemiology, clinical characteristics, and management. World J Clin Cases. 3(5):430-441.
Bolstad BM, Irizarry RA, Astrand M, Speed TP. 2003. A comparison of normalization methods for high density oligonucleotide array data based on variance and bias. Bioinformatics. 19(2):185-193.
Burakoff A, Lehman J, Fischer M, Staples JE, Lindsey NP. 2018. West nile virus and other nationally notifiable arboviral diseases - united states, 2016. MMWR Morb Mortal Wkly Rep. 67(1):13-17.
Busch MP, Kleinman SH, Tobler LH, Kamel HT, Norris PJ, Walsh I, Matud JL, Prince HE, Lanciotti RS, Wright DJ et al. 2008. Virus and antibody dynamics in acute west nile virus infection. J Infect Dis. 198(7):984-993.
Cao-Lormeau VM, Blake A, Mons S, Lastere S, Roche C, Vanhomwegen J, Dub T, Baudouin L, Teissier A, Larre P et al. 2016. Guillain-barre syndrome outbreak associated with zika virus infection in french polynesia: A case-control study. Lancet. 387(10027):1531-1539.
Capeding MR, Tran NH, Hadinegoro SR, Ismail HI, Chotpitayasunondh T, Chua MN, Luong CQ, Rusmil K, Wirawan DN, Nallusamy R et al. 2014. Clinical efficacy and safety of a novel tetravalent dengue vaccine in healthy children in asia: A phase 3, randomised, observer-masked, placebo-controlled trial. Lancet. 384(9951):1358-1365.
Cardosa MJ, Wang SM, Sum MS, Tio PH. 2002. Antibodies against prm protein distinguish between previous infection with dengue and japanese encephalitis viruses. BMC Microbiol. 2:9.
Castresana J. 2000. Selection of conserved blocks from multiple alignments for their use in phylogenetic analysis. Molecular biology and evolution. 17(4):540-552.
Cauchemez S, Besnard M, Bompard P, Dub T, Guillemette-Artur P, Eyrolle-Guignot D, Salje H, Van Kerkhove MD, Abadie V, Garel C et al. 2016. Association between zika virus and microcephaly in french polynesia, 2013-15: A retrospective study. Lancet. 387(10033):2125-2132.
Centers for Disease C, Prevention. 2003. Update: Detection of west nile virus in blood donations--united states, 2003. MMWR Morb Mortal Wkly Rep. 52(38):916-919.
Chabierski S, Barzon L, Papa A, Niedrig M, Bramson JL, Richner JM, Palu G, Diamond MS, Ulbert S. 2014. Distinguishing west nile virus infection using a recombinant envelope protein with mutations in the conserved fusion-loop. BMC Infect Dis. 14:246.
Chandra H, Reddy PJ, Srivastava S. 2011. Protein microarrays and novel detection platforms. Expert Rev Proteomics. 8(1):61-79.
Chavez JH, Silva JR, Amarilla AA, Moraes Figueiredo LT. 2010. Domain iii peptides from flavivirus envelope protein are useful antigens for serologic diagnosis and targets for immunization. Biologicals. 38(6):613-618.
Chuang YC, Wang SY, Lin YS, Chen HR, Yeh TM. 2013. Re-evaluation of the pathogenic roles of nonstructural protein 1 and its antibodies during dengue virus infection. J Biomed Sci. 20:42.
Chung KM, Diamond MS. 2008. Defining the levels of secreted non-structural protein ns1 after west nile virus infection in cell culture and mice. J Med Virol. 80(3):547-556.
Churdboonchart V, Bhamarapravati N, Peampramprecha S, Sirinavin S. 1991. Antibodies against dengue viral proteins in primary and secondary dengue hemorrhagic fever. Am J Trop Med Hyg. 44(5):481-493.

Cleton N, Koopmans M, Reimerink J, Godeke GJ, Reusken C. 2012. Come fly with me: Review of clinically important arboviruses for global travelers. J Clin Virol. 55(3):191-203.
Cleton NB, Godeke GJ, Reimerink J, Beersma MF, Doorn HR, Franco L, Goeijenbier M, Jimenez-Clavero MA, Johnson BW, Niedrig M et al. 2015. Spot the difference-development of a syndrome based protein microarray for specific serological detection of multiple flavivirus infections in travelers. PLoS Negl Trop Dis. 9(3):e0003580.
Collaborative group for studies on yellow fever v. 2014. Duration of post-vaccination immunity against yellow fever in adults. Vaccine. 32(39):4977-4984.
Colombage G, Hall R, Pavy M, Lobigs M. 1998. DNA-based and alphavirus-vectored immunisation with prm and e proteins elicits long-lived and protective immunity against the flavivirus, murray valley encephalitis virus. Virology. 250(1):151-163.
Cook S, Moureau G, Kitchen A, Gould EA, de Lamballerie X, Holmes EC, Harbach RE. 2012. Molecular evolution of the insect-specific flaviviruses. J Gen Virol. 93(Pt 2):223-234.
Crill WD, Hughes HR, Delorey MJ, Chang GJ. 2009. Humoral immune responses of dengue fever patients using epitope-specific serotype-2 virus-like particle antigens. PLoS One. 4(4):e4991.
Cui S, Pan Y, Lyu Y, Liang Z, Li J, Sun Y, Dou X, Tian L, Huo D, Chen L et al. 2017. Detection of yellow fever virus genomes from four imported cases in china. Int J Infect Dis. 60:93-95.
Dai L, Wang Q, Qi J, Shi Y, Yan J, Gao GF. 2016. Molecular basis of antibody-mediated neutralization and protection against flavivirus. IUBMB Life. 68(10):783-791.
Danis K, Papa A, Papanikolaou E, Dougas G, Terzaki I, Baka A, Vrioni G, Kapsimali V, Tsakris A, Kansouzidou A et al. 2011a. Ongoing outbreak of west nile virus infection in humans, greece, july to august 2011. Euro Surveill. 16(34).
Danis K, Papa A, Theocharopoulos G, Dougas G, Athanasiou M, Detsis M, Baka A, Lytras T, Mellou K, Bonovas S et al. 2011b. Outbreak of west nile virus infection in greece, 2010. Emerg Infect Dis. 17(10):1868-1872.
de Alwis R, de Silva AM. 2014. Measuring antibody neutralization of dengue virus (denv) using a flow cytometry-based technique. Methods Mol Biol. 1138:27-39.
de Alwis R, Smith SA, Olivarez NP, Messer WB, Huynh JP, Wahala WM, White LJ, Diamond MS, Baric RS, Crowe JE, Jr. et al. 2012. Identification of human neutralizing antibodies that bind to complex epitopes on dengue virions. Proc Natl Acad Sci U S A. 109(19):7439-7444.
de Barros VE, Saggioro FP, Neder L, de Oliveira Franca RF, Mariguela V, Chavez JH, Penharvel S, Forjaz J, da Fonseca BA, Figueiredo LT. 2011. An experimental model of meningoencephalomyelitis by rocio flavivirus in balb/c mice: Inflammatory response, cytokine production, and histopathology. Am J Trop Med Hyg. 85(2):363-373.
De Decker S, Vray M, Sistek V, Labeau B, Enfissi A, Rousset D, Matheus S. 2015. Evaluation of the diagnostic accuracy of a new dengue iga capture assay (platelia dengue iga capture, bio-rad) for dengue infection detection. PLoS Negl Trop Dis. 9(3):e0003596.
Dejnirattisai W, Supasa P, Wongwiwat W, Rouvinski A, Barba-Spaeth G, Duangchinda T, Sakuntabhai A, Cao-Lormeau VM, Malasit P, Rey FA et al. 2016. Dengue virus sero-cross-reactivity drives antibody-dependent enhancement of infection with zika virus. Nat Immunol. 17(9):1102-1108.
Dejnirattisai W, Wongwiwat W, Supasa S, Zhang X, Dai X, Rouvinski A, Jumnainsong A, Edwards C, Quyen NT, Duangchinda T et al. 2015. A new class of highly potent, broadly neutralizing antibodies isolated from viremic patients infected with dengue virus. Nat Immunol. 16(2):170-177.

Di Bonito P, Grasso F, Mochi S, Accardi L, Dona MG, Branca M, Costa S, Mariani L, Agarossi A, Ciotti M et al. 2006. Serum antibody response to human papillomavirus (hpv) infections detected by a novel elisa technique based on denatured recombinant hpv16 l1, l2, e4, e6 and e7 proteins. Infect Agent Cancer. 1:6.

Di Tommaso P, Moretti S, Xenarios I, Orobitg M, Montanyola A, Chang JM, Taly JF, Notredame C. 2011. T-coffee: A web server for the multiple sequence alignment of protein and rna sequences using structural information and homology extension. Nucleic acids research. 39(Web Server issue):W13-17.

Diamond MS. 2003. Evasion of innate and adaptive immunity by flaviviruses. Immunol Cell Biol. 81(3):196-206.

Diamond MS, Shrestha B, Mehlhop E, Sitati E, Engle M. 2003. Innate and adaptive immune responses determine protection against disseminated infection by west nile encephalitis virus. Viral Immunol. 16(3):259-278.

Dick GW, Kitchen SF, Haddow AJ. 1952. Zika virus. I. Isolations and serological specificity. Trans R Soc Trop Med Hyg. 46(5):509-520.

Dobler G. 2010. Zoonotic tick-borne flaviviruses. Vet Microbiol. 140(3-4):221-228.

Dowd KA, DeMaso CR, Pelc RS, Speer SD, Smith AR, Goo L, Platt DJ, Mascola JR, Graham BS, Mulligan MJ et al. 2016. Broadly neutralizing activity of zika virus-immune sera identifies a single viral serotype. Cell reports. 16(6):1485-1491.

Duangchinda T, Dejnirattisai W, Vasanawathana S, Limpitikul W, Tangthawornchaikul N, Malasit P, Mongkolsapaya J, Screaton G. 2010. Immunodominant t-cell responses to dengue virus ns3 are associated with dhf. Proc Natl Acad Sci U S A. 107(39):16922-16927.

Dudley DM, Aliota MT, Mohr EL, Weiler AM, Lehrer-Brey G, Weisgrau KL, Mohns MS, Breitbach ME, Rasheed MN, Newman CM et al. 2016. A rhesus macaque model of asian-lineage zika virus infection. Nat Commun. 7:12204.

Duffy MR, Chen TH, Hancock WT, Powers AM, Kool JL, Lanciotti RS, Pretrick M, Marfel M, Holzbauer S, Dubray C et al. 2009. Zika virus outbreak on yap island, federated states of micronesia. N Engl J Med. 360(24):2536-2543.

Duong V, Lambrechts L, Paul RE, Ly S, Lay RS, Long KC, Huy R, Tarantola A, Scott TW, Sakuntabhai A et al. 2015. Asymptomatic humans transmit dengue virus to mosquitoes. Proc Natl Acad Sci U S A. 112(47):14688-14693.

Dupont-Rouzeyrol M, O'Connor O, Calvez E, Daures M, John M, Grangeon JP, Gourinat AC. 2015. Co-infection with zika and dengue viruses in 2 patients, new caledonia, 2014. Emerg Infect Dis. 21(2):381-382.

Durieux C. 1956. Mass yellow fever vaccination in french africa south of sahara. In: Smithburn KC, Durieux, C., Koerber, R., Panna, H. A., Dick, G. W. A., Courtois, G., de Sousa Manso, C., Stuart, G., Bonnel, P. H., editor. Yellow fever vaccination. Geneva. p. 115-121.

Ebel GD. 2010. Update on powassan virus: Emergence of a north american tick-borne flavivirus. Annu Rev Entomol. 55:95-110.

Ebel GD, Kramer LD. 2004. Short report: Duration of tick attachment required for transmission of powassan virus by deer ticks. Am J Trop Med Hyg. 71(3):268-271.

Ecker M, Allison SL, Meixner T, Heinz FX. 1999. Sequence analysis and genetic classification of tick-borne encephalitis viruses from europe and asia. J Gen Virol. 80 (Pt 1):179-185.

Elong Ngono A, Shresta S. 2018. Immune response to dengue and zika. Annu Rev Immunol.

Fernandez S, Cisney ED, Tikhonov AP, Schweitzer B, Putnak RJ, Simmons M, Ulrich RG. 2011. Antibody recognition of the dengue virus proteome and implications for development of vaccines. Clin Vaccine Immunol. 18(4):523-532.

Fibriansah G, Tan JL, Smith SA, de Alwis R, Ng TS, Kostyuchenko VA, Jadi RS, Kukkaro P, de Silva AM, Crowe JE et al. 2015. A highly potent human antibody neutralizes dengue virus serotype 3 by binding across three surface proteins. Nat Commun. 6:6341.

Flamand M, Megret F, Mathieu M, Lepault J, Rey FA, Deubel V. 1999. Dengue virus type 1 nonstructural glycoprotein ns1 is secreted from mammalian cells as a soluble hexamer in a glycosylation-dependent fashion. J Virol. 73(7):6104-6110.

Flipse J, Smit JM. 2015. The complexity of a dengue vaccine: A review of the human antibody response. PLoS Negl Trop Dis. 9(6):e0003749.

Foy BD, Kobylinski KC, Chilson Foy JL, Blitvich BJ, Travassos da Rosa A, Haddow AD, Lanciotti RS, Tesh RB. 2011. Probable non-vector-borne transmission of zika virus, colorado, USA. Emerg Infect Dis. 17(5):880-882.

Garcia-Fruitos E, Gonzalez-Montalban N, Morell M, Vera A, Ferraz RM, Aris A, Ventura S, Villaverde A. 2005. Aggregation as bacterial inclusion bodies does not imply inactivation of enzymes and fluorescent proteins. Microb Cell Fact. 4:27.

Garske T, Van Kerkhove MD, Yactayo S, Ronveaux O, Lewis RF, Staples JE, Perea W, Ferguson NM, Yellow Fever Expert C. 2014. Yellow fever in africa: Estimating the burden of disease and impact of mass vaccination from outbreak and serological data. PLoS Med. 11(5):e1001638.

Gaunt MW, Sall AA, de Lamballerie X, Falconar AK, Dzhivanian TI, Gould EA. 2001. Phylogenetic relationships of flaviviruses correlate with their epidemiology, disease association and biogeography. J Gen Virol. 82(Pt 8):1867-1876.

Gershman MD, Angelo KM, Ritchey J, Greenberg DP, Muhammad RD, Brunette G, Cetron MS, Sotir MJ. 2017. Addressing a yellow fever vaccine shortage - united states, 2016-2017. MMWR Morb Mortal Wkly Rep. 66(17):457-459.

Gholam BI, Puksa S, Provias JP. 1999. Powassan encephalitis: A case report with neuropathology and literature review. CMAJ. 161(11):1419-1422.

Go YY, Balasuriya UB, Lee CK. 2014. Zoonotic encephalitides caused by arboviruses: Transmission and epidemiology of alphaviruses and flaviviruses. Clin Exp Vaccine Res. 3(1):58-77.

Goenaga S, Kenney JL, Duggal NK, Delorey M, Ebel GD, Zhang B, Levis SC, Enria DA, Brault AC. 2015. Potential for co-infection of a mosquito-specific flavivirus, nhumirim virus, to block west nile virus transmission in mosquitoes. Viruses. 7(11):5801-5812.

Gould EA, Higgs S. 2009. Impact of climate change and other factors on emerging arbovirus diseases. Trans R Soc Trop Med Hyg. 103(2):109-121.

Gowri Sankar S, Balaji T, Venkatasubramani K, Thenmozhi V, Dhananjeyan KJ, Paramasivan R, Tyagi BK, John Vennison S. 2014. Dengue ns1 and prm antibodies increase the sensitivity of acute dengue diagnosis test and differentiate from japanese encephalitis infection. J Immunol Methods. 407:116-119.

Grard G, Moureau G, Charrel RN, Lemasson JJ, Gonzalez JP, Gallian P, Gritsun TS, Holmes EC, Gould EA, de Lamballerie X. 2007. Genetic characterization of tick-borne flaviviruses: New insights into evolution, pathogenetic determinants and taxonomy. Virology. 361(1):80-92.

Grobbelaar AA, Weyer J, Moolla N, Jansen van Vuren P, Moises F, Paweska JT. 2016. Resurgence of yellow fever in angola, 2015-2016. Emerg Infect Dis. 22(10):1854-1855.

Groen J, Velzing J, Copra C, Balentien E, Deubel V, Vorndam V, Osterhaus AD. 1999. Diagnostic value of dengue virus-specific iga and igm serum antibody detection. Microbes Infect. 1(13):1085-1090.

Gromowski GD, Barrett AD. 2007. Characterization of an antigenic site that contains a dominant, type-specific neutralization determinant on the envelope protein domain iii (ed3) of dengue 2 virus. Virology. 366(2):349-360.
Gubler DJ, Suharyono W, Tan R, Abidin M, Sie A. 1981. Viraemia in patients with naturally acquired dengue infection. Bull World Health Organ. 59(4):623-630.
Guindon S, Dufayard JF, Lefort V, Anisimova M, Hordijk W, Gascuel O. 2010. New algorithms and methods to estimate maximum-likelihood phylogenies: Assessing the performance of phyml 3.0. Systematic biology. 59(3):307-321.
Gutierrez RA, Dawson GJ, Knigge MF, Melvin SL, Heynen CA, Kyrk CR, Young CE, Carrick RJ, Schlauder GG, Surowy TK et al. 1997. Seroprevalence of gb virus c and persistence of rna and antibody. J Med Virol. 53(2):167-173.
Guy B, Briand O, Lang J, Saville M, Jackson N. 2015. Development of the sanofi pasteur tetravalent dengue vaccine: One more step forward. Vaccine. 33(50):7100-7111.
Guzman MG, Kouri G. 2004. Dengue diagnosis, advances and challenges. Int J Infect Dis. 8(2):69-80.
Haddow AD, Schuh AJ, Yasuda CY, Kasper MR, Heang V, Huy R, Guzman H, Tesh RB, Weaver SC. 2012. Genetic characterization of zika virus strains: Geographic expansion of the asian lineage. PLoS Negl Trop Dis. 6(2):e1477.
Hadinegoro SR, Arredondo-Garcia JL, Capeding MR, Deseda C, Chotpitayasunondh T, Dietze R, Muhammad Ismail HI, Reynales H, Limkittikul K, Rivera-Medina DM et al. 2015. Efficacy and long-term safety of a dengue vaccine in regions of endemic disease. N Engl J Med. 373(13):1195-1206.
Halstead SB. 1979. In vivo enhancement of dengue virus infection in rhesus monkeys by passively transferred antibody. J Infect Dis. 140(4):527-533.
Halstead SB. 1988. Pathogenesis of dengue: Challenges to molecular biology. Science. 239(4839):476-481.
Halstead SB. 2007. Dengue. Lancet. 370(9599):1644-1652.
Halstead SB, Marchette NJ, Sung Chow JS, Lolekha S. 1976. Dengue virus replication enhancement in peripheral blood leukocytes from immune human beings. Proc Soc Exp Biol Med. 151(1):136-139.
Halstead SB, Rojanasuphot S, Sangkawibha N. 1983. Original antigenic sin in dengue. Am J Trop Med Hyg. 32(1):154-156.
Hayes EB. 2009. Zika virus outside africa. Emerg Infect Dis. 15(9):1347-1350.
Heinz FX, Mandl CW. 1993. The molecular biology of tick-borne encephalitis virus. Review article. APMIS. 101(10):735-745.
Heinz FX, Stiasny K. 2012. Flaviviruses and their antigenic structure. J Clin Virol. 55(4):289-295.
Hepburn MJ, Kortepeter MG, Pittman PR, Boudreau EF, Mangiafico JA, Buck PA, Norris SL, Anderson EL. 2006. Neutralizing antibody response to booster vaccination with the 17d yellow fever vaccine. Vaccine. 24(15):2843-2849.
Hermance ME, Thangamani S. 2015. Tick saliva enhances powassan virus transmission to the host, influencing its dissemination and the course of disease. J Virol. 89(15):7852-7860.
Hermann LL, Thaisomboonsuk B, Poolpanichupatam Y, Jarman RG, Kalayanarooj S, Nisalak A, Yoon IK, Fernandez S. 2014. Evaluation of a dengue ns1 antigen detection assay sensitivity and specificity for the diagnosis of acute dengue virus infection. PLoS Negl Trop Dis. 8(10):e3193.
Hewitt SN, Choi R, Kelley A, Crowther GJ, Napuli AJ, Van Voorhis WC. 2011. Expression of proteins in escherichia coli as fusions with maltose-binding protein to rescue non-

expressed targets in a high-throughput protein-expression and purification pipeline. Acta Crystallogr Sect F Struct Biol Cryst Commun. 67(Pt 9):1006-1009.
Hobson-Peters J. 2012. Approaches for the development of rapid serological assays for surveillance and diagnosis of infections caused by zoonotic flaviviruses of the japanese encephalitis virus serocomplex. J Biomed Biotechnol. 2012:379738.
Hollidge BS, Gonzalez-Scarano F, Soldan SS. 2010. Arboviral encephalitides: Transmission, emergence, and pathogenesis. J Neuroimmune Pharmacol. 5(3):428-442.
Hua RH, Chen NS, Qin CF, Deng YQ, Ge JY, Wang XJ, Qiao ZJ, Chen WY, Wen ZY, Liu WX et al. 2010. Identification and characterization of a virus-specific continuous b-cell epitope on the prm/m protein of japanese encephalitis virus: Potential application in the detection of antibodies to distinguish japanese encephalitis virus infection from west nile virus and dengue virus infections. Virol J. 7:249.
Innis BL, Nisalak A, Nimmannitya S, Kusalerdchariya S, Chongswasdi V, Suntayakorn S, Puttisri P, Hoke CH. 1989. An enzyme-linked immunosorbent assay to characterize dengue infections where dengue and japanese encephalitis co-circulate. Am J Trop Med Hyg. 40(4):418-427.
Ioos S, Mallet HP, Leparc Goffart I, Gauthier V, Cardoso T, Herida M. 2014. Current zika virus epidemiology and recent epidemics. Med Mal Infect. 44(7):302-307.
Iwamoto M, Jernigan DB, Guasch A, Trepka MJ, Blackmore CG, Hellinger WC, Pham SM, Zaki S, Lanciotti RS, Lance-Parker SE et al. 2003. Transmission of west nile virus from an organ donor to four transplant recipients. N Engl J Med. 348(22):2196-2203.
Kamata T, Natesan M, Warfield K, Aman MJ, Ulrich RG. 2014. Determination of specific antibody responses to the six species of ebola and marburg viruses by multiplexed protein microarrays. Clin Vaccine Immunol. 21(12):1605-1612.
Kang X, Li Y, Fan L, Lin F, Wei J, Zhu X, Hu Y, Li J, Chang G, Zhu Q et al. 2012. Development of an elisa-array for simultaneous detection of five encephalitis viruses. Virol J. 9:56.
Kaufman BM, Summers PL, Dubois DR, Cohen WH, Gentry MK, Timchak RL, Burke DS, Eckels KH. 1989. Monoclonal antibodies for dengue virus prm glycoprotein protect mice against lethal dengue infection. Am J Trop Med Hyg. 41(5):576-580.
Keasey S, Pugh C, Tikhonov A, Chen G, Schweitzer B, Nalca A, Ulrich RG. 2010. Proteomic basis of the antibody response to monkeypox virus infection examined in cynomolgus macaques and a comparison to human smallpox vaccination. PLoS One. 5(12):e15547.
Keasey SL, Pugh CL, Jensen SM, Smith JL, Hontz RD, Durbin AP, Dudley DM, O'Connor DH, Ulrich RG. 2017. Antibody responses to zika virus infections in environments of flavivirus endemicity. Clin Vaccine Immunol. 24(4).
Keasey SL, Schmid KE, Lee MS, Meegan J, Tomas P, Minto M, Tikhonov AP, Schweitzer B, Ulrich RG. 2009. Extensive antibody cross-reactivity among infectious gram-negative bacteria revealed by proteome microarray analysis. Mol Cell Proteomics. 8(5):924-935.
Kirkpatrick BD, Whitehead SS, Pierce KK, Tibery CM, Grier PL, Hynes NA, Larsson CJ, Sabundayo BP, Talaat KR, Janiak A et al. 2016. The live attenuated dengue vaccine tv003 elicits complete protection against dengue in a human challenge model. Science translational medicine. 8(330):330ra336.
Klasse PJ. 2014. Neutralization of virus infectivity by antibodies: Old problems in new perspectives. Advances in biology. 2014.
Kliks SC, Nimmanitya S, Nisalak A, Burke DS. 1988. Evidence that maternal dengue antibodies are important in the development of dengue hemorrhagic fever in infants. Am J Trop Med Hyg. 38(2):411-419.

Kopp A, Gillespie TR, Hobelsberger D, Estrada A, Harper JM, Miller RA, Eckerle I, Muller MA, Podsiadlowski L, Leendertz FH et al. 2013. Provenance and geographic spread of st. Louis encephalitis virus. MBio. 4(3):e00322-00313.

Kostyuchenko VA, Lim EX, Zhang S, Fibriansah G, Ng TS, Ooi JS, Shi J, Lok SM. 2016. Structure of the thermally stable zika virus. Nature. 533(7603):425-428.

Kraus AA, Messer W, Haymore LB, de Silva AM. 2007. Comparison of plaque- and flow cytometry-based methods for measuring dengue virus neutralization. J Clin Microbiol. 45(11):3777-3780.

Krogh A, Larsson B, von Heijne G, Sonnhammer EL. 2001. Predicting transmembrane protein topology with a hidden markov model: Application to complete genomes. Journal of molecular biology. 305(3):567-580.

Kuno G. 2003. Serodiagnosis of flaviviral infections and vaccinations in humans. Adv Virus Res. 61:3-65.

Kuno G, Chang GJ, Tsuchiya KR, Karabatsos N, Cropp CB. 1998. Phylogeny of the genus flavivirus. J Virol. 72(1):73-83.

Lanciotti RS, Kosoy OL, Laven JJ, Velez JO, Lambert AJ, Johnson AJ, Stanfield SM, Duffy MR. 2008. Genetic and serologic properties of zika virus associated with an epidemic, yap state, micronesia, 2007. Emerg Infect Dis. 14(8):1232-1239.

Laoprasopwattana K, Libraty DH, Endy TP, Nisalak A, Chunsuttiwat S, Vaughn DW, Reed G, Ennis FA, Rothman AL, Green S. 2005. Dengue virus (dv) enhancing antibody activity in preillness plasma does not predict subsequent disease severity or viremia in secondary dv infection. J Infect Dis. 192(3):510-519.

Larkin MA, Blackshields G, Brown NP, Chenna R, McGettigan PA, McWilliam H, Valentin F, Wallace IM, Wilm A, Lopez R et al. 2007. Clustal w and clustal x version 2.0. Bioinformatics. 23(21):2947-2948.

Larsen CP, Whitehead SS, Durbin AP. 2015. Dengue human infection models to advance dengue vaccine development. Vaccine. 33(50):7075-7082.

Lazaro-Olan L, Mellado-Sanchez G, Garcia-Cordero J, Escobar-Gutierrez A, Santos-Argumedo L, Gutierrez-Castaneda B, Cedillo-Barron L. 2008. Analysis of antibody response in human dengue patients from the mexican coast using recombinant antigens. Vector Borne Zoonotic Dis. 8(1):69-79.

Leonova GN, Kondratov IG, Ternovoi VA, Romanova EV, Protopopova EV, Chausov EV, Pavlenko EV, Ryabchikova EI, Belikov SI, Loktev VB. 2009. Characterization of powassan viruses from far eastern russia. Arch Virol. 154(5):811-820.

Leyssen P, De Clercq E, Neyts J. 2000. Perspectives for the treatment of infections with flaviviridae. Clin Microbiol Rev. 13(1):67-82, table of contents.

Lindenbach BD, Rice CM. 2003. Molecular biology of flaviviruses. Adv Virus Res. 59:23-61.

Lindenbach BD, Thiel, H. J., Rice, C. M. . 2007. Flaviviridae: The viruses and their replication. Philadelphia, USA: Lippincott William & Wilkins.

Mackenzie JM, Jones MK, Young PR. 1996. Immunolocalization of the dengue virus nonstructural glycoprotein ns1 suggests a role in viral rna replication. Virology. 220(1):232-240.

Mangada MM, Rothman AL. 2005. Altered cytokine responses of dengue-specific cd4+ t cells to heterologous serotypes. J Immunol. 175(4):2676-2683.

Mansfield KL, Horton DL, Johnson N, Li L, Barrett AD, Smith DJ, Galbraith SE, Solomon T, Fooks AR. 2011. Flavivirus-induced antibody cross-reactivity. J Gen Virol. 92(Pt 12):2821-2829.

Mansfield KL, Johnson N, Phipps LP, Stephenson JR, Fooks AR, Solomon T. 2009. Tick-borne encephalitis virus - a review of an emerging zoonosis. J Gen Virol. 90(Pt 8):1781-1794.

Mansuy JM, Dutertre M, Mengelle C, Fourcade C, Marchou B, Delobel P, Izopet J, Martin-Blondel G. 2016. Zika virus: High infectious viral load in semen, a new sexually transmitted pathogen? Lancet Infect Dis. 16(4):405.

Matusan AE, Kelley PG, Pryor MJ, Whisstock JC, Davidson AD, Wright PJ. 2001a. Mutagenesis of the dengue virus type 2 ns3 proteinase and the production of growth-restricted virus. J Gen Virol. 82(Pt 7):1647-1656.

Matusan AE, Pryor MJ, Davidson AD, Wright PJ. 2001b. Mutagenesis of the dengue virus type 2 ns3 protein within and outside helicase motifs: Effects on enzyme activity and virus replication. J Virol. 75(20):9633-9643.

McCracken MK, Gromowski GD, Friberg HL, Lin X, Abbink P, De La Barrera R, Eckles KH, Garver LS, Boyd M, Jetton D et al. 2017. Impact of prior flavivirus immunity on zika virus infection in rhesus macaques. PLoS Pathog. 13(8):e1006487.

Mehlhop E, Ansarah-Sobrinho C, Johnson S, Engle M, Fremont DH, Pierson TC, Diamond MS. 2007. Complement protein c1q inhibits antibody-dependent enhancement of flavivirus infection in an igg subclass-specific manner. Cell Host Microbe. 2(6):417-426.

Meltzer E. 2012. Arboviruses and viral hemorrhagic fevers (vhf). Infect Dis Clin North Am. 26(2):479-496.

Messer WB, de Alwis R, Yount BL, Royal SR, Huynh JP, Smith SA, Crowe JE, Jr., Doranz BJ, Kahle KM, Pfaff JM et al. 2014. Dengue virus envelope protein domain i/ii hinge determines long-lived serotype-specific dengue immunity. Proc Natl Acad Sci U S A. 111(5):1939-1944.

Meyer D., Dimitriadou E., Hornik K., Weingessel A., Leisch F., Chang C., Lin C. 2015. Support vector machines. Misc Functions of the Department of Statistics, Probability Theory Group (Formerly: E1071), TU Wien (August 5, 2015). https://cran.r-project.org/web/packages/e1071/e1071.pdf.

Mittal R, Nguyen D, Debs LH, Patel AP, Liu G, Jhaveri VM, SI SK, Mittal J, Bandstra ES, Younis RT et al. 2017. Zika virus: An emerging global health threat. Front Cell Infect Microbiol. 7:486.

Miyaji KT, Avelino-Silva VI, Simoes M, Freire MD, Medeiros CR, Braga PE, Neves MA, Lopes MH, Kallas EG, Sartori AM. 2017. Prevalence and titers of yellow fever virus neutralizing antibodies in previously vaccinated adults. Rev Inst Med Trop Sao Paulo. 59:e2.

Mohr EL, Stapleton JT. 2009. Gb virus type c interactions with hiv: The role of envelope glycoproteins. J Viral Hepat. 16(11):757-768.

Monath T CM, Teuwen DE. 2008. Yellow fever vaccine. In: Plotkin SA OW, Offit PA, editor. Vaccines. 5th ed. Philadelphia, PA: Saunders Elsevier. p. 959-1055.

Monath TP. 2001. Yellow fever: An update. Lancet Infect Dis. 1(1):11-20.

Monath TP, Woodall JP, Gubler DJ, Yuill TM, Mackenzie JS, Martins RM, Reiter P, Heymann DL. 2016. Yellow fever vaccine supply: A possible solution. Lancet. 387(10028):1599-1600.

Muller DA, Young PR. 2013. The flavivirus ns1 protein: Molecular and structural biology, immunology, role in pathogenesis and application as a diagnostic biomarker. Antiviral Res. 98(2):192-208.

Murray KO, Koers E, Baraniuk S, Herrington E, Carter H, Sierra M, Kilborn C, Arafat R. 2009. Risk factors for encephalitis from west nile virus: A matched case-control study using hospitalized controls. Zoonoses Public Health. 56(6-7):370-375.

Musso D, Nilles EJ, Cao-Lormeau VM. 2014. Rapid spread of emerging zika virus in the pacific area. Clin Microbiol Infect. 20(10):O595-596.

Muyanja E, Ssemaganda A, Ngauv P, Cubas R, Perrin H, Srinivasan D, Canderan G, Lawson B, Kopycinski J, Graham AS et al. 2014. Immune activation alters cellular and humoral responses to yellow fever 17d vaccine. J Clin Invest. 124(7):3147-3158.

Nallamsetty S, Austin BP, Penrose KJ, Waugh DS. 2005. Gateway vectors for the production of combinatorially-tagged his6-mbp fusion proteins in the cytoplasm and periplasm of escherichia coli. Protein science : a publication of the Protein Society. 14(12):2964-2971.

Natesan M, Jensen SM, Keasey SL, Kamata T, Kuehne AI, Stonier SW, Lutwama JJ, Lobel L, Dye JM, Ulrich RG. 2016. Human survivors of disease outbreaks caused by ebola or marburg virus exhibit cross-reactive and long-lived antibody responses. Clin Vaccine Immunol. 23(8):717-724.

Natesan M, Ulrich RG. 2010. Protein microarrays and biomarkers of infectious disease. Int J Mol Sci. 11(12):5165-5183.

Ng JK, Zhang SL, Tan HC, Yan B, Martinez JM, Tan WY, Lam JH, Tan GK, Ooi EE, Alonso S. 2014. First experimental in vivo model of enhanced dengue disease severity through maternally acquired heterotypic dengue antibodies. PLoS Pathog. 10(4):e1004031.

Notredame C, Higgins DG, Heringa J. 2000. T-coffee: A novel method for fast and accurate multiple sequence alignment. Journal of molecular biology. 302(1):205-217.

Oehler E, Watrin L, Larre P, Leparc-Goffart I, Lastere S, Valour F, Baudouin L, Mallet H, Musso D, Ghawche F. 2014. Zika virus infection complicated by guillain-barre syndrome--case report, french polynesia, december 2013. Euro Surveill. 19(9).

Palmer I, Wingfield PT. 2012. Preparation and extraction of insoluble (inclusion-body) proteins from escherichia coli. Current protocols in protein science / editorial board, John E Coligan [et al]. Chapter 6:Unit6 3.

Patkar CG, Kuhn RJ. 2008. Yellow fever virus ns3 plays an essential role in virus assembly independent of its known enzymatic functions. J Virol. 82(7):3342-3352.

Paz-Bailey G, Rosenberg ES, Doyle K, Munoz-Jordan J, Santiago GA, Klein L, Perez-Padilla J, Medina FA, Waterman SH, Gubern CG et al. 2017. Persistence of zika virus in body fluids - preliminary report. N Engl J Med Overseas Ed. 2017.

Perera R, Kuhn RJ. 2008. Structural proteomics of dengue virus. Curr Opin Microbiol. 11(4):369-377.

Pierson TC, Kielian M. 2013. Flaviviruses: Braking the entering. Curr Opin Virol. 3(1):3-12.

Pincus S, Mason PW, Konishi E, Fonseca BA, Shope RE, Rice CM, Paoletti E. 1992. Recombinant vaccinia virus producing the prm and e proteins of yellow fever virus protects mice from lethal yellow fever encephalitis. Virology. 187(1):290-297.

Prince HE, Tobler LH, Lape-Nixon M, Foster GA, Stramer SL, Busch MP. 2005. Development and persistence of west nile virus-specific immunoglobulin m (igm), iga, and igg in viremic blood donors. J Clin Microbiol. 43(9):4316-4320.

Prince HE, Tobler LH, Yeh C, Gefter N, Custer B, Busch MP. 2007. Persistence of west nile virus-specific antibodies in viremic blood donors. Clin Vaccine Immunol. 14(9):1228-1230.

Priyamvada L, Cho A, Onlamoon N, Zheng NY, Huang M, Kovalenkov Y, Chokephaibulkit K, Angkasekwinai N, Pattanapanyasat K, Ahmed R et al. 2016. B cell responses during secondary dengue virus infection are dominated by highly cross-reactive, memory-derived plasmablasts. J Virol. 90(12):5574-5585.

Pugh C, Brown ES, Quinn X, Korman L, Dyas BK, Ulrich RG, Pittman PR. 2016. Povidone iodine ointment application to the vaccination site does not alter immunoglobulin g antibody response to smallpox vaccine. Viral Immunol. 29(6):361-366.

Pugh C, Keasey S, Korman L, Pittman PR, Ulrich RG. 2014. Human antibody responses to the polyclonal dryvax vaccine for smallpox prevention can be distinguished from responses

to the monoclonal replacement vaccine acam2000. Clin Vaccine Immunol. 21(6):877-885.
Ramon A, Senorale-Pose M, Marin M. 2014. Inclusion bodies: Not that bad. Front Microbiol. 5:56.
Ramos HJ, Lanteri MC, Blahnik G, Negash A, Suthar MS, Brassil MM, Sodhi K, Treuting PM, Busch MP, Norris PJ et al. 2012. Il-1beta signaling promotes cns-intrinsic immune control of west nile virus infection. PLoS Pathog. 8(11):e1003039.
Rasmussen SA, Jamieson DJ, Honein MA, Petersen LR. 2016. Zika virus and birth defects--reviewing the evidence for causality. N Engl J Med. 374(20):1981-1987.
Reed W, Carroll JS, Agramonte A. 1901. The etiology of yellow fever.: An additional note. Journal of the American Medical Association. XXXVI(7):431-440.
Reimann CA, Hayes EB, DiGuiseppi C, Hoffman R, Lehman JA, Lindsey NP, Campbell GL, Fischer M. 2008. Epidemiology of neuroinvasive arboviral disease in the united states, 1999-2007. Am J Trop Med Hyg. 79(6):974-979.
Reisen WK, Lothrop HD, Wheeler SS, Kennsington M, Gutierrez A, Fang Y, Garcia S, Lothrop B. 2008. Persistent west nile virus transmission and the apparent displacement st. Louis encephalitis virus in southeastern california, 2003-2006. Journal of medical entomology. 45(3):494-508.
Rivino L, Lim MQ. 2017. Cd4(+) and cd8(+) t-cell immunity to dengue - lessons for the study of zika virus. Immunology. 150(2):146-154.
Rodenhuis-Zybert IA, van der Schaar HM, da Silva Voorham JM, van der Ende-Metselaar H, Lei HY, Wilschut J, Smit JM. 2010. Immature dengue virus: A veiled pathogen? PLoS Pathog. 6(1):e1000718.
Rodenhuis-Zybert IA, Wilschut J, Smit JM. 2011. Partial maturation: An immune-evasion strategy of dengue virus? Trends Microbiol. 19(5):248-254.
Roehrig JT. 2003. Antigenic structure of flavivirus proteins. Adv Virus Res. 59:141-175.
Roehrig JT, Nash D, Maldin B, Labowitz A, Martin DA, Lanciotti RS, Campbell GL. 2003. Persistence of virus-reactive serum immunoglobulin m antibody in confirmed west nile virus encephalitis cases. Emerg Infect Dis. 9(3):376-379.
Russell PK, Udomsakdi S, Halstead SB. 1967. Antibody response in dengue and dengue hemorrhagic fever. Jpn J Med Sci Biol. 20 Suppl:103-108.
Sabin AB. 1952. Research on dengue during world war ii. Am J Trop Med Hyg. 1(1):30-50.
Saeed AI, Sharov V, White J, Li J, Liang W, Bhagabati N, Braisted J, Klapa M, Currier T, Thiagarajan M et al. 2003. Tm4: A free, open-source system for microarray data management and analysis. BioTechniques. 34(2):374-378.
Saito Y, Moi ML, Takeshita N, Lim CK, Shiba H, Hosono K, Saijo M, Kurane I, Takasaki T. 2016. Japanese encephalitis vaccine-facilitated dengue virus infection-enhancement antibody in adults. BMC Infect Dis. 16(1):578.
Sampathkumar P. 2003. West nile virus: Epidemiology, clinical presentation, diagnosis, and prevention. Mayo Clin Proc. 78(9):1137-1143; quiz 1144.
Schmaljohn AL, McClain D. 1996. Alphaviruses (togaviridae) and flaviviruses (flaviviridae). In: th, Baron S, editors. Medical microbiology. Galveston (TX).
Schuler-Faccini L, Ribeiro EM, Feitosa IM, Horovitz DD, Cavalcanti DP, Pessoa A, Doriqui MJ, Neri JI, Neto JM, Wanderley HY et al. 2016. Possible association between zika virus infection and microcephaly - brazil, 2015. MMWR Morb Mortal Wkly Rep. 65(3):59-62.
Schweitzer BK, Chapman NM, Iwen PC. 2009. Overview of theflaviviridaewith an emphasis on the japanese encephalitis group viruses. Laboratory Medicine. 40(8):493-499.
Seligman SJ. 2008. Constancy and diversity in the flavivirus fusion peptide. Virol J. 5:27.

Selvey LA, Dailey L, Lindsay M, Armstrong P, Tobin S, Koehler AP, Markey PG, Smith DW. 2014. The changing epidemiology of murray valley encephalitis in australia: The 2011 outbreak and a review of the literature. PLoS Negl Trop Dis. 8(1):e2656.

Shrestha B, Brien JD, Sukupolvi-Petty S, Austin SK, Edeling MA, Kim T, O'Brien KM, Nelson CA, Johnson S, Fremont DH et al. 2010. The development of therapeutic antibodies that neutralize homologous and heterologous genotypes of dengue virus type 1. PLoS Pathog. 6(4):e1000823.

Silva JR, Romeiro MF, Souza WM, Munhoz TD, Borges GP, Soares OA, Campos CH, Machado RZ, Silva ML, Faria JL et al. 2014. A saint louis encephalitis and rocio virus serosurvey in brazilian horses. Rev Soc Bras Med Trop. 47(4):414-417.

Simmonds P, Becher P, Bukh J, Gould EA, Meyers G, Monath T, Muerhoff S, Pletnev A, Rico-Hesse R, Smith DB et al. 2017. Ictv virus taxonomy profile: Flaviviridae. J Gen Virol. 98(1):2-3.

Simmons M, Burgess T, Lynch J, Putnak R. 2010. Protection against dengue virus by non-replicating and live attenuated vaccines used together in a prime boost vaccination strategy. Virology. 396(2):280-288.

Singh MP, Majumdar M, Singh G, Goyal K, Preet K, Sarwal A, Mishra B, Ratho RK. 2010. Ns1 antigen as an early diagnostic marker in dengue: Report from india. Diagn Microbiol Infect Dis. 68(1):50-54.

Sirohi D, Chen Z, Sun L, Klose T, Pierson TC, Rossmann MG, Kuhn RJ. 2016. The 3.8 a resolution cryo-em structure of zika virus. Science. 352(6284):467-470.

Smit JM, Moesker B, Rodenhuis-Zybert I, Wilschut J. 2011. Flavivirus cell entry and membrane fusion. Viruses. 3(2):160-171.

Smith JL, Pugh, C.L., Cisney, E.D., Keasey, S.L., Guevara, C., Ampuero, J.S., Comach, G., Gomez, D., Ochoa-Diaz, M., Hontz, R.D., and Ulrich, R.G. 2018. Human antibody responses to emerging mayaro virus and cocirculating alphavirus infections examined by using structural proteins from nine new and old world lineages. mSphere. 3(2).

Solomon T, Dung NM, Kneen R, Gainsborough M, Vaughn DW, Khanh VT. 2000. Japanese encephalitis. J Neurol Neurosurg Psychiatry. 68(4):405-415.

Solomon T, Mallewa M. 2001. Dengue and other emerging flaviviruses. J Infect. 42(2):104-115.

Solomon T, Winter PM. 2004. Neurovirulence and host factors in flavivirus encephalitis--evidence from clinical epidemiology. Arch Virol Suppl. (18):161-170.

Song BH, Yun SI, Woolley M, Lee YM. 2017. Zika virus: History, epidemiology, transmission, and clinical presentation. J Neuroimmunol. 308:50-64.

Sonnhammer EL, von Heijne G, Krogh A. 1998. A hidden markov model for predicting transmembrane helices in protein sequences. Proceedings / International Conference on Intelligent Systems for Molecular Biology ; ISMB International Conference on Intelligent Systems for Molecular Biology. 6:175-182.

Stadler K, Allison SL, Schalich J, Heinz FX. 1997. Proteolytic activation of tick-borne encephalitis virus by furin. J Virol. 71(11):8475-8481.

Stapleton JT, Foung S, Muerhoff AS, Bukh J, Simmonds P. 2011. The gb viruses: A review and proposed classification of gbv-a, gbv-c (hgv), and gbv-d in genus pegivirus within the family flaviviridae. J Gen Virol. 92(Pt 2):233-246.

Sun P, Kochel TJ. 2013. The battle between infection and host immune responses of dengue virus and its implication in dengue disease pathogenesis. ScientificWorldJournal. 2013:843469.

Sundaresh S, Randall A, Unal B, Petersen JM, Belisle JT, Hartley MG, Duffield M, Titball RW, Davies DH, Felgner PL et al. 2007. From protein microarrays to diagnostic antigen

discovery: A study of the pathogen francisella tularensis. Bioinformatics. 23(13):i508-518.
Talavera G, Castresana J. 2007. Improvement of phylogenies after removing divergent and ambiguously aligned blocks from protein sequence alignments. Systematic biology. 56(4):564-577.
Ter Meulen J, Koulemou K, Wittekindt T, Windisch K, Strigl S, Conde S, Schmitz H. 1998. Detection of lassa virus antinucleoprotein immunoglobulin g (igg) and igm antibodies by a simple recombinant immunoblot assay for field use. J Clin Microbiol. 36(11):3143-3148.
Tesh RB, Travassos da Rosa AP, Guzman H, Araujo TP, Xiao SY. 2002. Immunization with heterologous flaviviruses protective against fatal west nile encephalitis. Emerg Infect Dis. 8(3):245-251.
Tomizaki KY, Usui K, Mihara H. 2010. Protein-protein interactions and selection: Array-based techniques for screening disease-associated biomarkers in predictive/early diagnosis. FEBS J. 277(9):1996-2005.
Troupin C, Picard-Meyer E, Dellicour S, Casademont I, Kergoat L, Lepelletier A, Dacheux L, Baele G, Monchatre-Leroy E, Cliquet F et al. 2017. Host genetic variation does not determine spatio-temporal patterns of european bat 1 lyssavirus. Genome Biol Evol. 9(11):3202-3213.
Valdes K, Alvarez M, Pupo M, Vazquez S, Rodriguez R, Guzman MG. 2000. Human dengue antibodies against structural and nonstructural proteins. Clin Diagn Lab Immunol. 7(5):856-857.
van der Schaar HM, Rust MJ, Waarts BL, van der Ende-Metselaar H, Kuhn RJ, Wilschut J, Zhuang X, Smit JM. 2007. Characterization of the early events in dengue virus cell entry by biochemical assays and single-virus tracking. J Virol. 81(21):12019-12028.
VanBlargan LA, Mukherjee S, Dowd KA, Durbin AP, Whitehead SS, Pierson TC. 2013. The type-specific neutralizing antibody response elicited by a dengue vaccine candidate is focused on two amino acids of the envelope protein. PLoS Pathog. 9(12):e1003761.
Vasilakis N, Cardosa J, Hanley KA, Holmes EC, Weaver SC. 2011. Fever from the forest: Prospects for the continued emergence of sylvatic dengue virus and its impact on public health. Nat Rev Microbiol. 9(7):532-541.
Vaughn DW, Green S, Kalayanarooj S, Innis BL, Nimmannitya S, Suntayakorn S, Endy TP, Raengsakulrach B, Rothman AL, Ennis FA et al. 2000. Dengue viremia titer, antibody response pattern, and virus serotype correlate with disease severity. J Infect Dis. 181(1):2-9.
Viral and immune parameters of dengue and wnv in donors: Blood safety implications. 2012. [accessed]. https://biolincc.nhlbi.nih.gov/static/studies/wnv/MOP.pdf.
Vratskikh O, Stiasny K, Zlatkovic J, Tsouchnikas G, Jarmer J, Karrer U, Roggendorf M, Roggendorf H, Allwinn R, Heinz FX. 2013. Dissection of antibody specificities induced by yellow fever vaccination. PLoS Pathog. 9(6):e1003458.
Wahala WM, Huang C, Butrapet S, White LJ, de Silva AM. 2012. Recombinant dengue type 2 viruses with altered e protein domain iii epitopes are efficiently neutralized by human immune sera. J Virol. 86(7):4019-4023.
Wahala WM, Kraus AA, Haymore LB, Accavitti-Loper MA, de Silva AM. 2009. Dengue virus neutralization by human immune sera: Role of envelope protein domain iii-reactive antibody. Virology. 392(1):103-113.
Wahala WM, Silva AM. 2011. The human antibody response to dengue virus infection. Viruses. 3(12):2374-2395.

Wan SW, Lin CF, Wang S, Chen YH, Yeh TM, Liu HS, Anderson R, Lin YS. 2013a. Current progress in dengue vaccines. J Biomed Sci. 20:37.
Wan SW, Lin CF, Yeh TM, Liu CC, Liu HS, Wang S, Ling P, Anderson R, Lei HY, Lin YS. 2013b. Autoimmunity in dengue pathogenesis. J Formos Med Assoc. 112(1):3-11.
Wasserman S, Tambyah PA, Lim PL. 2016. Yellow fever cases in asia: Primed for an epidemic. Int J Infect Dis. 48:98-103.
Waugh DS. 2016. The remarkable solubility-enhancing power of escherichia coli maltose-binding protein. Postepy Biochem. 62(3):377-382.
Weaver SC, Costa F, Garcia-Blanco MA, Ko AI, Ribeiro GS, Saade G, Shi PY, Vasilakis N. 2016. Zika virus: History, emergence, biology, and prospects for control. Antiviral Res. 130:69-80.
Weaver SC, Reisen WK. 2010. Present and future arboviral threats. Antiviral Res. 85(2):328-345.
Weiskopf D, Angelo MA, de Azeredo EL, Sidney J, Greenbaum JA, Fernando AN, Broadwater A, Kolla RV, De Silva AD, de Silva AM et al. 2013. Comprehensive analysis of dengue virus-specific responses supports an hla-linked protective role for cd8+ t cells. Proc Natl Acad Sci U S A. 110(22):E2046-2053.
Whitehead SS, Blaney JE, Durbin AP, Murphy BR. 2007. Prospects for a dengue virus vaccine. Nat Rev Microbiol. 5(7):518-528.
Wieten RW, Jonker EF, van Leeuwen EM, Remmerswaal EB, Ten Berge IJ, de Visser AW, van Genderen PJ, Goorhuis A, Visser LG, Grobusch MP et al. 2016. A single 17d yellow fever vaccination provides lifelong immunity; characterization of yellow-fever-specific neutralizing antibody and t-cell responses after vaccination. PLoS One. 11(3):e0149871.
Williams KL, Wahala WM, Orozco S, de Silva AM, Harris E. 2012. Antibodies targeting dengue virus envelope domain iii are not required for serotype-specific protection or prevention of enhancement in vivo. Virology. 429(1):12-20.
Xiao SY, Guzman H, da Rosa AP, Zhu HB, Tesh RB. 2003. Alteration of clinical outcome and histopathology of yellow fever virus infection in a hamster model by previous infection with heterologous flaviviruses. Am J Trop Med Hyg. 68(6):695-703.
Yoshii K, Sunden Y, Yokozawa K, Igarashi M, Kariwa H, Holbrook MR, Takashima I. 2014. A critical determinant of neurological disease associated with highly pathogenic tick-borne flavivirus in mice. J Virol. 88(10):5406-5420.
Zhou Y, Austin SK, Fremont DH, Yount BL, Huynh JP, de Silva AM, Baric RS, Messer WB. 2013. The mechanism of differential neutralization of dengue serotype 3 strains by monoclonal antibody 8a1. Virology. 439(1):57-64.
Zika open-research portal. 2016. [accessed]. https://zika.labkey.com/project/OConnor/begin.view.